Automatic modulation classification system for OFDM signals

M Rossouw

https://orcid.org/0000-0001-5138-6669

Dissertation accepted in fulfilment of the requirements for the degree Master of Engineering in Computer and Electronic Engineering at the Potchefstroom campus of the North-West University

Supervisor: Dr M Ferreira

Graduation: May 2020

Student number: 24117102

Acknowledgements

"Then everything you do will bring glory to God through Jesus Christ.
All glory and power to him forever and ever!"
— 1 Peter 4:11 NLT

To my study leader, Dr Melvin Ferreira: Thank you for all your guidance and support through the years. Thank you for always believing in me.

To my parents: Thank you for always supporting me in everything I do and for all the opportunities you have given me.

To everyone who has served on student structures with me: Thank you for showing me that there is more to life.

To all my friends during my time at university: Thank you for being there for me.

Abstract

Automatic modulation classification (AMC) is the process of automatically determining the modulation technique used in a received signal. An important part of identifying an unknown signal is to determine its modulation parameters; therefore an important part of the automatic modulation classification (AMC) of orthogonal frequency-division multiplexing (OFDM) signals is to determine the modulation parameters of the signal.

The purpose of this research is to explore and evaluate existing methods of blindly determining the parameters of an OFDM signal, as well as determining if OFDM is present in a signal of interest (SOI). Improvements to and novel uses of existing feature extraction and parameter recognition techniques are also explored and evaluated. These techniques include the Giannakis–Tsatsanis test and a MUltiple SIgnal Classification (MUSIC) based test to determine the number of OFDM sub-carriers.

It was determined that the Giannakis–Tsatsanis test could not be used to distinguish OFDM signals from several other modulation techniques. A MUSIC algorithm based test to determine the number of sub-carriers present in an OFDM signal was also evaluated. A shortcoming of this test, namely that it is computationally intensive, was addressed by improving the test to use the MATLAB® `pmusic` function. This greatly reduced the computational complexity of the test. Finally, it was determined that this pMUSIC algorithm could also be used to determine the presence of OFDM, thereby addressing a shortcoming of existing methods by developing a suitable method.

Keywords: *Automatic Modulation Classification, OFDM, parameter estimation*

Opsomming

Outomatiese modulasieklassifikasie is die proses waarin die modulasieskema van ′n ontvangde sein outomaties bepaal word. ′n Belangrike aspek van om ′n onbekende sein te identifiseer is om die modulasieparameters daarvan te bepaal. Daarom is dit belangrik om die modulasieparameters van ′n Ortogonale Frekwensie Verdeelde Multipleksering (OFDM) sein te bepaal as dit outomaties geklassifiseer word.

Die doel van hierdie navorsing is om bestaande metodes om blindelings die teenwoordigheid en parameters van ′n OFDM-sein te bepaal, te verken en te evalueer. Verbeterings aan en ongewone gebruike van bestaande kenmerkonttrekking- en parameter-herkenningstegnieke is ook verken en geëvalueer. Hierdie tegnieke sluit die Giannakis–Tsatsanis-toets en ′n MUltiple SIgnal Classification (MUSIC) gebaseerde toets vir die aantal OFDM sub-draers in.

Dit was bevind dat die Giannakis–Tsatsanis-toets nie gebruik kan word om OFDM-seine van verskeie ander modulasieskemas te onderskei nie. ′n MUSIC-algoritme gebaseerde toets om die aantal sub-draers in ′n OFDM-sein te bepaal is ook geëvalueer. ′n Tekortkoming van hierdie toets, naamlik dat dit rekenintensief is, is aangespreek deur die toets te verbeter deur die gebruik van die MATLAB® `pmusic`-funksie. Dit het die rekenintensiteit van die toets aansienlik verbeter. Laastens is dit bevind dat hierdie pMUSIC algoritme ook gebruik kan word om die teenwoordigheid van OFDM te bepaal. Hierdeur is ′n tekortkoming van ′n bestaande metode aangespreek deur ′n gepaste metode te ontwikkel.

Sleutelwoorde: *Outomatiese Modulasieklassifikasie, OFDM, parameterskatting*

Table of Contents

List of Figures

List of Tables

List of Abbreviations and Acronyms

ACI adjacent channel interference

ADSL asymmetric digital subscriber line

ALRT average likelihood ratio test

AMC automatic modulation classification

AMR automatic modulation recognition

AWGN additive white Gaussian noise

COFDM coded orthogonal frequency-division multiplexing

COST European Cooperation in Science and Technology

CP cyclic prefix

CS cyclic suffix

DAB Digital Audio Broadcasting

DMT discrete multi-tone

DSB double sideband

DVB Digital Video Broadcasting

E-UTRA Evolved Universal Terrestrial Radio Access

EPA Extended Pedestrian A

ETU Extended Typical Urban

EVA Extended Vehicular A

FB feature-based

FEC forward error correction

FPR false positive rate

FSK frequency-shift keying

GI guard interval

GLRT generalised likelihood ratio test

GMSK Gaussian minimum shift keying

GSM Global System for Mobile communications

HLRT hybrid likelihood ratio test

ICI inter-carrier interference

IEEE Institute of Electrical and Electronics Engineers

IFFT inverse fast Fourier transform

ISI inter symbol interference

ITU-R International Telecommunication Union Radiocommunication Sector

LB likelihood-based

LTE Long Term Evolution

MC-CDMA multi-carrier code-division multiple access

MIMO multiple input, multiple output

MISO multiple input, single output

ML Machine Learning

ML maximum likelihood

MSE mean squared error

MUSIC MUltiple SIgnal Classification

OFDM orthogonal frequency-division multiplexing

PAM pulse-amplitude modulation

pdf probability density function

PDP power delay profile

P/S parallel to serial

PSD power spectral density

PSK phase-shift keying

QAM quadrature amplitude modulation

ROC receiver operating characteristic

SISO single input, single output

SOI signal of interest

S/P serial to parallel

SSB single sideband

TDL tapped delay line

TPR true positive rate

ZP zero padding

List of Symbols

M	estimated number of sub-carriers
N_c	number of sub-carriers
N_d	number of data containing sub-carriers
N_e	number of samples received
N_g	number of guard carriers
N_s	number of symbols
T_s	sample duration
T_{sym}	symbol duration
f_D	maximum Doppler shift
f_k	sub-carrier frequency
k	sub-carrier index
M	modulation order

Chapter 1

Research Proposal

This chapter will give a background of the research problem and provide a research proposal for the study.

1.1 Introduction

There are many modulation techniques widely used for the transmission of radio signals [1–3]. There are situations in which a signal is received, but the modulation technique is unknown. This creates the need to determine the modulation technique of a received signal automatically.

Automatic modulation classification (AMC) is the process of automatically determining the modulation technique used in a received signal [4]. This process can also be called automatic modulation recognition (AMR) [5]. There are several applications for AMC in both military and civilian domains. In the military environment, the first step towards decoding adversarial communications would be to determine the modulation technique used [4]. When the modulation type is known, the signal can also be jammed more effectively [4]. In the civilian environment, AMC is used in the field of cognitive radio. In cognitive radio communications, the modulation technique is changed based on the channel conditions [5, 6]. For the receiver to be able to keep up with these modulation technique changes, it has to perform AMC on the received signal [4]. Another application is that of spectrum monitoring and enforcing [7]. Regulators want to determine if a specific section of the spectrum is being used in the way that it is licensed to be used [8]. AMC can help them determine the type of signal that is present.

1.2 Background and Rationale

1.2.1 AMC System Overview

An AMC system consists of different parts. Firstly a signal is received through a channel. Feature extraction is then performed on the received signal. Lastly, a classifier uses the extracted features to determine the modulation used. Figure 1.1 illustrates this process.

Figure 1.1: The AMC process.

1.2.2 Properties of a Good Classifier

According to Zhu and Nandi [4], a good modulation classifier has the following characteristics:

1. Accurate
2. Robust
3. Computationally efficient
4. Versatile

In this context, accuracy is defined as the percentage of times that a classifier can correctly determine the modulation type used [4]. Robustness means that the classifier can function in a wide variety of channels [4] and has a degree of immunity towards interference and noise. The computational efficiency of a classifier refers to how powerful the hardware that it runs on needs to be [4]. Versatility refers to how many modulation methods the classifier can detect [4].

It is also important that the modulation classification happens fast enough [9].

These properties will be important in evaluating and comparing existing and new AMC algorithms and methods.

1.2.3 AMC techniques

The AMC techniques to be investigated include the Giannakis–Tsatsanis test and a MUltiple SIgnal Classification (MUSIC) based test to determine the number of sub-carriers. These tests can then be used as an AMC system to determine the presence of orthogonal frequency-division multiplexing (OFDM) and determine the number of OFDM sub-carriers.

1.2.4 Channels

There are various different channel models used in the wireless telecommunication literature [1–4, 10]. The most common channel models used for AMC is [4, 11, 12]:

1. Additive white Gaussian noise (AWGN)
2. non-Gaussian noise
3. Fading (including Rayleigh and Rician)
4. Frequency and Phase shifts

1.3 Literature Review

Chapter 2 provides a detailed literature study. From this, it can be seen that most of the recent work is on digital modulation techniques and not analogue modulation techniques. There is also limited research done on AMC of OFDM signals. The channel models used in the research varies, but most of the work is done in an AWGN channel. There is some work done in non-Gaussian and fading channels, and little work done in physical, real-world channels.

1.4 Purpose and Problem Statement

An important part of identifying an unknown signal is to determine its modulation parameters [13], therefore an important part of the automatic modulation classification (AMC) of OFDM signals is to determine the modulation parameters of the signal.

The purpose of this research is to explore and evaluate existing methods of blindly determining the parameters of an OFDM signal, as well as determining if OFDM is present in a signal of interest (SOI). Improvements to and novel uses of existing feature extraction and parameter recognition techniques will also be explored and evaluated.

1.5 Research Objectives

The objectives of this research are to:

1. Identify the applicable OFDM modulations that are commonly used in OFDM-based signals.

2. Identify the modulation parameters used in these signals and how they vary between signals.

3. Identify the appropriate tests for parameter extraction, such as the Giannakis–Tsatsanis test and a MUSIC based tests.

4. Evaluate existing tests for parameter extraction, using metrics such as accuracy, robustness, computational efficiency and versatility.

5. Develop or improve tests for parameter extraction by applying existing tests in novel ways and developing new tests.

6. Perform experiments in increasingly realistic channels, such as AWGN and multi-path channels.

1.6 Contributions and Limitations

This study contributes by creating an AMC system for OFDM signals that can distinguish OFDM signals from other digital modulation schemes and determine the number of sub-carriers in an OFDM signal. During the study, practical tests and validations of simulations will take place, and the study will add to the body of knowledge on the subject.

The goal of this study is not to develop new features or new classifiers, but only to implement existing features and classifiers. The study is limited to OFDM signals.

The scope of this study is limited as follows. Only standard OFDM signals are considered and therefore coded orthogonal frequency-division multiplexing (COFDM), Wavelet-OFDM and multi-carrier code-division multiple access (MC-CDMA) OFDM signals are excluded from the work done here. This study will also only consider single input, single output (SISO) systems and will not look at multiple input, multiple output (MIMO) or multiple input, single output (MISO) systems. This is done in order to limit the extent of the tests that are done.

A finite solution space will also be determined for the parameters by limiting the number of possible outcomes of a test. This means that for example, when testing the number of sub-carriers (N_c), only $N_c \in \{16, 32, 64, 128, 256\}$ will be considered and not $N_c \in \mathbb{N}$.

1.7 Dissertation Overview

The rest of the dissertation is organised as follows:

- Chapter 2 provides a literature study that explores the theoretical background and literature related to the study.
- Chapter 3 provides initial experiments that are done by implementing various tests in an AWGN channel.
- Chapter 4 expands on these initial experiments by repeating the tests in various channels, including, AWGN and multi-path channel models.
- Chapter 5 provides the verification and validation of the tests performed in Chapters 3 and 4.
- Chapter 6 provides a conclusion to the dissertation.

Chapter 2

Literature Study

This chapter explores the theoretical background and literature related to the study. It looks at existing AMC techniques and how these techniques are implemented. It also provides an overview of the channel conditions in which tests of this nature are typically done. Next, it provides an overview of OFDM signals, as well as existing techniques to determine the parameters of an OFDM signal. Finally, it looks at the parameters of typical OFDM signals.

2.1 Analogue and Digital Modulation

Most AMC algorithms can only be used on analogue modulations or digital modulations [4]. There are, however, techniques that can be used for both as they classify the received signal as analogue or digital as part of their classification process [5,8].

Recent development focuses on digital signals, although there are recent studies in which the algorithm that was developed can classify both analogue and digital signals [5,8].

2.2 Likelihood-based vs Feature-based

AMC techniques can be divided into two categories, namely likelihood-based (LB) and feature-based (FB) [6].

2.2.1 Likelihood-based Methods

The likelihood-based (LB) method of AMC uses the probability density function (pdf) of the received signal, together with various statistical hypothesis tests to determine the modulation technique [6]. This technique is also sometimes called distribution test-based or decision theoretic-based [4]. This method is more computationally complex than the feature-based method [4, 8]. This complexity is caused by the calculation of natural logarithms in the likelihood function and the need for more signal samples [4]. LB methods are the most popular way of doing AMC [4]. This method produces high-accuracy classifiers when perfect channel model and channel state parameters are known [4]. It is therefore not well suited for scenarios in which the channel conditions are not entirely known.

The LB method is based on hypothesis testing [4]. The most common tests used are maximum likelihood (ML), average likelihood ratio test (ALRT), generalised likelihood ratio test (GLRT) and hybrid likelihood ratio test (HLRT) [4, 6].

2.2.2 Feature-based Methods

Feature-based (FB) methods look at the features of the signal when classifying [4, 6]. One of these features is the variance of the centred normalised signal amplitude [4, 6]. This is a measure of how the signal amplitude changes and can be used to differentiate between modulation techniques where the amplitude should stay the same, such as phase-shift keying (PSK), and techniques where it should change, such as quadrature amplitude modulation (QAM) [4]. Another feature used is the standard deviation of the absolute value of the non-linear component of the instantaneous phase [4]. This feature allows the distinction between modulation techniques that have information in their phase (e.g. PSK) and those that do not (e.g. ASK) [4]. These, and other, features each separate the modulation techniques into groups based on what method the modulation technique uses to carry information. By testing various features against the received signal, it is possible to determine the modulation technique used. Whether features are tested hierarchically or all at once has an effect on the performance of the system [8]. Testing the features all at once is expected to yield a system with better performance [8]. For analogue modulation techniques, feature-based methods are preferred [4,8]. However, Xiao [14] has developed a likelihood-based AMC algorithm for analogue signals.

2.3 Channel Conditions

Most AMC research is done on signals transmitted through an AWGN channel [4,6]. More recent research however, also takes channel conditions such as fading channels and impulse noises into consideration [4, 11]. During the development of AMC algorithms, a signal model is used. For an AMC algorithm to work well in practice, the signal model has to be very accurate [4]. Some fading channel models used also take the Doppler effect into consideration [4]. Chavali and Da Silva have developed a likelihood-based technique that uses non-Gaussian Noise [11]. Wu *et al.* have developed a feature-based AMC technique that works in a multipath channel [15].

2.3.1 AWGN Channel

The simplest non-ideal channel that is commonly used for tests is the additive white Gaussian noise (AWGN) channel [3]. In practice, this noise can be caused by the thermal noise of the electronic components used in the transmitter and receiver, as well as interference during transmission [3]. This noise has a constant power spectral density (PSD) over all frequencies and has an infinite bandwidth [16].

2.3.2 Fading Channels [1]

Fading occurs when a signal experiences rapid changes in its amplitude, phase or multipath delay over a short period or short distance. This is caused by more than one version of the same signal arriving at the receiver with slightly different delays. These delays are caused by the multipath propagation of the signal, where each of the signal versions that arrive at the receiver followed a different route.

Fading has the following effects on a signal:

1. The signal experiences rapid changes in its signal strength over a short period or short distance.
2. Varying Doppler shifts on the different multipath signals causes the random frequency modulation of the signal.
3. Multipath propagation delays cause echoes in the signal.

The movement of surrounding objects can cause these effects to vary in time, although the transmitter and receiver are stationary.

Antenna space diversity can be used to counter fading by preventing deep fading nulls.

The following factors influence fading:

1. Multipath propagation
2. Speed between transmitter and receiver
3. Speed of surrounding objects
4. The bandwidth of the signal

There are different types of fading:

1. Flat fading, in which only the amplitude is affected, and the change is constant over the bandwidth of the signal.
2. Frequency selective fading, in which different frequencies in the bandwidth of the signal experiences different amplitude changes.
3. Fast fading, in which the amplitude, phase and delay changes in the signal happen faster than the changes in the signal.
4. Slow fading, in which the amplitude, phase and delay changes in the signal happen slower than the changes in the signal.

The most common fading channel models used are Rayleigh and Rician. These models only take the amplitude effect of fading into account and does not consider the phase and delay effects that fading can have and are also not frequency selective. There is a two-ray Rayleigh fading model that does take multipath time delays into account.

2.3.3 Tapped Delay Line Channel Models

One of the very common types of channel model for multi-path channels is the tapped delay line (TDL) channel model [10,17]. TDL channel models are usually defined for a specific scenario, such as [10,17]:

- Indoor residential
- Indoor office
- Factories and airports
- Tunnels and mines
- Typical Urban

- Typical Rural
- Bad Urban
- Hilly Terrain
- Pedestrian
- Vehicular

Two of the most popular TDL channel models are COST 207 and ITU-R M.1225 [10,18].

The COST 207 [19] channel models were developed by the European Cooperation in Science and Technology (COST) from extensive measurements throughout Europe [18]. They are the basis of the Global System for Mobile communications (GSM) channel models [18]. They include typical urban, bad urban, typical rural and hilly terrain scenarios [10,18].

The ITU-R M.1225 [20] channel models were developed by the International Telecommunication Union Radiocommunication Sector (ITU-R) for use in third-generation cellular systems [18]. They include indoor, pedestrian and vehicular models [10,18].

2.4 Machine Learning

Machine Learning (ML) techniques have been used with success for solving the problem of classifying things based on their features [21]. It is, therefore also suited for feature-based AMC [4]. In the ML process, the system is taught how to recognise items by applying it to a test set of items with known outcomes [21]. The system is then tested against another set of test data [21]. There are already several studies done where ML is used for feature-based AMC; however, all of these were done in an AWGN channel and by means of simulations [7,22–24].

2.5 Comparison of Existing AMC Techniques (Related Work)

Dobre *et al.* [6] provide a comparison of AMC techniques that existed in 2007. This section will, therefore, focus on techniques developed since then and builds on the existing body of knowledge. Table 2.1 shows a comparison of existing techniques.

To do this comparison, an extensive literature survey was done, and the relevant aspects of each study were extracted. These aspects are the year the study was done, whether the method is likelihood-based (LB) or feature-based (FB), which modulations were considered, and which channels were used in the study. Where OFDM is listed as one of the modulation schemes, OFDM was one of the modulation schemes that had to be distinguished from the others, and where OFDM is listed as a channel, the related work focused on the inner modulation of OFDM, thereby seeing it as a channel for the relevant modulation scheme.

From this, it can be seen that most of the recent work is on digital modulation techniques and not analogue modulation techniques. There is also limited research done on AMC of OFDM signals. The channel models used in the research varies, but most of the work is done in an AWGN channel. There is little work done in multipath channels, as well as physical, real-world channels.

Other OFDM AMC related work is also discussed in Sections 2.11 to 2.13.

Table 2.1: Comparison of existing AMC techniques.

Author(s)	Year	Method	Modulations	Channel(s)
Wu *et al.* [15]	2008	FB	BPSK, QPSK	Rayleigh
Choqueuse *et al.* [25]	2009	LB	BPSK, QPSK, 16-PSK, 16-QAM	MIMO, Rayleigh, AWGN
Wang and Wang [12]	2010	LB	QAM, PSK	AWGN, flat-fading, OFDM, non-Gaussian noise, phase and frequency offset
Headley and Da Silva [26]	2011	LB	BPSK, QPSK, 8-PSK, 16-QAM, 64-QAM	flat-fading
Aslam *et al.* [7]	2012	FB	BPSK, QPSK, QAM-16, QAM-64	noise
Xiao [14]	2012	LB, FB	AM, SSB, DSB, FM	AWGN
Popoola and van Olst [27,28]	2012, 2013	FB	AM, DSB, SSB, FM, 2-ASK, 4-ASK, 2-FSK, BPSK, QPSK, OFDM, 16-QAM, 64-QAM	AWGN, hardware
Chavali and Da Silva [11]	2013	LB	PAM, PSK, QAM	time-correlated non-Gaussian noise
Zhu *et al.* [22]	2013	FB	4-QAM, 16-QAM, 64-QAM	AWGN, phase offset
Mühlhaus *et al.* [29]	2013	FB	BPSK, QPSK, 8-PSK, 16-QAM, 64-QAM	spatially multiplexed MIMO
Benedetto *et al.* [5]	2016	FB	FM, AM, SSB, BPSK, QPSK, 8-PSK, 16-PSK, 4-ASK, 2-FSK, 4-FSK, GMSK, 8-QAM, 16-QAM, 32-QAM, 64-QAM	noise and phase offset

2.6 Existing Features

Yu [8] has categorised the features and methods used into the following groups:

1. Phase based approaches
2. M-th order power law based approaches
3. Zero-crossing based approaches
4. Statistical moments based approaches
5. Wavelet transform based approaches

2.7 OFDM

Orthogonal frequency-division multiplexing (OFDM) is a digital signal transmission scheme that can be seen as both a modulation technique and a multiplexing technique [30]. In an OFDM signal, the channel is divided into sub-carriers, and each of these sub-carriers is used to transmit data in parallel [31]. Figure 2.1 shows this basic principle of OFDM modulation and demodulation for the case where the number of sub-carriers (N_c) is 4.

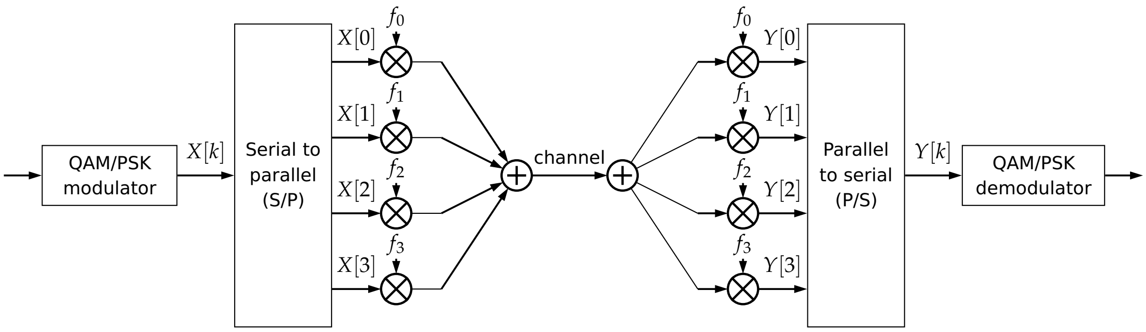

Figure 2.1: Signal diagram of the principle of OFDM modulation [10,32].

OFDM is robust against frequency selective fading [30] because when a frequency selective fading channel is divided into sub-carriers, each of the sub-carriers can be approximated by a flat fading channel [10]. OFDM is spectrally efficient [31], especially when more than 64 sub-carriers are used [10]. Because of the mathematical orthogonality of the sub-carriers, it is possible to arrange the carriers in such a way that the sidebands of the carriers can overlap without interference [30]. This can be seen in Figure 2.2, where it is shown that all the other sub-carriers are zero at the frequency of a sub-carrier [32]. This allows for efficient use of the available spectrum. One of the disadvantages of OFDM is that it is sensitive to frequency offset [30, 31]. Figure 2.2 shows the frequency spectrum of the OFDM sub-carriers for the case where the number of sub-carriers (N_c) is 4.

Figure 2.3 shows the block diagram of a typical OFDM system. Each of the blocks will now be discussed in more detail.

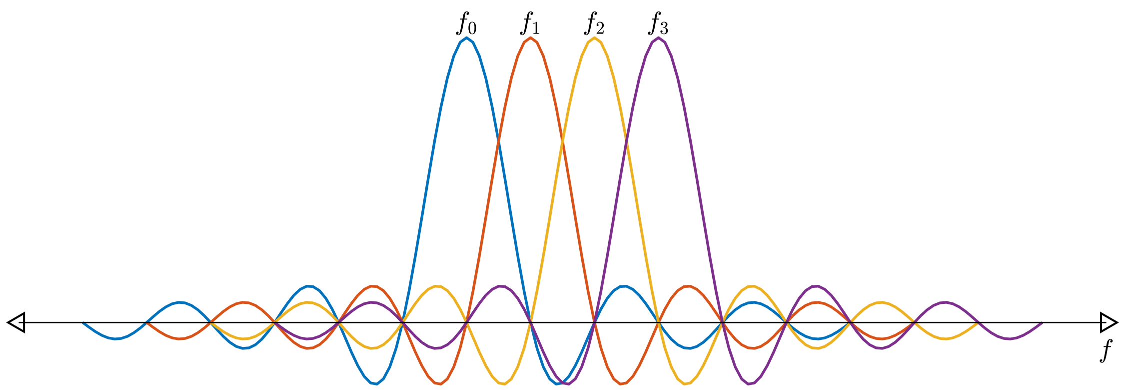

Figure 2.2: The frequency spectrum of the OFDM sub-carriers [2, 10, 32].

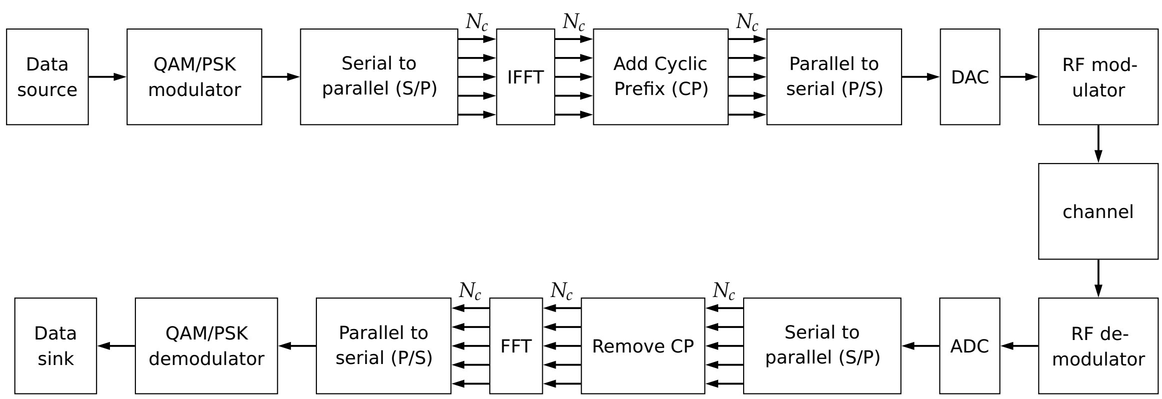

Figure 2.3: Block diagram of a typical OFDM system [2, 10, 31, 32].

2.7.1 Inner Modulation

The OFDM process starts with modulating the data that has to be sent with a single carrier modulation scheme such as M-PSK or M-QAM [10], where M is the modulation order, typically $M \in \{4, 8, 16, 32, 64\}$. This is known as the inner modulation of the OFDM signal [10]. Each of the modulated symbols has a duration of T_s.

2.7.2 Serial to Parallel

The data is then split into N_c parallel streams, and as part of the serial to parallel (S/P) conversion process each symbol's duration is lengthened to $M = N_c T_s$ [10]. The data is then put through an N_c-point inverse fast Fourier transform (IFFT) which modulates the parallel streams onto N_c sub-carriers [10]. The use of an IFFT for this purpose is a mathematical trick that is explained and derived in [10].

2.7.3 Guard Interval

The next step in the process is to add a cyclic prefix (CP) to each of the symbols. During this step, the last part of each symbol is added at the beginning of the symbol [10]. This is done in order to prevent the inter symbol interference (ISI) that is caused by a multipath channel [10]. The duration of this CP has to be longer than the maximum multipath delay of the channel in order to prevent both ISI and inter-carrier interference (ICI) [10]. The ICI is caused by the ISI causing the sub-carriers to lose orthogonality [10]. In some OFDM implementations, a cyclic suffix (CS) or zero padding (ZP) is used instead of a CP [10]. The fact that a signal contains a CP or CS can be used to determine the symbol length (M) of a received signal by autocorrelating the signal [33]. This CP, CS or ZP is known as the guard interval (GI) [10].

2.7.4 Parallel to Serial

The next step is to convert the N_c parallel streams into a single stream by means of a parallel to serial (P/S) converter [10]. Finally, the signal is converted to an analogue form and modulated to the carrier frequency before being transmitted over the channel [10]. The whole process then reversed on the receiving side in order to recover the transmitted data.

2.7.5 Sub-carrier Spacing

The frequencies used for the sub-carriers are $f_k = k/M$ (where k is the sub-carrier index and f_k is the sub-carrier frequency) which means that the complex time-domain representation of the signals are given by $e^{j2\pi f_k t}$ where in each case $k \in \mathbb{Z}$ and $0 \leq k \leq N_c - 1$ and the signals are time-limited to $0 \leq t \leq M$ for each of the OFDM symbols [10].

2.7.6 Guard Carriers

OFDM signals have large out-of-band power which can cause adjacent channel interference (ACI) [10]. To counteract this effect, OFDM sometimes make use of virtual carriers, also called guard carriers [10]. These guard carriers are unused sub-carriers at both ends of the spectrum used by the signal [10]. Figure 2.4 shows an example of an OFDM signal with 4 sub-carriers, where there is one guard carrier at each end. In this case, f_0 and f_3 are the guard carriers, and f_1 and f_2 are data-bearing sub-carriers.

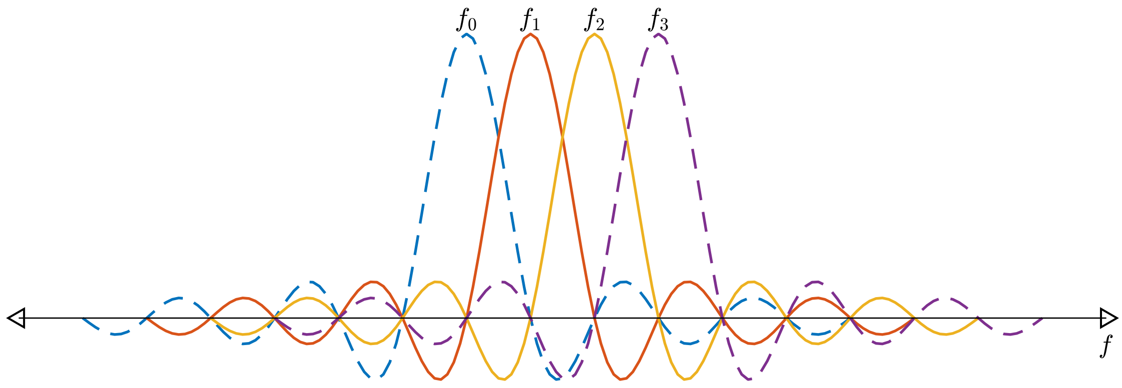

Figure 2.4: The frequency spectrum of OFDM with guard carriers.

2.8 OFDM Parameters

The modulation of one OFDM signal can be different from that of another OFDM signal. These variations are caused by the parameters of the modulation being different in each signal [10,31,34]. The parameters of OFDM modulation include:

- The number of sub-carriers [34]
- Sub-carrier spacing [34]
- How sub-carriers are used [10]
- The use, type and length of a guard interval (GI) [10,33,34]
- Symbol length [31,33]
- The channel estimation technique used [10,31]
- If built-in forward error correction (FEC) is used [10,31]
- Inner modulation [10,33]

2.9 Common OFDM Use Cases and Channel Models

Technologies where OFDM is typically encountered include Digital Audio Broadcasting (DAB) [35], Digital Video Broadcasting (DVB) [36], Wi-Fi (IEEE 802.11) and Long Term Evolution (LTE) [34]. LTE uses the Evolved Universal Terrestrial Radio Access (E-UTRA) radio interface protocol [37]. Table 2.2 shows a comparison of these signals and Table 2.3 shows the frequencies of the bands mentioned in Table 2.2, as it is applicable to ITU-R Region 1, of which South-Africa is part.

The key takeaways from this comparison are:

1. The frequency bands in which civilian OFDM signals are commonly found can range from 47 MHz to 5 GHz.
2. The number of sub-carriers can vary from 12 to 27 841.
3. The sub-carrier spacing can vary from 279 Hz to 2500 kHz.
4. The most common inner modulations are QPSK, 16-QAM, and 64-QAM, although others are also used.
5. The typical bandwidth of an OFDM signal can vary from 1.536 MHz to 160 MHz.
6. The different channel models, as discussed below.

These parameters and their typical ranges will be important during the experimental design of Chapters 3 and 4 to ensure that the experiments are done using realistic values for these parameters. It should also be noted that all of these signals make use of a cyclic prefix (CP).

2.9.1 Channel Model: DAB

The channel model proposed by the DAB standard is a SISO Rayleigh power delay profile (PDP) model with a Doppler shift, which is implemented using a TDL model [42].

Table 2.2: Comparison of common OFDM signals.

	DAB [35]	DVB-T2 [36]	Wi-Fi [38]	LTE [34,39,40]
Frequency band	Band I, II and III	Band III, IV and V [41]	2.4 GHz and 5 GHz	450 MHz to 3700 MHz
Number of sub-carriers	1536	853 to 27 841	64 [2]	12 to 1200
Sub-carrier spacing	1 kHz	279 Hz to 8929 Hz (8 MHz channel)	78.125 kHz, 156.25 kHz, 312.5 kHz, 625 kHz, 1250 kHz and 2500 kHz	15 kHz
Inner modulation	$\pi/4$-shift D-QPSK	QPSK, 16-QAM, 64-QAM, 256-QAM	BPSK, QPSK, 16-QAM, 64-QAM	QPSK, 16-QAM, 64-QAM, 256-QAM
Typical bandwidth	1.536 MHz	1.7 MHz, 5 MHz, 6 MHz, 7 MHz and 8 MHz	5 MHz, 10 MHz, 20 MHz, 40 MHz, 80 MHz and 160 MHz	dynamically adjusted
Channel model specification	ETSI TS 103 461 D [42]	ETSI TS 102 831 14.1 [43] ETSI TR 101 190 9.4 [44]	TGn and TGac [45,46]	3GPP TS 36.104 B [47]

Table 2.3: ITU-R Region 1 frequencies as applicable to South Africa.

Band	Frequency range [MHz]
I [48]	47 to 68
II [49]	87.5 to 108
III [50,51]	174 to 238; 246 to 254
IV [50]	470 to 582
V [50]	582 to 862

2.9.2 Channel Model: DVB-T2

The DVB-T2 standard proposes several channel models, including [43, 44]:

- SISO AWGN channels
- SISO Rayleigh and Rician TDL models
- SISO COST 207 [19] derived mobile channels
- MISO Rayleigh and Rician models

2.9.3 Channel Model: Wi-Fi

The IEEE 802.11 standard proposes several channel models, including [45]:

- SISO Rayleigh TDL models as described in ETSI EP BRAN 3ERI085B [52]
- SISO Rayleigh and Rician TDL models based on the above models
- MIMO Rayleigh and Rician models

2.9.4 Channel Model: LTE

The LTE standard proposes several channel models, including [47]:

- AWGN models
- SISO Rayleigh TDL models
- MIMO models

2.10 Discrete Multi-tone

Discrete multi-tone (DMT) is a modulation scheme that is very similar to OFDM that is typically used in wired communication links such as asymmetric digital subscriber line (ADSL) [31, 32]. The difference between OFDM and DMT is that DMT has an additional feature called bit-loading [31]. This means that the data rate of all the bins (as sub-carriers are called in DMT) are not the same, but they are varied according to the noise level of each of the bins in order to maximise data throughput [31]. The similarities between DMT and OFDM means that the feature detection techniques of DMT can also be applied to OFDM.

2.11 Cyclostationary Analysis

There are several techniques for estimating the parameters of an OFDM signal that are based on the cyclostationary analysis of the signal [53–56]. These techniques can be used to estimate parameters such as the symbol period, the number of sub-carriers, the carrier frequency offset and the cyclic prefix length [53–56]. These techniques do, however, depend on the presence of a CP, which although it is very common, is not used by all signals [10].

2.12 Test for Single-carrier vs Multi-carrier

Before performing tests to determine the parameters of an OFDM signal, the presence of an OFDM signal needs to be established; therefore, methods to determine this are also explored.

The Giannakis–Tsatsanis test [57] can be used to determine if a received signal is single-carrier of multi-carrier based [33, 58]. This test works on the principle of multi-carrier modulations such as OFDM being asymptotically Gaussian [58]. Since OFDM is a multi-carrier based signal, this test can be used to determine if OFDM is present. It has been successfully used for this purpose in AMC systems [33,58,59].

The original test has been simplified and implemented by Akmouche [58] and has been further simplified by Azarmanesh [59]. The steps given by [59] are as follows:

1. Compute the fourth-order cumulant of both the real and imaginary parts of the received signal [59]:

$$c_{4r}(0,t,t) = -\frac{1}{N_e}\sum_{i=t}^{N-t-1}\left(x_r^4(i) + x_r^2(i)x_r(i+t)x_r(i-t)\right) \tag{2.1}$$

$$c_{4j}(0,t,t) = -\frac{1}{N_e}\sum_{i=t}^{N-t-1}\left(x_j^4(i) + x_j^2(i)x_j(i+t)x_j(i-t)\right) \tag{2.2}$$

   where N_e is the number of samples received, and x_r and x_j are the real and imaginary parts of the received signal.

2. Form the vectors $\mathbf{c_r}$ and $\mathbf{c_j}$ from these cumulants [59].

3. Compute the covariance matrices of these vectors [59]:

$$\Sigma_{c_r} = \text{cov}\ \{c_{4r}(0,\eta_u,\eta_u), c_{4r}(0,\eta_v,\eta_v)\} \tag{2.3}$$

$$\Sigma_{c_j} = \text{cov}\ \left\{c_{4j}(0,\eta_u,\eta_u), c_{4j}(0,\eta_v,\eta_v)\right\} \tag{2.4}$$

4. The threshold value can then be calculated [59]:

$$d_{G,4} = \sup\ \left(\mathbf{c_r}^T\Sigma_{c_r}^{-1}\mathbf{c_r}, \mathbf{c_j}^T\Sigma_{c_j}^{-1}\mathbf{c_j}\right) \tag{2.5}$$

5. If $d_{G,4} < \tau_G$, then $x(i)$ is a multi-carrier signal, where τ_G is a threshold value that has to be determined experimentally [59].

2.13 Test for the Number of Sub-carriers

An OFDM signal is made up of a number of sub-carriers. This number varies between different implementations of OFDM [31,34]. In practice, the number of sub-carriers can vary from 12 to 27 841 (see Table 2.2). A variation of the MUSIC (MUltiple SIgnal Classification) algorithm [60] can be used to determine the number of sub-carriers that are present in a signal [61]. In this algorithm, the covariance terms $r(\tau)$ are first calculated as follows [61]:

$$r(\tau) = \frac{1}{N_c - \tau} \sum_{i=\tau+1}^{N_e} x(i) \cdot x^*(i - \tau) \tag{2.6}$$

where N_e is the number of samples received, N_c is the number of sub-carriers, τ is a time delay in the interval $[0; N_c - 1]$ and $\tau \in \mathbb{Z}$, and x is the received signal [61]. The covariance matrix $\mathbf{R}$ is then formed as follows [61]:

$$\mathbf{R} = \begin{pmatrix} r(0) & r(1) & \cdots & r(N_c-2) & r(N_c-1) \\ r^*(1) & r(0) & \cdots & r(N_c-3) & r(N_c-2) \\ \vdots & \vdots & \ddots & \vdots & \vdots \\ r^*(N_c-1) & r^*(N_c) & \cdots & r^*(1) & r(0) \end{pmatrix} \tag{2.7}$$

This next step is to perform eigenvalue decomposition on the matrix. This produces the diagonal matrix $\mathbf{R_d}$, which contains the eigenvalues [61]:

$$\mathbf{R_d} = \begin{pmatrix} \lambda_1 & 0 & \cdots & \cdots & \cdots & \cdots & \cdots \\ 0 & \lambda_2 & 0 & \cdots & \cdots & \cdots & \cdots \\ \cdots & \cdots & \ddots & \cdots & \cdots & \cdots & \cdots \\ \cdots & \cdots & 0 & \lambda_{N_c} & 0 & \cdots & \cdots \\ \cdots & \cdots & \cdots & 0 & \sigma_b^2 & 0 & \cdots \\ \cdots & \cdots & \cdots & \cdots & \cdots & \ddots & \cdots \\ \cdots & \cdots & \cdots & \cdots & \cdots & 0 & \sigma_b^2 \end{pmatrix} \tag{2.8}$$

where $\lambda_1, \lambda_2, \ldots, \lambda_{N_c}$ are the eigenvalues representing signal and noise, and σ_b^2 is the variance of the noise [60, 61]. Normally, $\lambda_i > \sigma_b^2, \forall i \in 1, 2, \ldots, N_c$ [61]. As $\mathbf{R_d}$ contains N_c eigenvalues that are larger than σ_b^2, the number of sub-carriers can be determined [61].

The problem is that this algorithm uses the number of sub-carriers (N_c) in its calculations, but this is the value that needs to be calculated [61]. The solution to this is to start the algorithm with an estimation of the number of sub-carriers and iterate until a viable solution appears [61].

2.14 Conclusion

In this chapter, it was shown that there are several existing AMC techniques that employ a variety of methods to achieve their goal. Out of these methods, there are few that focus on OFDM signals. These AMC techniques are tested in a variety of channel models, but mainly AWGN channels; these channel models were also discussed. The theoretical background behind OFDM signals was discussed and the related modulation parameters and their typical values given. Tests for determining the presence of OFDM signals and the parameters of these signals were shown.

These tests will be implemented and evaluated in the following chapter. Improvements to and novel uses of these tests will also be provided.

Chapter 3

Initial Experiments

This chapter will explore the tests provided in Sections 2.8 and 2.12 by means of experiments in a simulated environment. The results are also given and discussed. Improvements to and novel uses of these tests will also be explored.

3.1 General Experimental Setup

The tests were performed in a simulation environment using MATLAB® R2018a. The test setup as developed by the author will now be explained. The MATLAB® Communications System Toolbox was used to generate random signals and to send them through AWGN channels of varying SNR as described in each section. A diagram of the experimental setup is shown in Figure 3.1. In each case, the baseband signal was used, and the signal was synchronised. The number of symbols used in each test is described in each section. The components of the experimental setup will be discussed below.

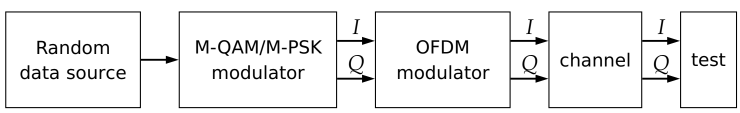

Figure 3.1: The experimental setup.

3.1.1 Random Data Source

Randomly generated data is used as the input to the system. This data is generated using the `randi` MATLAB® function. It generates a stream of pseudorandom integers in the range [0; M] where M is the modulation order of the M-QAM/M-PSK modulator.

3.1.2 M-QAM/M-PSK modulator

The M-QAM/M-PSK modulator maps these integers to the different modulation symbols in an I/Q stream. This is implemented using the `comm.QPSKModulator`, `comm.PSKModulator` and `comm.RectangularQAMModulator` MATLAB® system objects.

3.1.3 OFDM modulator

The OFDM modulator maps these symbols onto OFDM symbols. This is implemented using the `comm.OFDMModulator` MATLAB® system object.

3.1.4 Channel

The signal is then sent through an AWGN channel. This is implemented using the `awgn` MATLAB® function. The SNR of the channel is varied, as described in each section.

3.1.5 Test

Finally, the signal is subjected to the appropriate test as described in each section.

3.2 Single-carrier vs Multi-carrier

The Giannakis–Tsatsanis test can be used to determine if a received signal is single-carrier or multi-carrier based, as explained in Section 2.12. In this section, the test will be performed using the MATLAB® code provided in [59].

3.2.1 Experimental Setup

The original Giannakis–Tsatsanis test [57] has been simplified and implemented by Akmouche [58] and has been further simplified by Azarmanesh [59].

The algorithm and related equations, as explained in Section 2.12, were implemented using the MATLAB® code provided by [59]. This test follows the following procedure:

1. Compute the fourth-order cumulant of both the real and imaginary parts of the received signal.
2. From the vectors $\mathbf{c_r}$ and $\mathbf{c_j}$ from these cumulants.
3. Compute the covariance matrices of these vectors.
4. Compare this covariance value to a threshold.

Generated signals of various modulations were generated and sent through AWGN channels with an SNR of both 30 dB and 10 dB. In each case, the test was performed on 512 random samples, and each test was repeated 100 times.

3.2.2 Understanding the Results

Figure 3.2 shows an example of the results of the Giannakis–Tsatsanis test as done in this section. The horizontal line is the threshold for this example. Everything above the line represents signals that are determined to not be OFDM and everything below the line represents signals that are determined to be OFDM. The top rectangle represents signals that were correctly identified as not being OFDM and the bottom rectangle represents signals that were identified as being OFDM but are in fact not OFDM. This is known as a false positive or type I error [62].

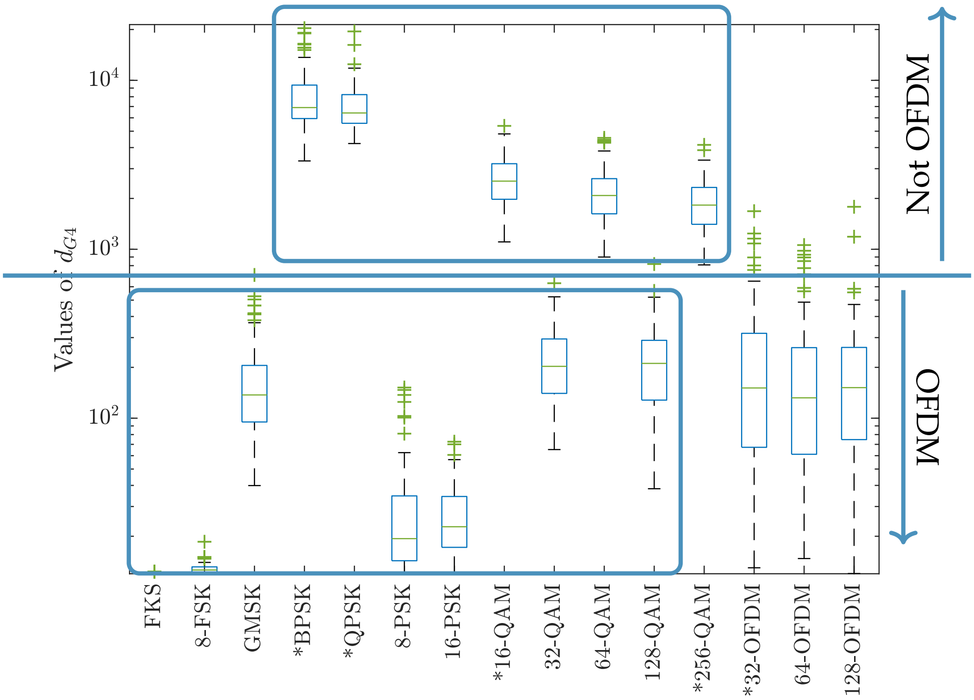

Figure 3.2: Example of the results of the Giannakis–Tsatsanis test.

3.2.3 Results and Interpretation

The test was first performed on the same modulations as in the original paper [58], i.e. BPSK, QPSK, 16-QAM, 256-QAM and 32-OFDM. The results obtained in the tests are shown in Figure 3.3 and Table 3.1. Modulation techniques indicated with an asterisk (*) were evaluated in the original paper [58]. As can be expected, the test yielded similar results. However, when this test is performed on other modulation techniques, it can not successfully distinguish OFDM from these modulation techniques. The only other modulation technique on which this test was successful is 64-QAM. The effect of a different number of OFDM sub-carriers was also evaluated. The test works by thresholding parameter d_{G4}. Table 3.2 shows the accuracy of this test for the case where the threshold of d_{G4} is set to 1000 and in a 30 dB AWGN channel. This value was chosen visually from Figure 3.3. The run-time for the tests in Table 3.2 (100 iterations for each modulation scheme, a total of 1500 iterations) is 8 seconds (using an Intel i7-7700) — this will become important in Section 3.6. As can be seen from the results, not all modulation techniques can be distinguished from OFDM with this test. If the test was able to successfully distinguish non-OFDM signals from OFDM signals, a clear vertical separation would have been seen in Figure 3.3. An example of that this looks like will be seen later in Figure 3.16a.

Table 3.1: Results of the Giannakis–Tsatsanis Test.

	average d_{G4} value in channels	
Modulation	AWGN 10 dB	AWGN 30 dB
FSK	16	12
8-FSK	46	13
GMSK	150	146
*BPSK	4512	7631
*QPSK	4191	7319
8-PSK	41	30
16-PSK	39	26
*16-QAM	2417	2624
32-QAM	248	260
64-QAM	2117	2042
128-QAM	242	244
*256-QAM	2149	2058
*32-OFDM	212	222
64-OFDM	218	215
128-OFDM	190	175

*Modulation techniques evaluated in the original paper [58]

3.2.4 Conclusion

From these results, it can be seen that the Giannakis–Tsatsanis test can be successfully used to distinguish OFDM from BPSK, QPSK, 16-QAM, 64-QAM and 256-QAM, but it cannot distinguish OFDM from 2-FSK, 8-FSK, GMSK, 8-PSK, 16-PSK, 32-QAM and 128-QAM. This makes it unsuitable for determining the presence of OFDM.

Table 3.2: Accuracy of the Giannakis–Tsatsanis Test.

	% results	
Modulation	OFDM	not OFDM
FSK	100	
8-FSK	100	
GMSK	100	
*BPSK		100
*QPSK		100
8-PSK	100	
16-PSK	100	
*16-QAM		100
32-QAM	100	
64-QAM		100
128-QAM	100	
*256-QAM	4	96
*32-OFDM	99	1
64-OFDM	99	1
128-OFDM	100	

*Modulation techniques evaluated in the original paper [58]

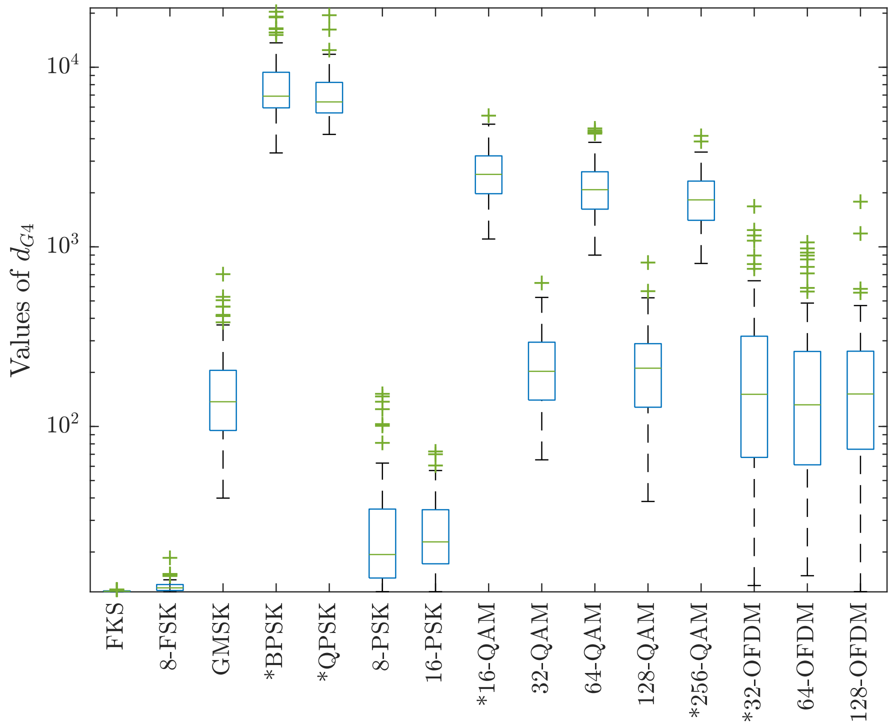

(a) 30 dB SNR AGWN channel.

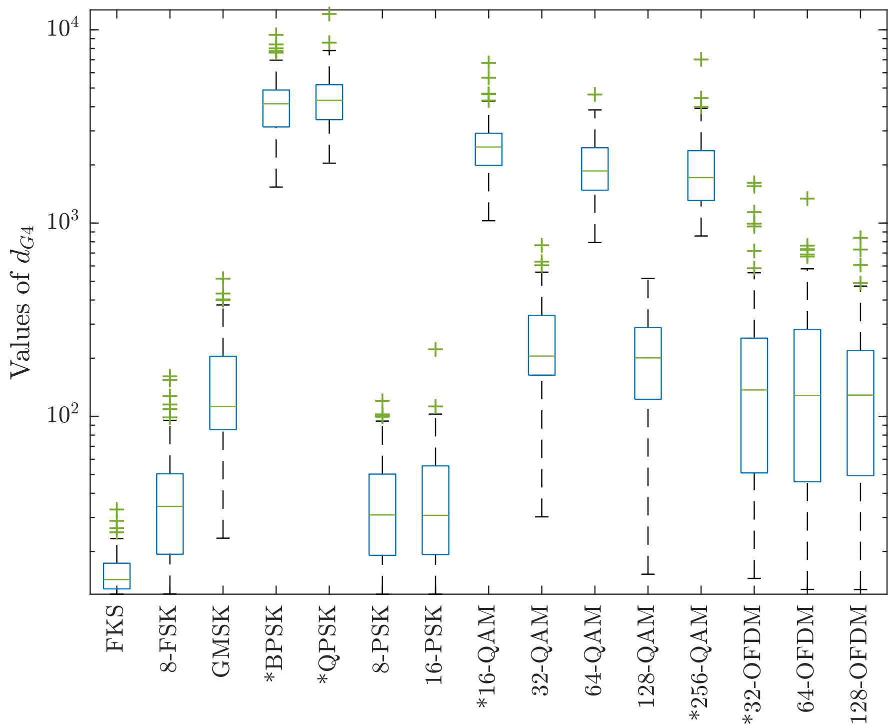

(b) 10 dB SNR AGWN channel.

Figure 3.3: Box plots for the results of 100 Giannakis–Tsatsanis tests on different modulation techniques. Modulation techniques indicated with an asterisk (*) were evaluated in the original paper [58].

3.3 Number of Sub-carriers Using MUSIC

3.3.1 Experimental Setup

The algorithm and related equations, as explained in Section 2.13, were implemented in MATLAB®. The MATLAB® implementation of the algorithm was done by the author. The specific way of visually interpreting the results was also done by the author.

This test follows the following procedure:

1. Calculate the covariance terms as in (2.6).
2. Populate the covariance matrix **R** as in (2.7).
3. Perform eigenvalue decomposition on **R**, resulting in $\mathbf{R_d}$ as in (2.8).
4. Plot the resulting eigenvalues that form the diagonal of $\mathbf{R_d}$.

This procedure is then repeated for different initial value estimations for the sub-carriers (M) until the actual number of sub-carriers (N_c) is found. This condition is explained in Section 3.3.2.

The interpretation of these plots, as developed by the author, is described in Section 3.3.3.

The MATLAB® Communications System Toolbox was used to generate an OFDM signal. Tests were performed with different numbers of sub-carriers, as well as various combinations of the number of sub-carriers in use. The number of sub-carriers tested are $N_c \in \{16, 32, 64, 128, 256\}$. In each test, 100 OFDM symbols were used. After being sent through an AWGN channel with an SNR of 30 dB, the received signal was tested to see if the number of sub-carriers can be determined. As shown in Section 2.13, the test requires that an estimate of the number of sub-carriers is given. Runs were done with this estimate being smaller than, equal to, and larger than the actual number of sub-carriers in order to see how the test responds to these different initial values.

3.3.2 Understanding the Results

The crux of this method, as well as the key to understanding the results, can be seen by comparing Figures 3.4b and 3.4c. For values of T_{sym} where $M \leq N_c$, the resulting plot will be similar to Figure 3.4b and for values of M where $M > N_c$, the resulting plot will be similar to Figure 3.4c. From this the value of N_c can then be determined by examining a series of plots for different values of M.

3.3.3 Results and Interpretation

In order to interpret the results of the test, the eigenvalues resulting from the tests were plotted. Figure 3.4 shows the results where the number of sub-carriers (N_c) is 64 and different initial value estimations for the sub-carriers (M) were used. Figure 3.5 shows the results of the test for 128 sub-carriers. The test is repeated in Figure 3.6 for 256 sub-carriers. In these tests, no guard carriers were used; therefore, all the sub-carriers carried data.

From these graphs, it can be seen that for $M > N_c$ the graph produces a sharp point at N_c, but there are no sharp points produces for $M \leq N_c$. This does however not hold for $M \gg N_c$, and it only works for up to about $M \approx N_c + 10$. This means that the initial value estimate used for the number of sub-carriers should be reasonably close in order for the test to work. Additionally, when all the sub-carriers are used, there is a sharp point in the graph at $M - N_c + 1$. As can be seen in the graphs, the minimum and maximum values are a lot more extreme when $M = N_c + 1$. This can be used to increase the confidence that the correct value for N_c has been found.

In the paper detailing the test [61], no information is given about how the test will react to the inclusion of guard carriers in the signal. The author has, however, through experimentation discovered that this test could also be used to determine the use of guard carriers in a signal. Figure 3.7 shows the results of the test for the case where there are 4 guard-carriers (N_g), two on each side of the data. This means that there are 60 sub-carriers that contain data (N_d). As can be seen in the graphs, the left sharp point moves to $M - N_d + 1$ when guard carriers are included and can, therefore, be used to determine the number of sub-carriers that contain data and the number of guard carriers. The sharp point at the right side of the graph remains at the same point, indicating the total number of sub-carriers. Figure 3.8 shows this test for 128 sub-carriers and 8 guard bands. In Figure 3.9 the test is done for 256 sub-carriers and 16 guard bands. It can also be seen that the left point is less pronounced when $M = N_c + 1$ than when $M \approx N_c + 10$, but the inverse is true for the right point. Therefore, it would be best to determine the total number of sub-carriers when $M = N_c + 1$ and to determine the number of sub-carriers use when $M \approx N_c + 10$. This only appears to work on signals with symmetrical guard carriers where the same amount of guard carriers are present at both ends of the spectrum.

This test requires more iterations to be able to detect a higher number of sub-carriers. Each iteration also requires more computations than the previous one. The complexity of this algorithm is approximately $\mathcal{O}(n^3)$. This makes the test unpractical for large numbers of sub-carriers. On the computer that was used for this test (Intel i7-7700, 16 GB RAM), a single iteration of the test took 222 seconds with $N_c = 256$ and $N_s = 200$. The test would therefore not be practical on a PC for more than 256 sub-carriers.

3.3.4 Conclusion

As can be seen from these results, this test can be successfully used to determine both the total number of sub-carriers and the number of sub-carriers in use for an OFDM signal. This is done by a visual examination of a graph of the results as outlined above. The next step would be to write an algorithm that can perform this test automatically by interpreting the results of the test. This was, however, not done, because a more computationally efficient test was developed in Section 3.4.

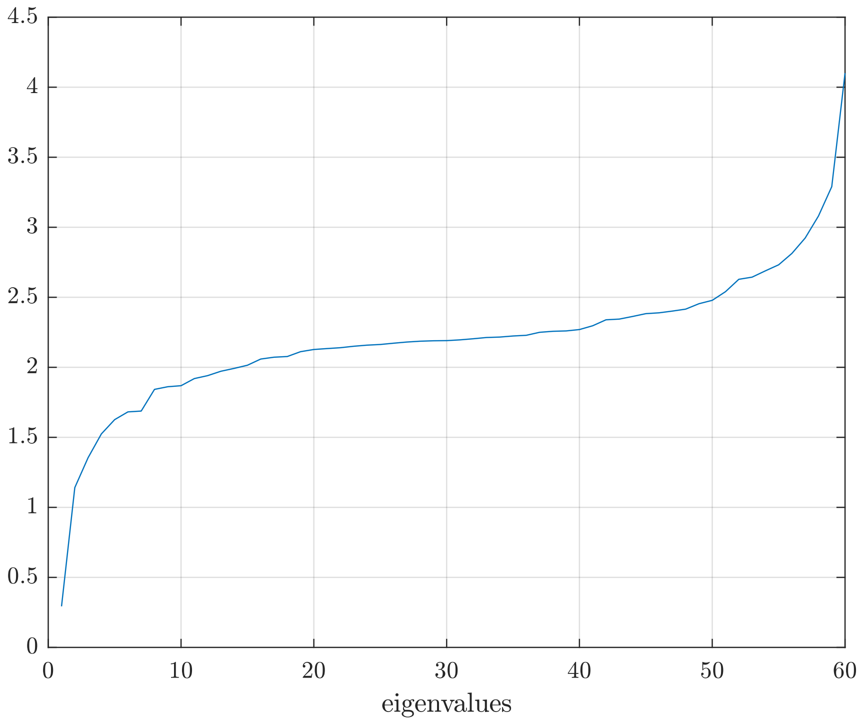

(a) $M = 60$

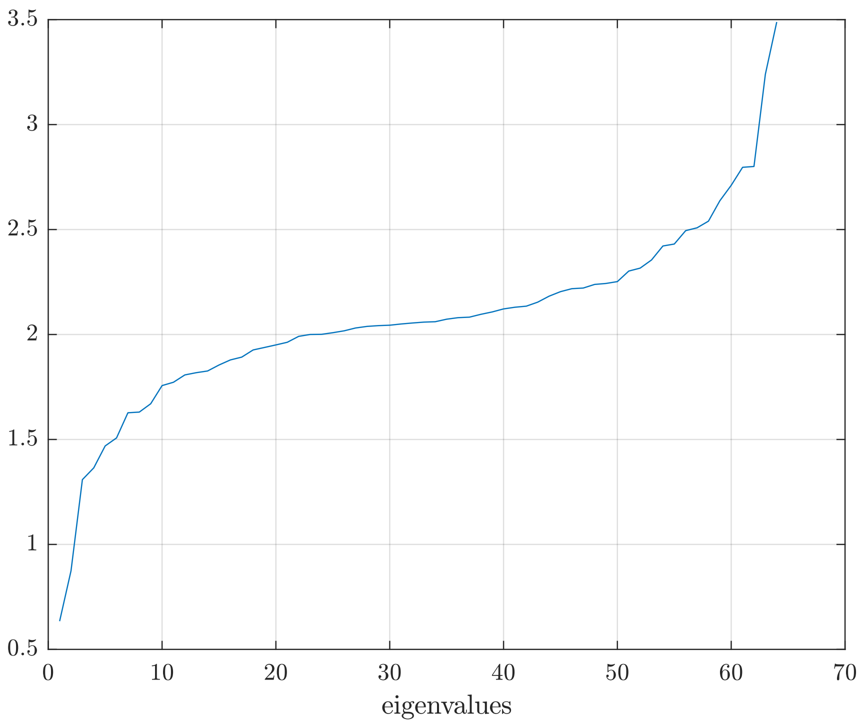

(b) $M = 64$

Figure 3.4: Results of the MUSIC sub-carrier test for $N_c = 64$, all sub-carriers used.

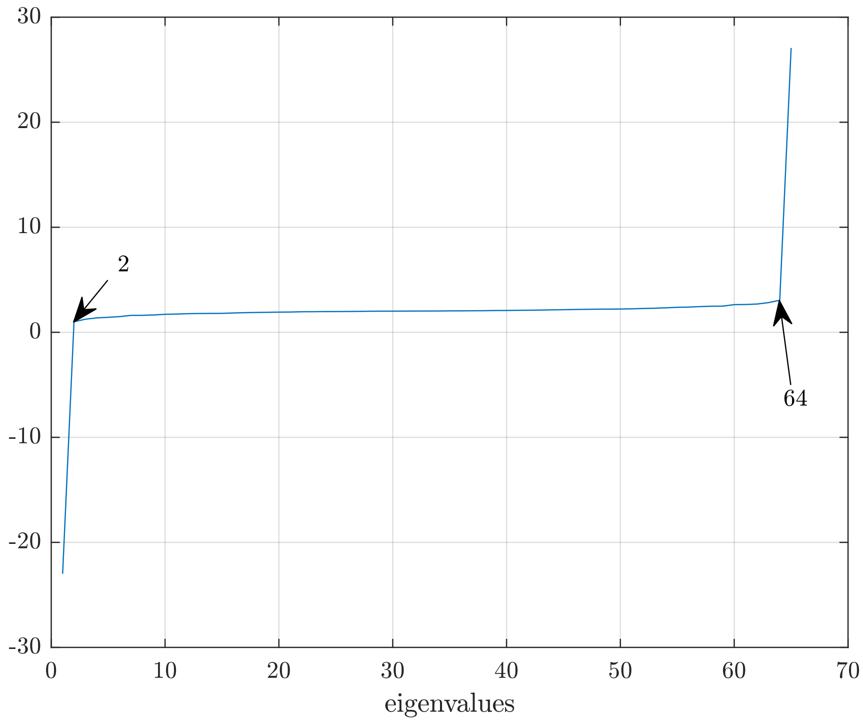

(c) $M = 65$

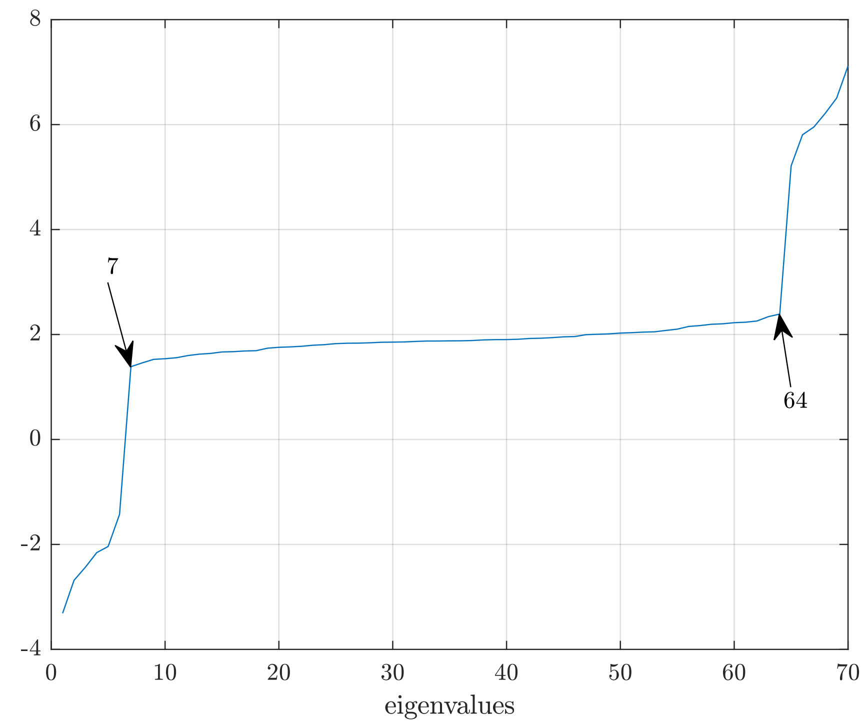

(d) $M = 70$

Figure 3.4: Results of the MUSIC sub-carrier test for $N_c = 64$, all sub-carriers used.

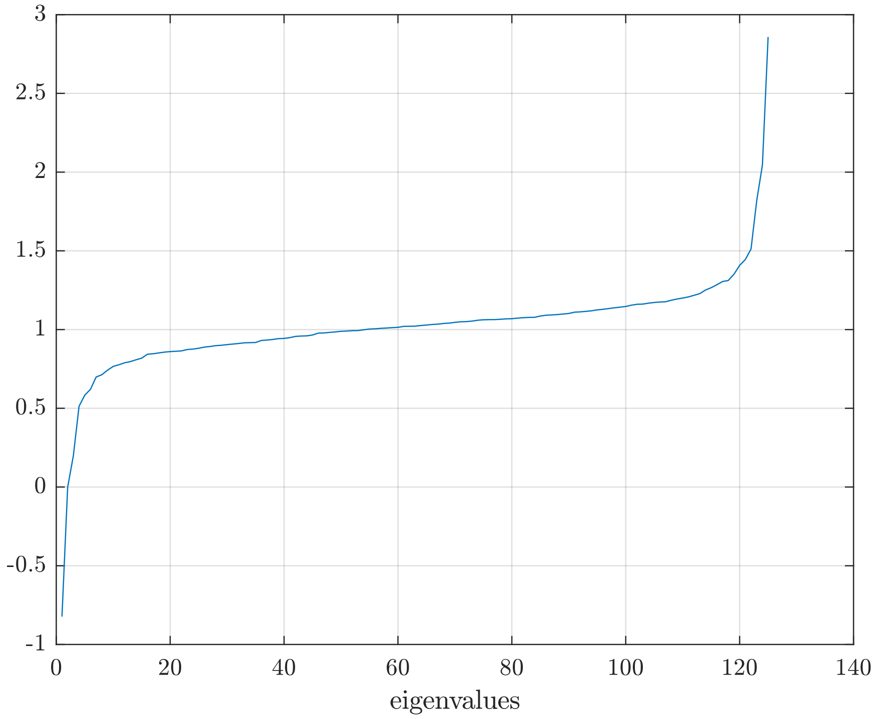

(a) $M = 125$

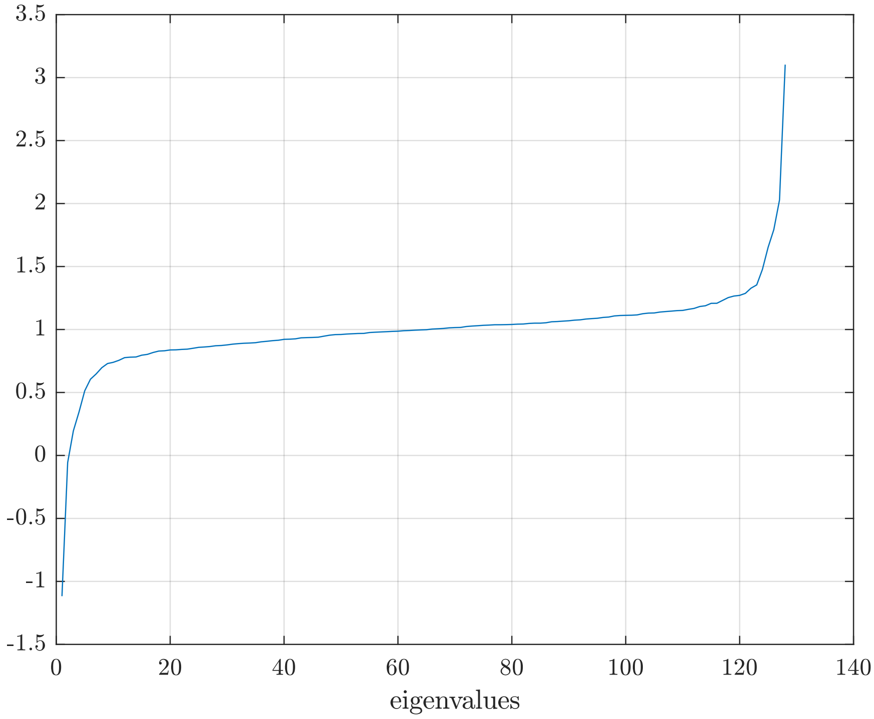

(b) $M = 128$

Figure 3.5: Results of the MUSIC sub-carrier test for $N_c = 128$, all sub-carriers used.

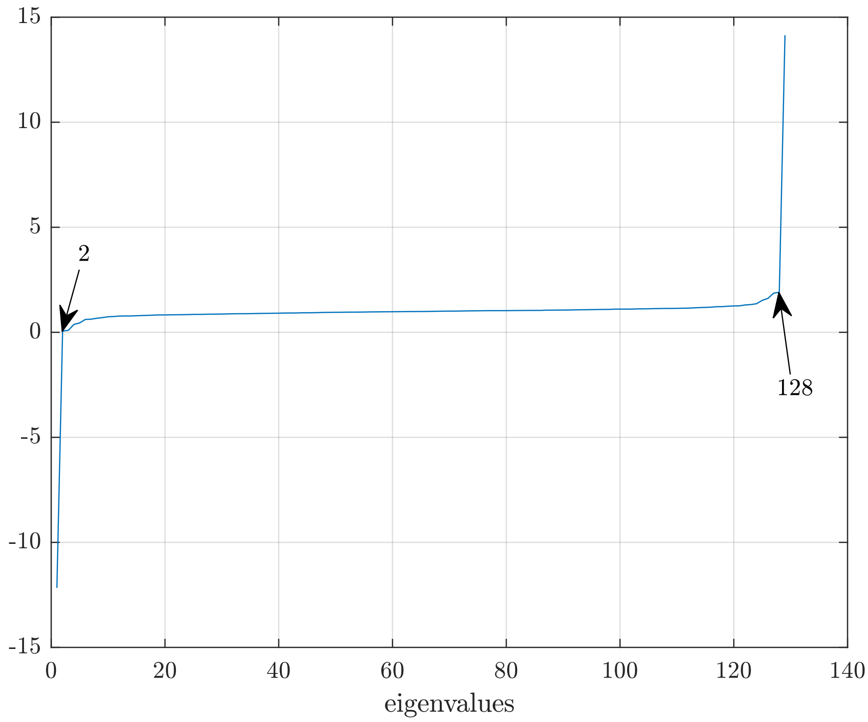

(c) $M = 129$

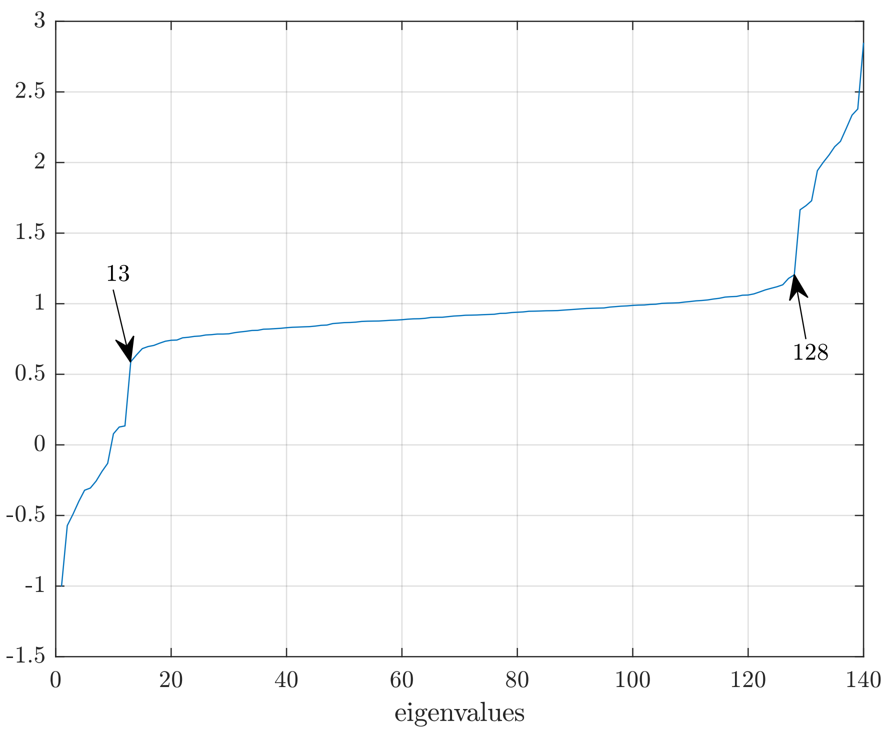

(d) $M = 140$

Figure 3.5: Results of the MUSIC sub-carrier test for $N_c = 128$, all sub-carriers used.

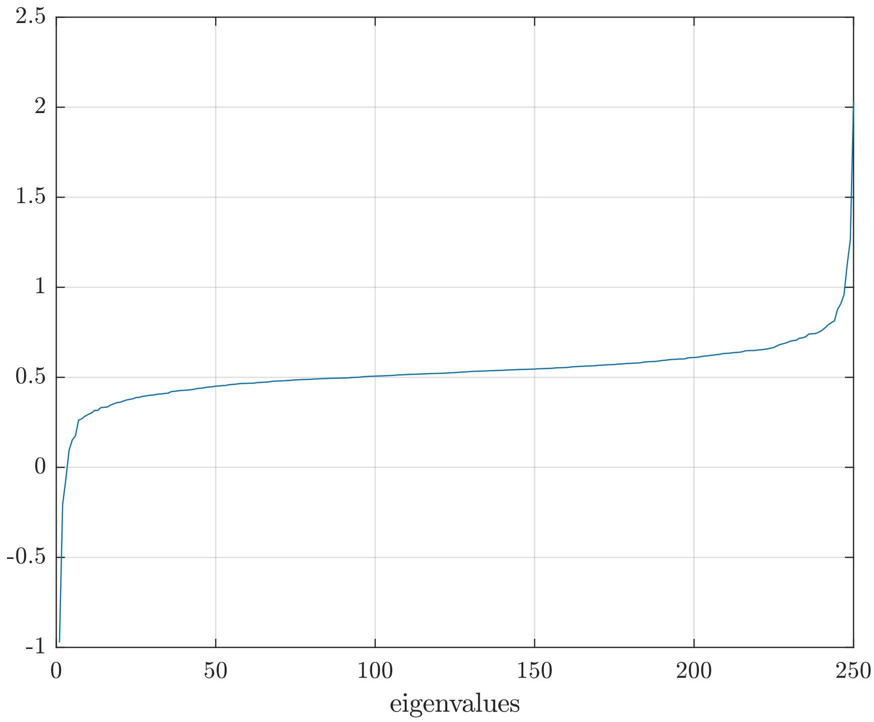

(a) $M = 250$

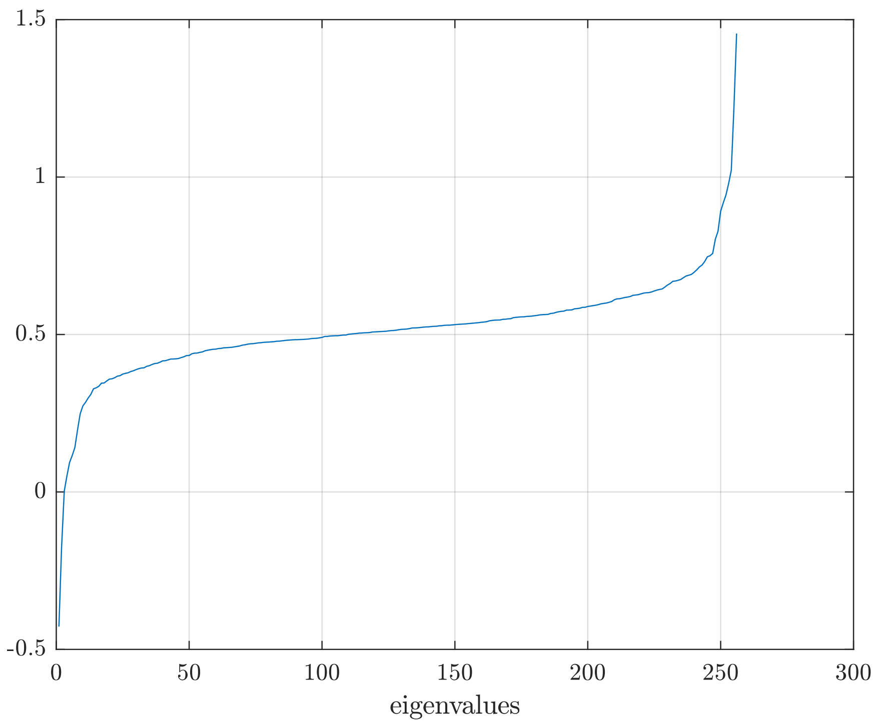

(b) $M = 256$

Figure 3.6: Results of the MUSIC sub-carrier test for $N_c = 256$, all sub-carriers used.

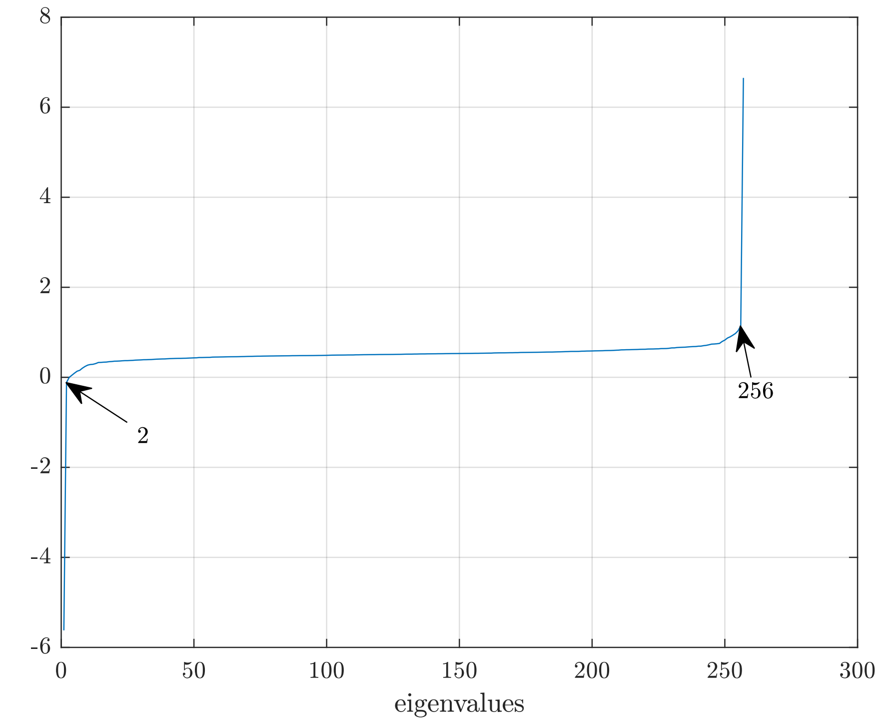

(c) $M = 257$

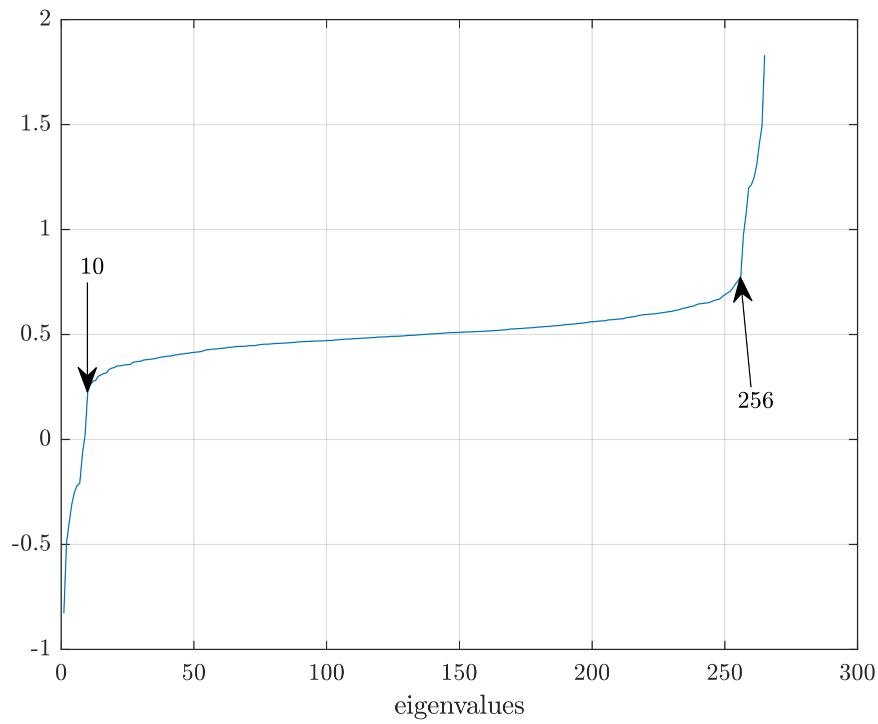

(d) $M = 265$

Figure 3.6: Results of the MUSIC sub-carrier test for $N_c = 256$, all sub-carriers used.

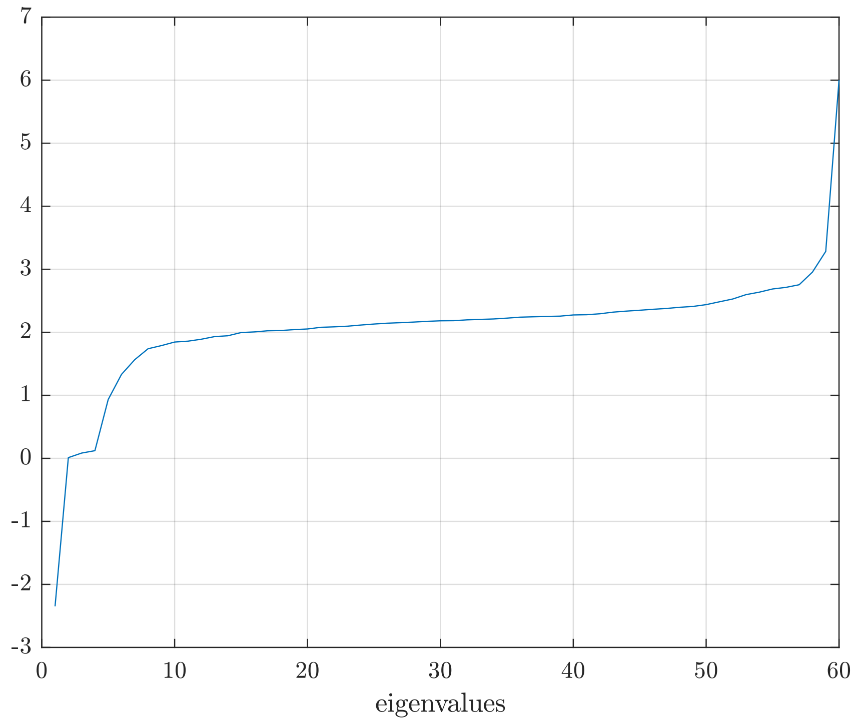

(a) $M = 60$

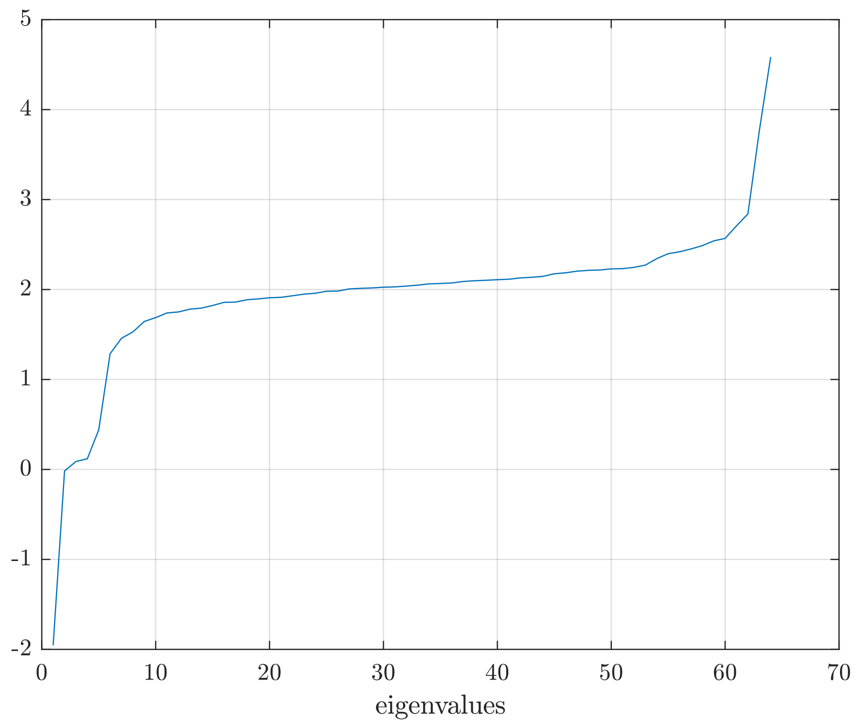

(b) $M = 64$

Figure 3.7: Results of the MUSIC sub-carrier test for $N_c = 64$, $N_g = 4$.

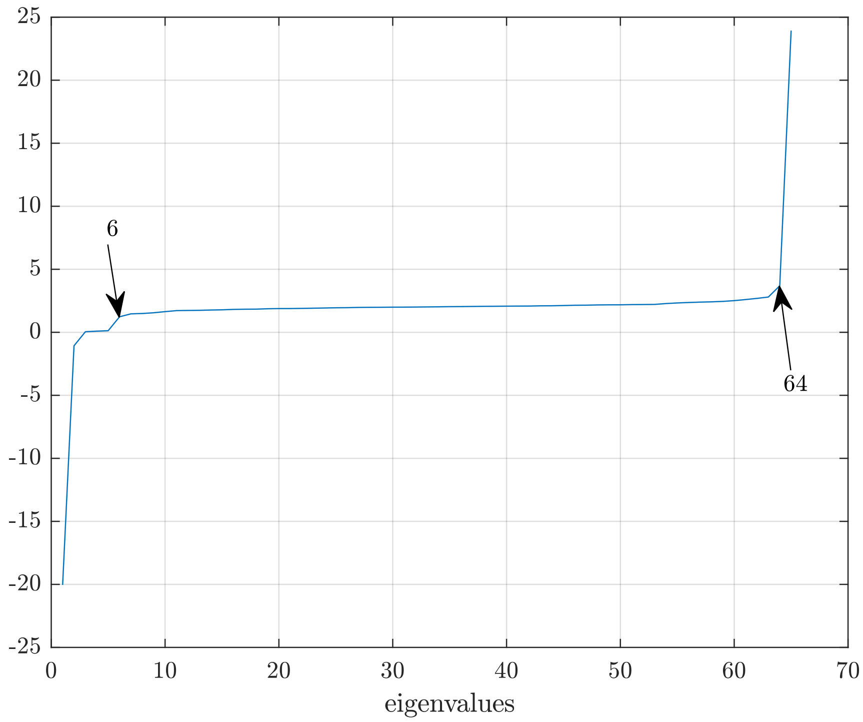

(c) $M = 65$

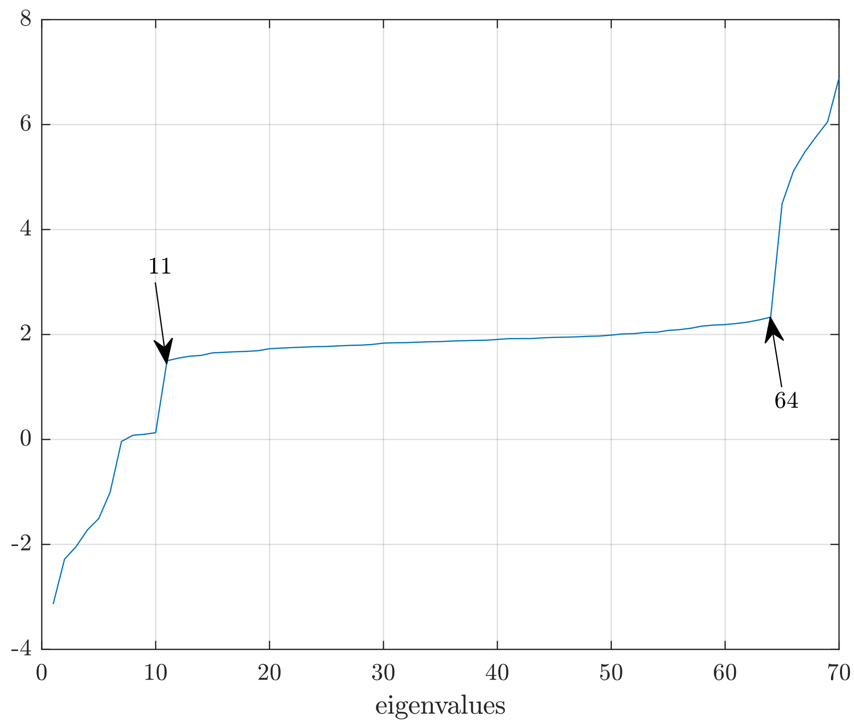

(d) $M = 70$

Figure 3.7: Results of the MUSIC sub-carrier test for $N_c = 64$, $N_g = 4$.

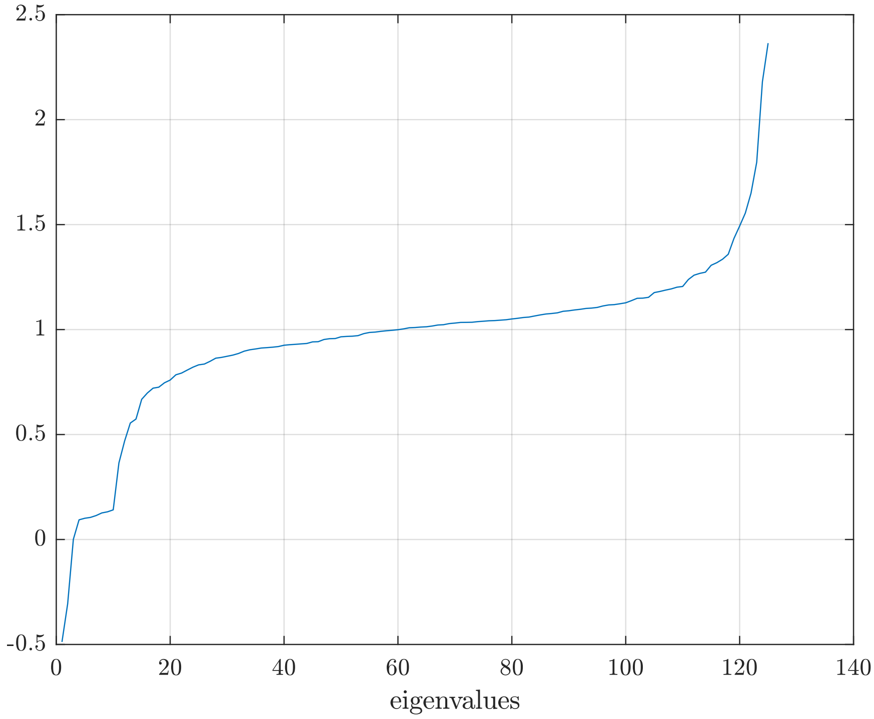

(a) $M = 125$

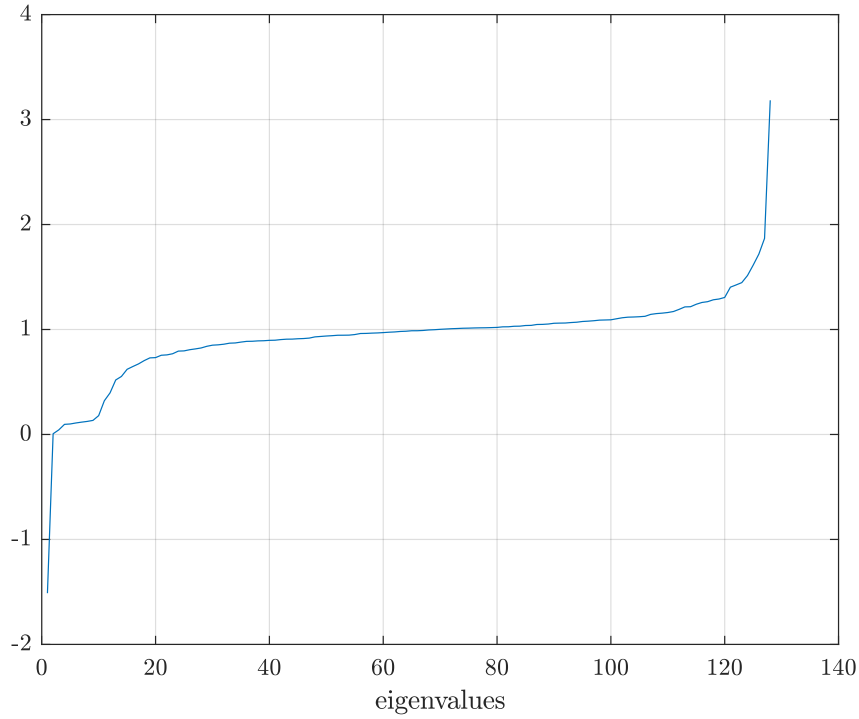

(b) $M = 128$

Figure 3.8: Results of the MUSIC sub-carrier test for $N_c = 128$, $N_g = 8$.

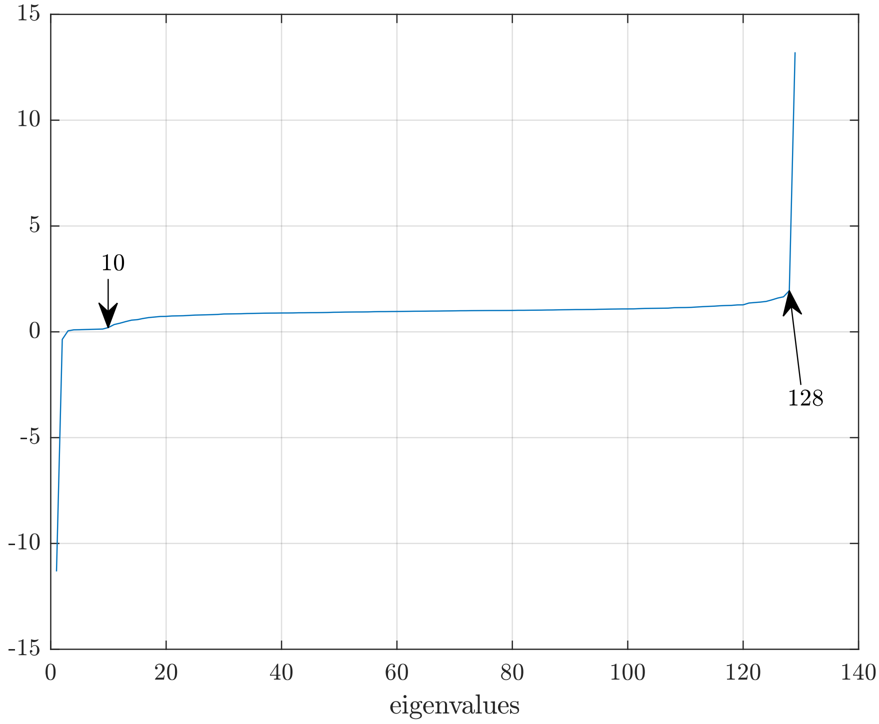

(c) $M = 129$

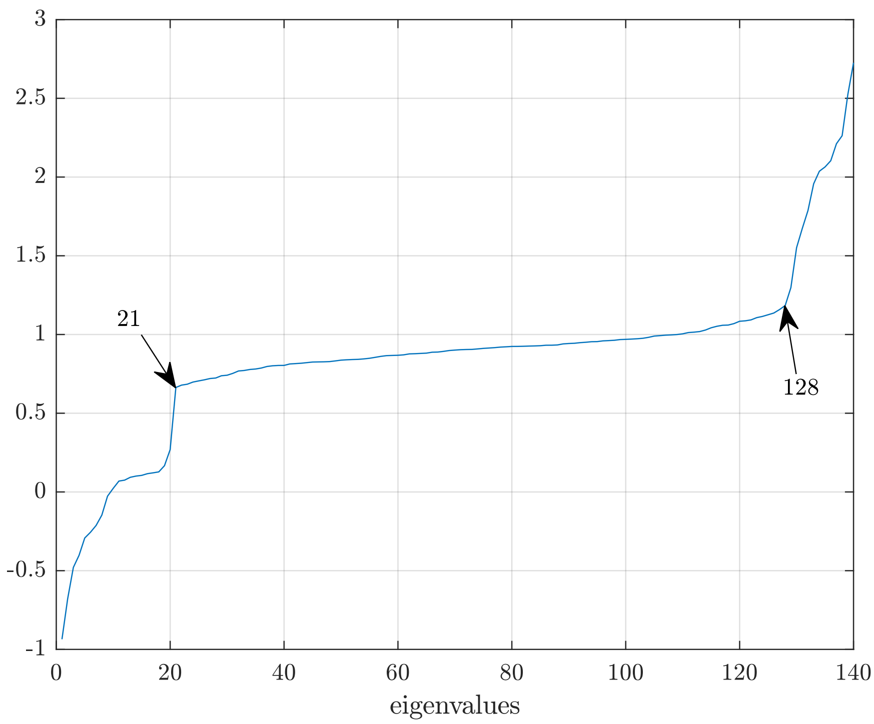

(d) $M = 140$

Figure 3.8: Results of the MUSIC sub-carrier test for $N_c = 128$, $N_g = 8$.

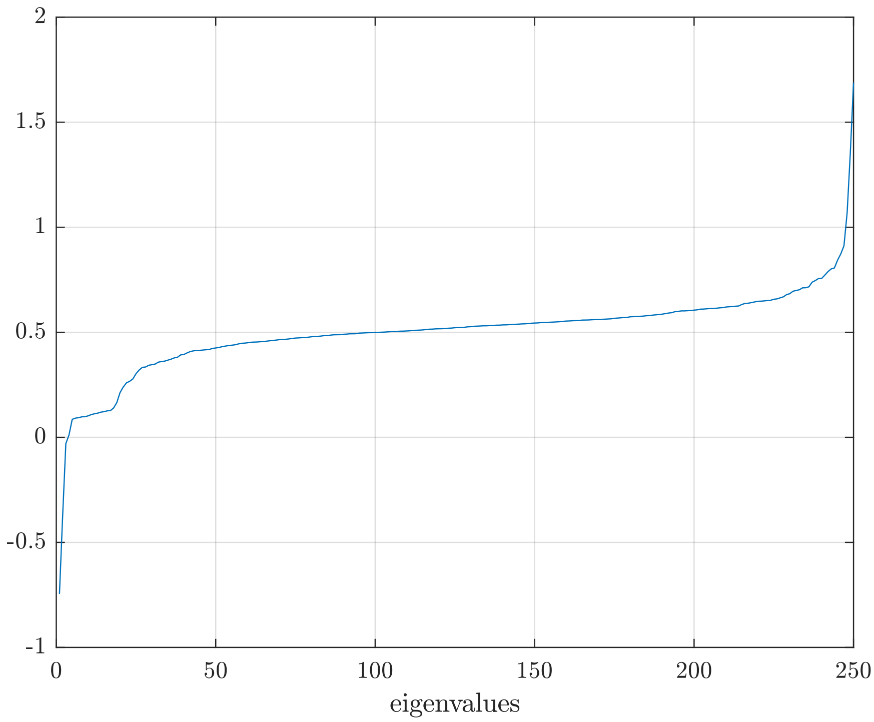

(a) $M = 250$

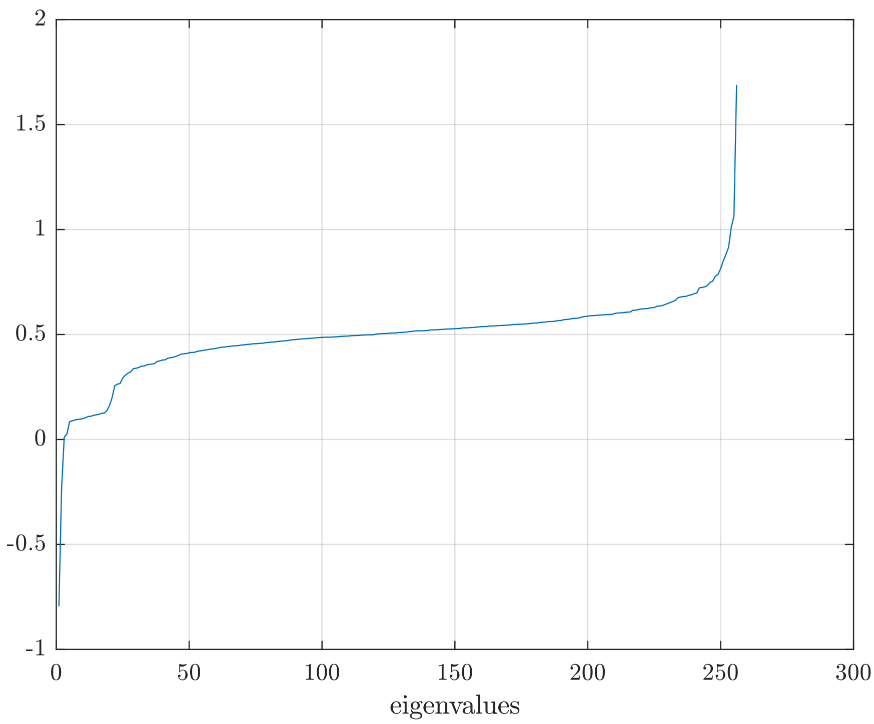

(b) $M = 256$

Figure 3.9: Results of the MUSIC sub-carrier test for $N_c = 256$, $N_g = 16$.

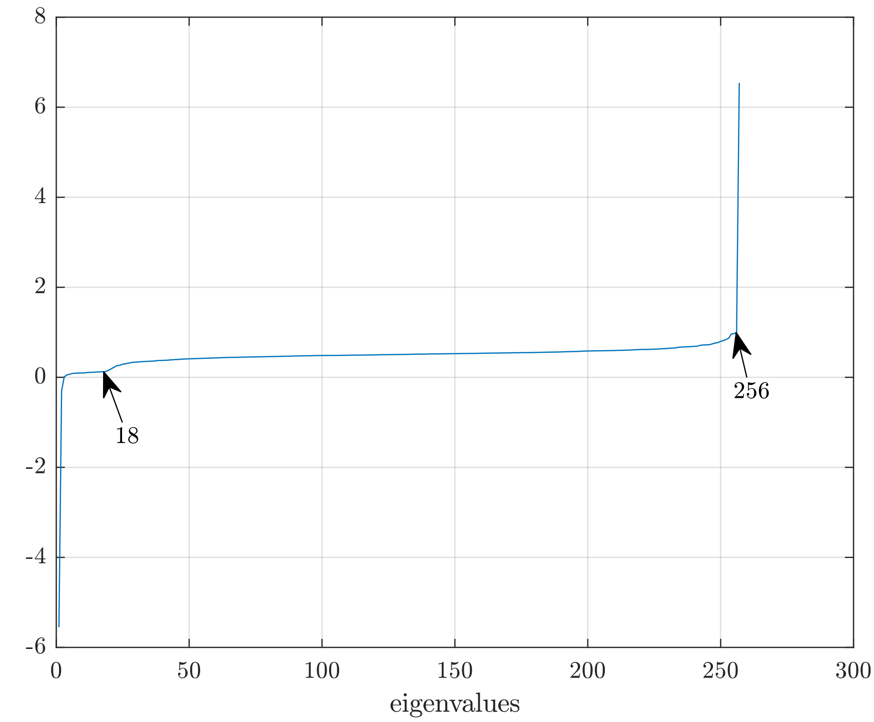

(c) $M = 257$

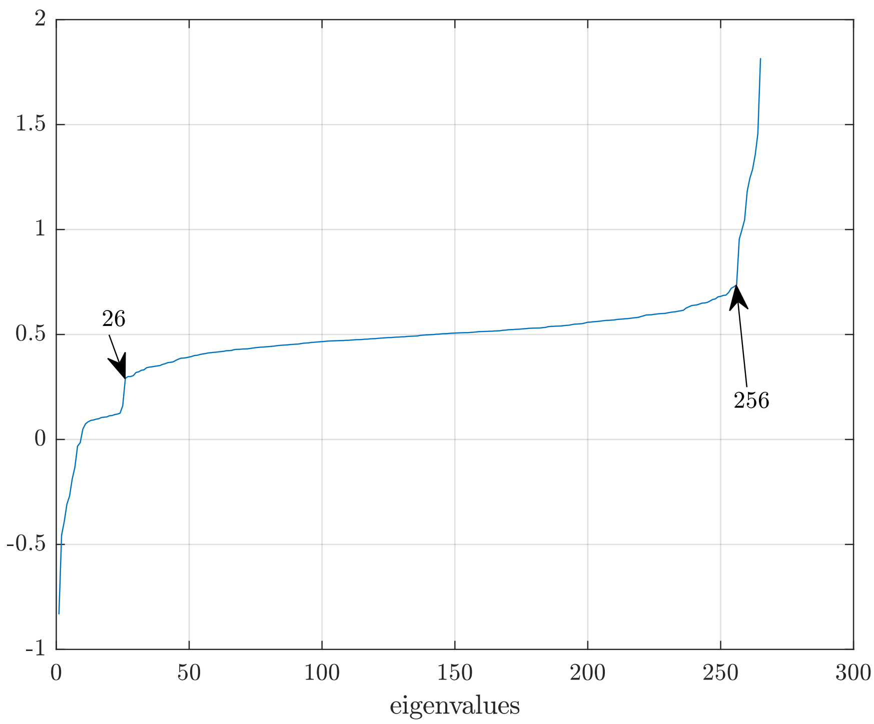

(d) $M = 265$

Figure 3.9: Results of the MUSIC sub-carrier test for $N_c = 256$, $N_g = 16$.

3.4 Number of Sub-carriers Using pMUSIC

3.4.1 Introduction

As the algorithm used in Section 3.3 uses the MUSIC algorithm to compute the answer, an optimisation of the algorithm was developed by the author using the MATLAB® function `pmusic`, which computes the pseudospectrum using the MUSIC algorithm. The test has the same limitation as the original test in that it needs an initial value for the number of sub-carriers before it can determine the number of sub-carriers. As in the original test, this can be solved by iterating over a number of initial values. It does, however, perform significantly faster than the original algorithm.

3.4.2 Experimental Setup

The `pmusic` function as used in this section is a numeric way of calculating the MUSIC algorithm as explained in Section 2.13 with the trade-off that it is less computationally intensive, but produces less accurate results.

The MATLAB® Communications System Toolbox was used to generate an OFDM signal. Tests were performed with different numbers of sub-carriers. In these tests, 100 and 300 OFDM symbols were used. After being sent through an AWGN channel with an SNR of 30 dB, as well as 10 dB, the received signal was tested to see if the number of sub-carriers can be determined.

Listing 3.1 shows the algorithm used in the test. In line 2, the pseudospectrum is calculated using the MUSIC algorithm. In line 3, the peaks of this spectrum are located, which are then counted in line 4.

Due to the iterative nature of the test, the test needs to be repeated over a range of values. This is done with variable `i` and the `for`-loop in lines 1 and 5 of the listing. The test reaches a result when a number of consecutive inputs give the same output.

This consistent output is the number of sub-carriers. This is done by determining the mode and frequency of the modal value of the output in line 6. The modal frequency required for a result is a threshold value that has to be determined experimentally.

Listing 3.1: MATLAB® code for the pMUSIC based algorithm

```
1 for i=1:150
2     [S,w] = pmusic(receivedSignal,i,2048);
3     [pks,locs] = findpeaks(S);
4     carriersdet(i) = length(pks);
5 end
6 [M,F] = mode(carriersdet);
```

3.4.3 Understanding the Results

Figure 3.10 shows an example of the results of the pMUSIC test as done in this section. The test works by comparing an estimated (initial) value to a test result corresponding to an actual value. At a certain point in the test, the test result stabilizes on an actual value over a range of initial values. This is shown in the rectangle in Figure 3.10. This stable test result is the number of sub-carriers (N_c) as determined by the test.

3.4.4 Results and Interpretation

Figure 3.11 shows the results of the test for various values of the number of sub-carriers (N_c) and the number of symbols (N_s). In these tests, the initial value was swept from 1 to 150 while the output of the test was observed. As can be seen in the results, the output stabilises at a value if the input is close to the correct value for the number of sub-carriers. This behaviour can also be used to save time by stopping the test when the output stabilises instead of testing all the values. The accuracy of the test will be quantified in Chapter 4.

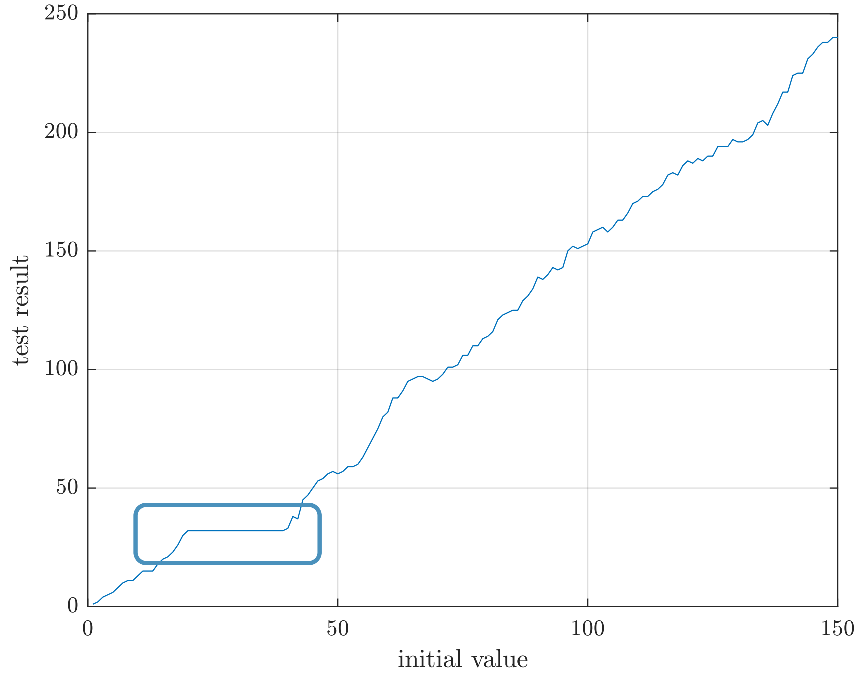

Figure 3.10: Example of the results of the pMUSIC test.

Figure 3.12 shows the results when guard carriers are used. From this, it can be seen that the test does not perform well when guard carriers are used. The output of this test, as seen on the y-axis does not stabilise as in the case where guard carriers are not used.

In some cases, the test determines the number of sub-carriers to be one less than the actual value. The frequency of this occurrence is discussed in Section 4.1. This can be solved by defining a limited solution space, in this case, $N_c \in \{16, 32, 64, 128, 256\}$, and discarding or rounding values outside the solution space.

To successfully detect a higher number of sub-carriers, a higher number of samples are required. This can be seen by comparing Figures 3.11c and 3.11d.

Recall that a single iteration of the MUSIC test took 222 s. By comparison , a single iteration of the pMUSIC test under the same conditions ($N_c = 256, N_s = 200$) took 4 seconds. Therefore, this test performs significantly faster.

3.4.5 Conclusion

This test can be successfully used to determine the number of sub-carriers present in an OFDM signal and requires significantly less time than the MUSIC algorithm implemented in Section 3.3. It does not, however, perform well when all the sub-carriers are not used.

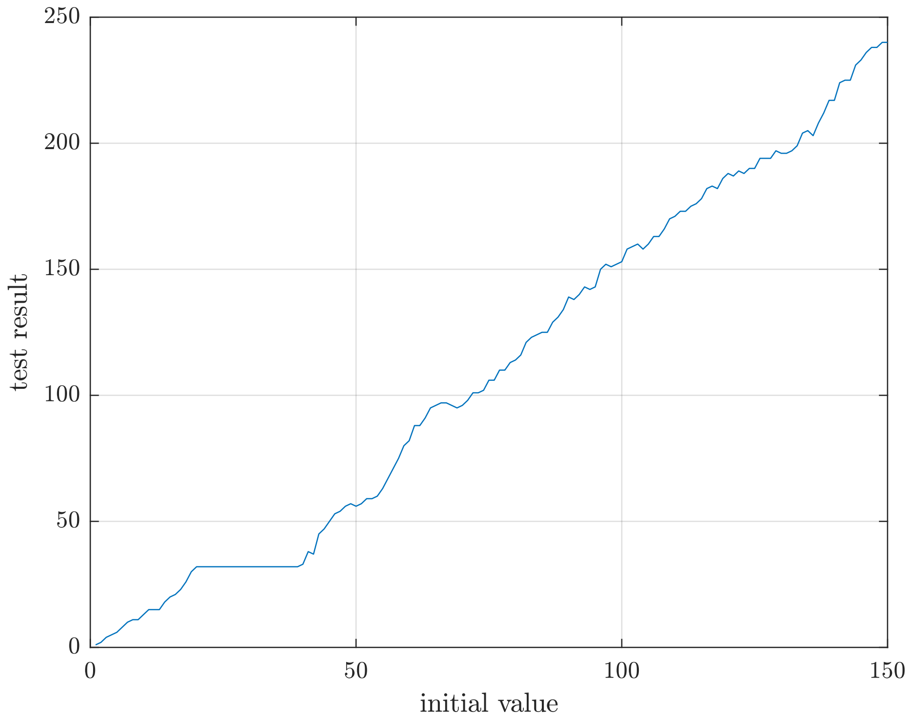

(a) $N_c = 32,\ N_s = 100,\ \text{SNR} = 30\,\text{dB}$

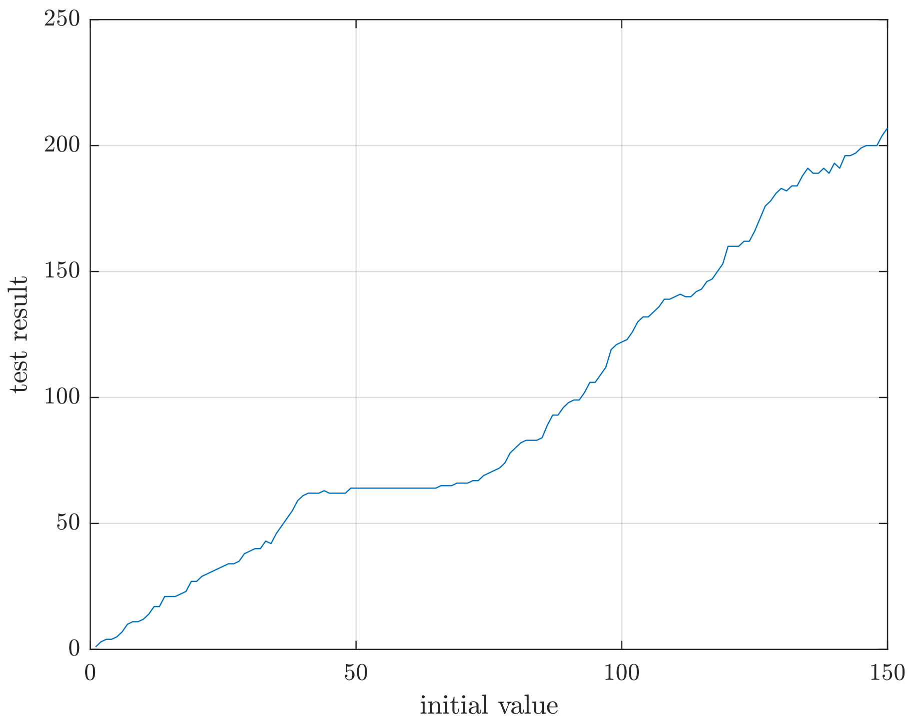

(b) $N_c = 64,\ N_s = 100,\ \text{SNR} = 30\,\text{dB}$

Figure 3.11: Results of the pMUSIC test.

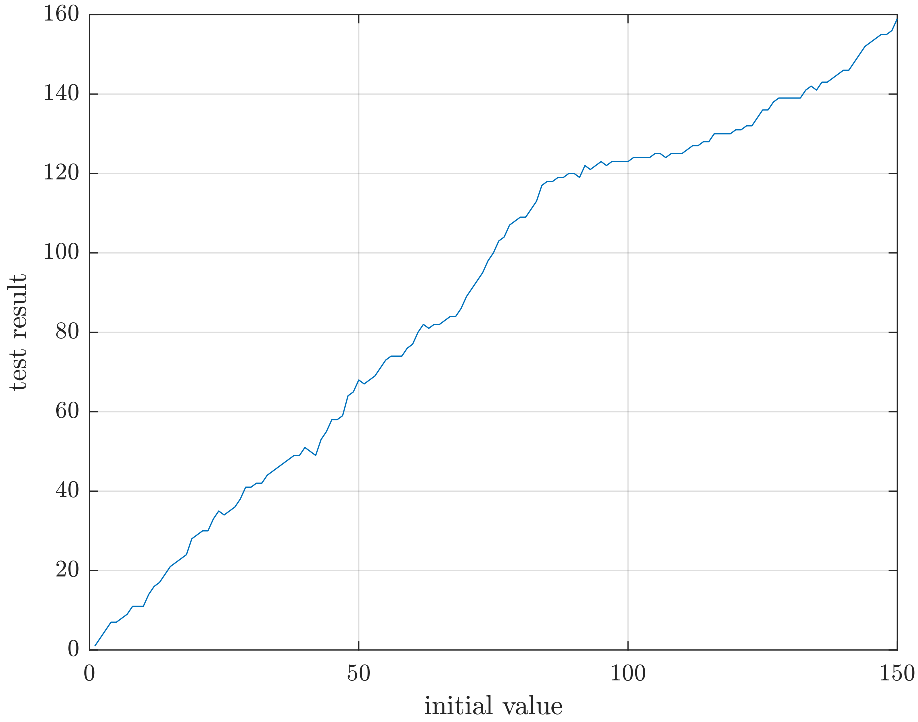

(c) $N_c = 128,\ N_s = 100,\ \text{SNR} = 30\,\text{dB}$

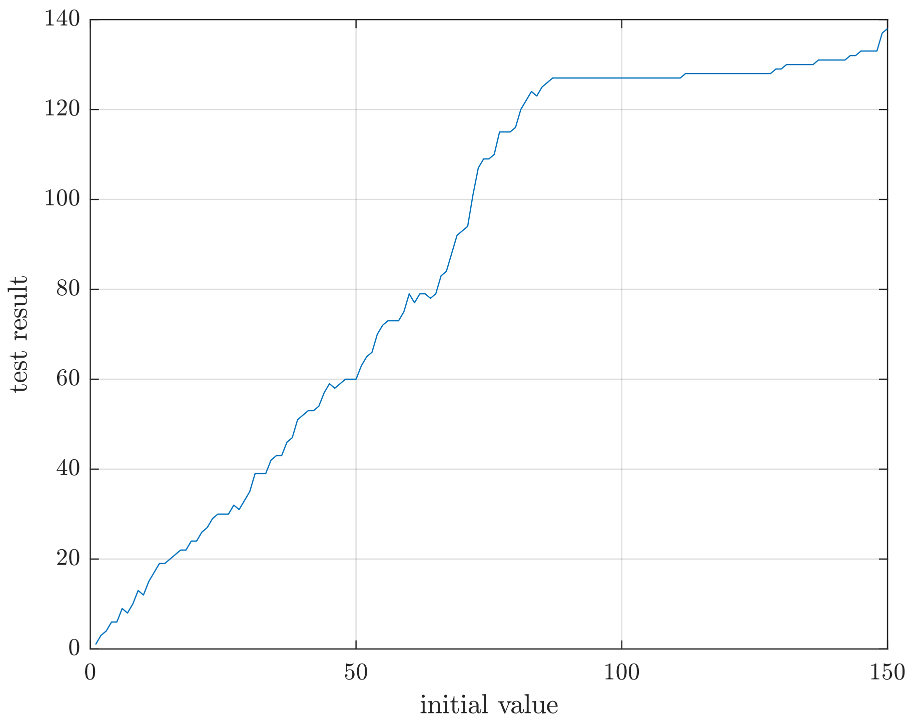

(d) $N_c = 128,\ N_s = 300,\ \text{SNR} = 30\,\text{dB}$

Figure 3.11: Results of the pMUSIC test.

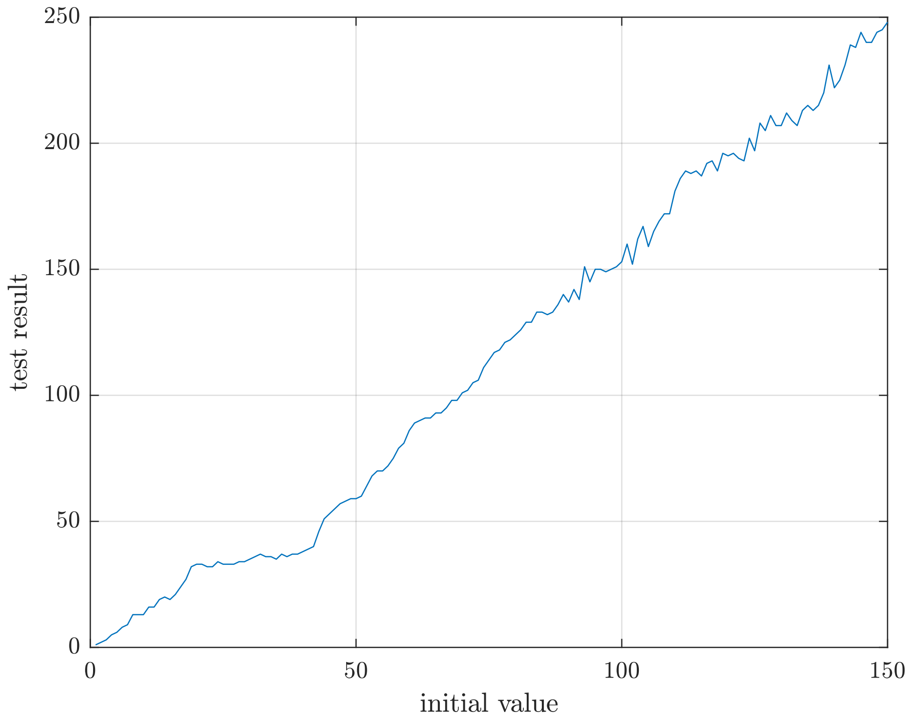

(a) $N_c = 32, \; N_s = 300$

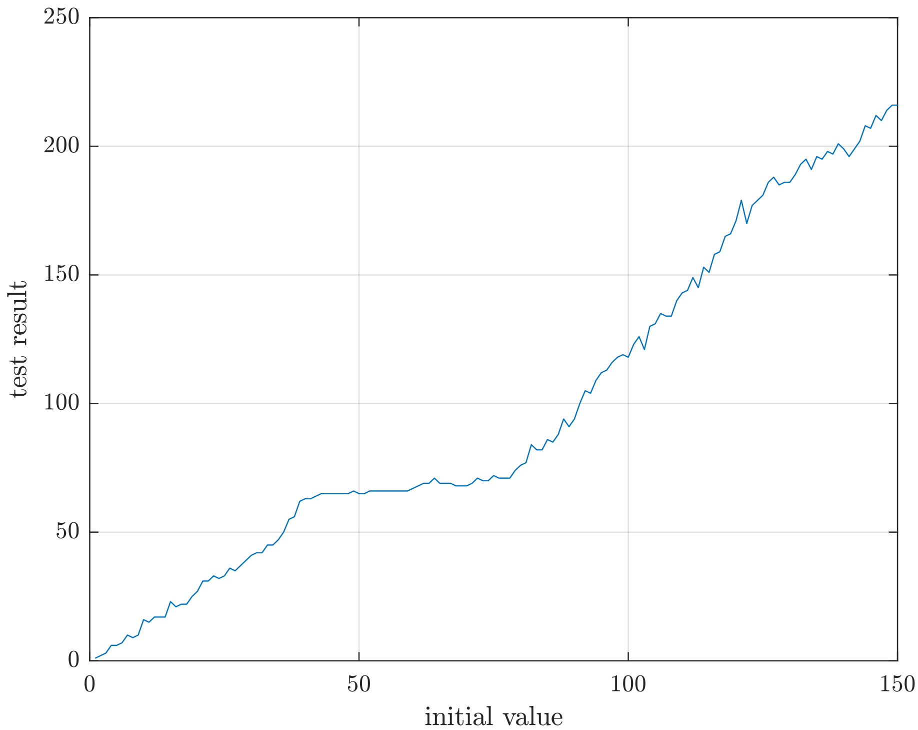

(b) $N_c = 64, \; N_s = 300$

Figure 3.12: Results of the pMUSIC test using guard carriers. SNR $= 30\,\text{dB}, \; N_g = 4$

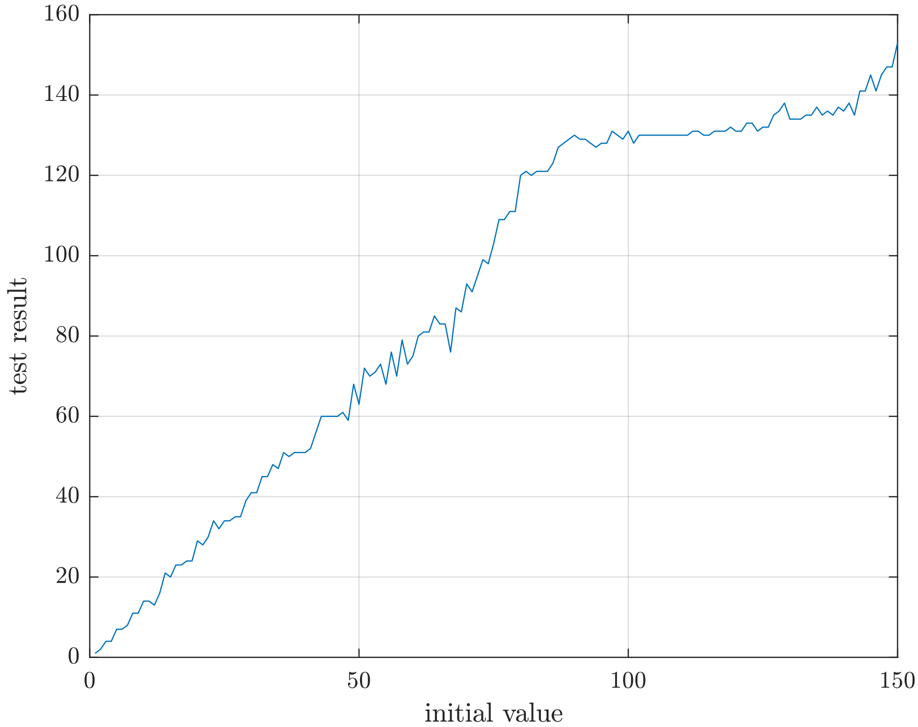

(c) $N_c = 128,\ N_s = 300$

Figure 3.12: Results of the pMUSIC test using guard carriers. SNR $= 30\,\text{dB},\ N_g = 4$

3.5 Sub-carrier Spacing Using pMUSIC

It was also determined that the pMUSIC algorithm used in Section 3.4 could also be used to determine the location of the OFDM sub-carriers. This test was developed by looking at the location of the peaks in the pseudospectrum.

3.5.1 Experimental setup

The experimental setup for this test is the same as for the previous test. The algorithm differs in that it uses the location of the MUSIC peaks instead of the number of peaks.

3.5.2 Results and Conclusion

The results of the test can be seen in Figure 3.13. The spectrum of the signal is shown, and the detected positions of the sub-carriers are indicated by the stars. It can be seen that this test can successfully determine the locations of the sub-carriers.

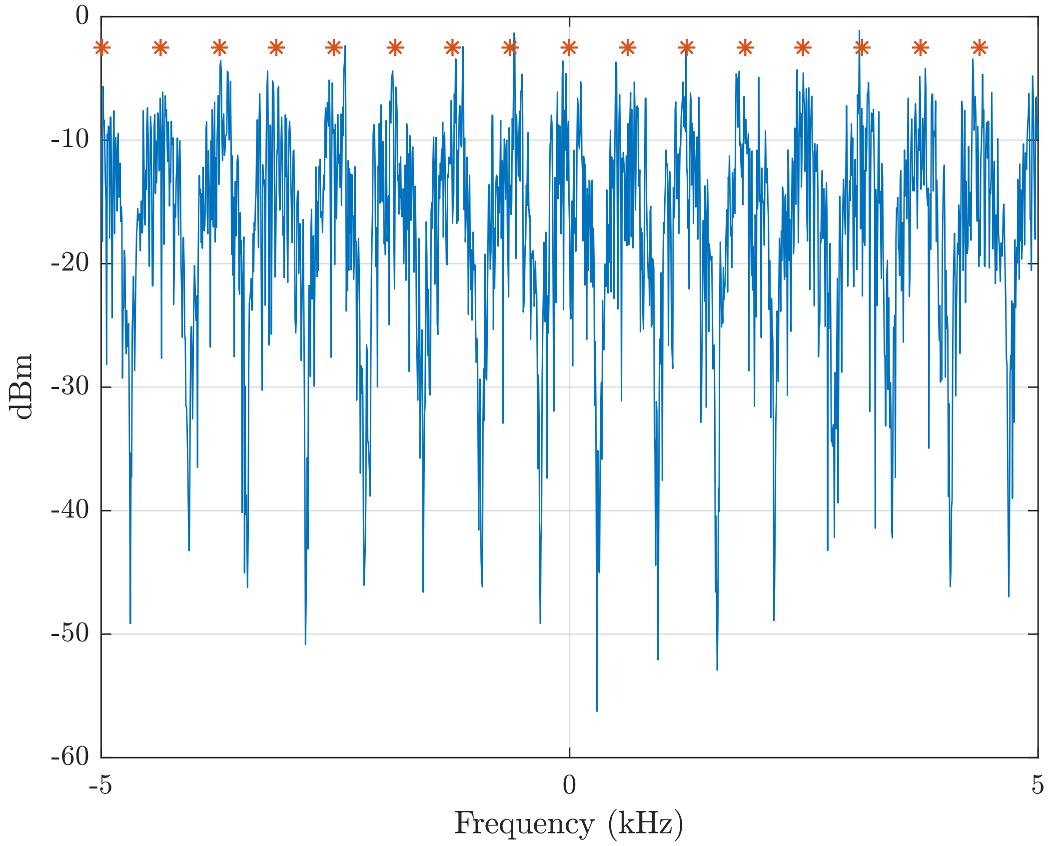

Figure 3.13: Sub-carrier spacing using pMUSIC.

3.6 Using pMUSIC to Determine if OFDM is Present

Because the Giannakis–Tsatsanis test performed in Section 3.2 was not successful, the behaviour of the pMUSIC test as performed in Section 3.4 on signals that are not OFDM was explored to see if this test can be used to determine the presence of OFDM in an SOI. As the non-OFDM signals do not contain any sub-carriers, it can be expected that testing these signals for the number of sub-carriers will yield an inconclusive result; therefore, this test was developed by the author.

3.6.1 Experimental Setup

The experimental setup for this section is the same as in Section 3.2, but the pMUSIC test was applied to the signals instead of the Giannakis–Tsatsanis test. This test was additionally performed on 16-FSK and 32-FSK signals as well.

The test that was developed works as follows. The modal frequency is compared to a threshold value. If the modal frequency is above the threshold, the signal is determined to be OFDM, but if the modal frequency is below or equal to the threshold, the signal is determined not to be OFDM. The threshold value is to be determined experimentally.

3.6.2 Determining the Modal Frequency Threshold

Determining the value to be used for the modal frequency is a trade-off between type I and type II errors, where a type I error would be saying that a signal is not OFDM when it is OFDM (false positive), and a type II error would be saying that a signal is OFDM when it is not OFDM (false negative) [62].

Table 3.3 shows the percentage of times a signal was identified as OFDM for different modal frequencies from 1 to 15. This was done in a 30 dB AWGN channel. Table 3.4 and Figure 3.14 shows the percentage of each error type in these results. From this it can be seen that the least errors are made when using a modal frequency threshold of 7; therefore, this will be used in the remainder of this experiment.

Table 3.3 also shows the true positive rate (TPR) and false positive rate (FPR) of each modal frequency which is then used to graph the receiver operating characteristic (ROC) curve as shown in Figure 3.15. An ROC curve is a visual way of showing the

Table 3.3: Percentage of signals identified as OFDM using a specific modal frequency.

modal frequency	1	2	3	4	5	6	7	8
FSK	100	100	99	78	45	21	12	7
8-FSK	100	100	100	85	45	18	5	2
GMSK	100	100	96	60	18	12	4	1
BPSK	100	100	100	85	42	13	3	1
QPSK	100	100	95	49	15	1	1	0
8-PSK	100	100	97	46	15	4	0	0
16-PSK	100	100	92	55	21	6	1	1
16-QAM	100	100	90	44	17	4	1	0
32-QAM	100	100	93	49	13	4	2	0
64-QAM	100	100	93	45	21	3	1	1
128-QAM	100	100	98	52	12	0	0	0
256-QAM	100	100	95	45	13	2	1	0
32-OFDM	100	100	100	100	100	100	100	100
64-OFDM	100	100	100	100	100	100	100	100
128-OFDM	100	100	100	100	100	99	97	89
modal frequency	9	10	11	12	13	14	15	
FSK	3	1	1	0	0	0	0	
8-FSK	1	0	0	0	0	0	0	
GMSK	0	0	0	0	0	0	0	
BPSK	0	0	0	0	0	0	0	
QPSK	0	0	0	0	0	0	0	
8-PSK	0	0	0	0	0	0	0	
16-PSK	0	0	0	0	0	0	0	
16-QAM	0	0	0	0	0	0	0	
32-QAM	0	0	0	0	0	0	0	
64-QAM	0	0	0	0	0	0	0	
128-QAM	0	0	0	0	0	0	0	
256-QAM	0	0	0	0	0	0	0	
32-OFDM	99	97	91	87	83	77	69	
64-OFDM	100	100	100	100	100	100	100	
128-OFDM	76	65	58	49	38	34	22	

accuracy of a binary classifier [63]. An ideal classifier would have an ROC curve that passes through the point (0,1) [63]. This ROC is near to the ideal case, showing that the classifier has a high accuracy. This accuracy is quantified later in Table 3.6.

Table 3.4: Percentage of errors using a specific modal frequency.

modal frequency	type I	type II	combined	TPR	FPR
1	0	100	50	0	0
2	0	100	50	0	0
3	0	95.7	47.8	0.04	0
4	0	57.8	28.9	0.42	0
5	0	23.1	11.5	0.77	0
6	0.3	7.3	3.8	0.93	0
7	1.0	2.6	1.8	0.97	0.01
8	3.7	1.1	2.4	0.99	0.04
9	8.3	0.3	4.3	1	0.08
10	12.7	0.1	6.4	1	0.13
11	17.0	0.1	8.5	1	0.17
12	21.3	0	10.7	1	0.21
13	26.3	0	13.2	1	0.26
14	29.7	0	14.8	1	0.30
15	36.3	0	18.2	1	0.36

3.6.3 Understanding the Results

The results of this test are presented and interpreted in the same way as the test done in Section 3.2.

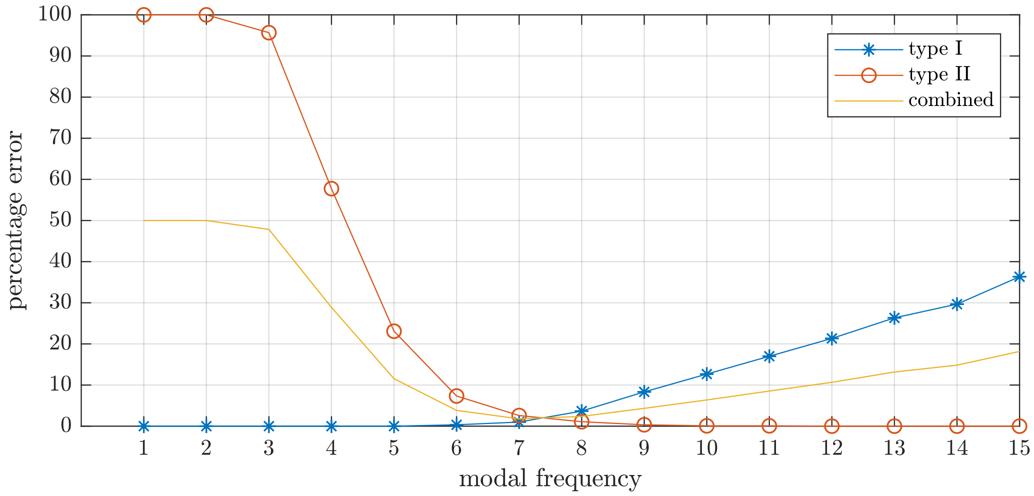

Figure 3.14: Percentage of errors using a specific modal frequency.

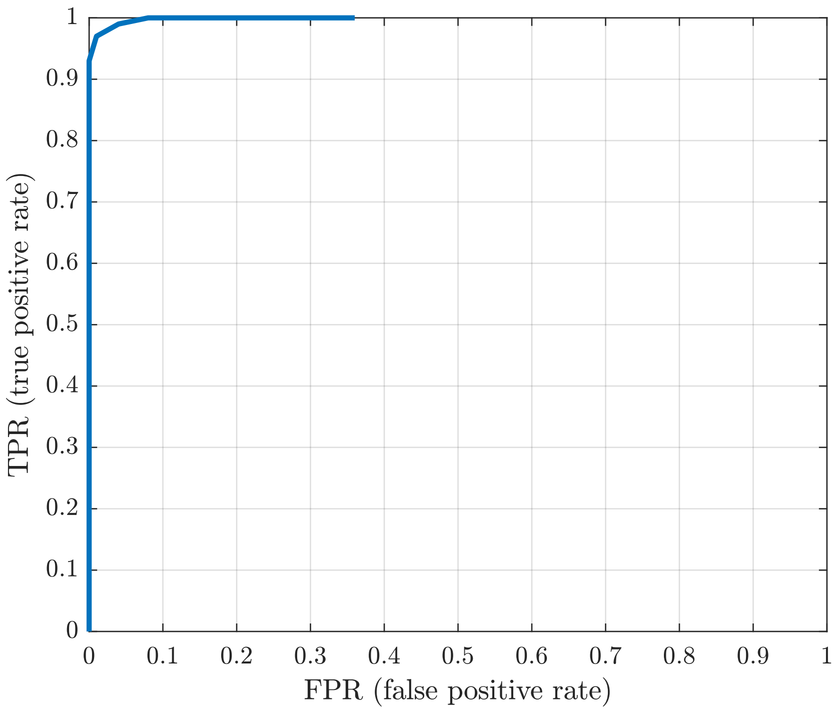

Figure 3.15: Receiver operating characteristic (ROC) of the pMUSIC test.

3.6.4 Results and Conclusion

The results of 100 iterations of this test on various different modulation schemes are shown in Figure 3.16 and Table 3.5. It was determined that a threshold modal frequency of 7 could be used to distinguish OFDM signals from non-OFDM signals in a 30 dB SNR AWGN channel. This can also be seen in Figure 3.16a where there is a clear horizontal separation between the OFDM and non-OFDM signals. However, the test does not perform well in a 10 dB environment. It can be seen in Figure 3.16b that there is practically no horizontal separation between the OFDM and non-OFDM signals.

One shortcoming of this test is because it is iterative, an inconclusive result does not guarantee the absence of an OFDM signal as it can also mean that an OFDM signal is present that contains more sub-carriers that the maximum value of the iteration. This can be solved by limiting the solution space to OFDM signals where $N_c \in \{1, \ldots, n\}$. In this case, $n = 150$.

Table 3.6 shows the accuracy of this test for the case where the threshold of the modal frequency is set to 7 and in a 30 dB AWGN channel. This value was chosen in Section 3.6.2. In comparing Table 3.6 to Table 3.2, it can be seen that the pMUSIC based test can distinguish OFDM from amongst more modulation schemes than the Giannakis–Tsatsanis test can. This increased versatility comes at a significant cost, namely computational complexity. The run-time for all of the tests in Table 3.6 (100 iterations for each modulation scheme, a total of 1500 iterations) was approximately 3 hours while the run-time for the tests in Table 3.2 is 8 seconds (using an Intel i7-7700). It can be argued that this trade-off is worth it considering the increase in versatility, but it will need to be evaluated for the scenario in which the test is used.

Therefore, this test can be successfully used to determine the presence or absence of an OFDM signal within a predefined scope.

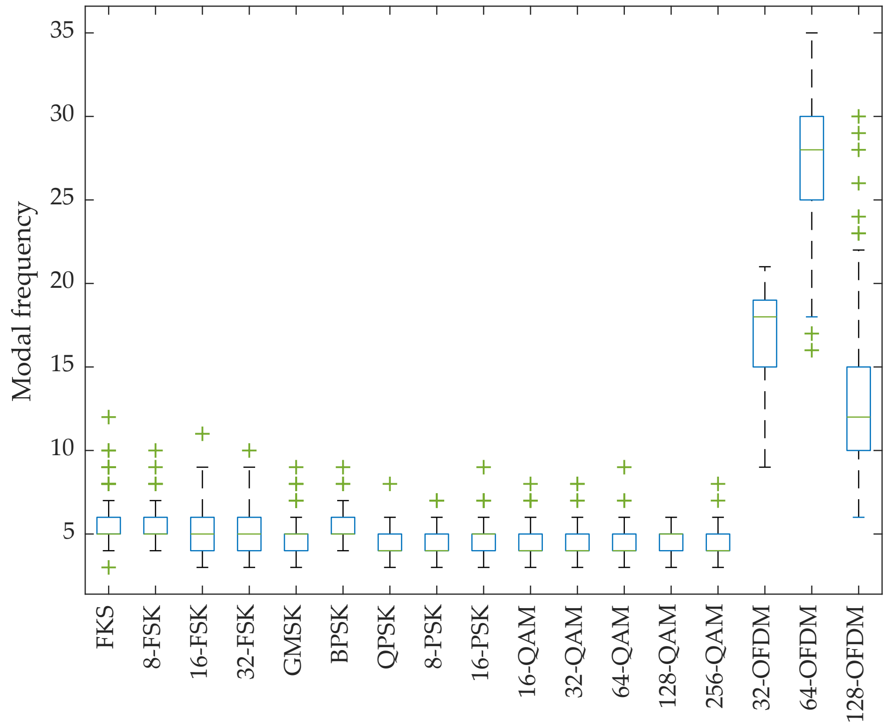

(a) 30 dB SNR AGWN channel.

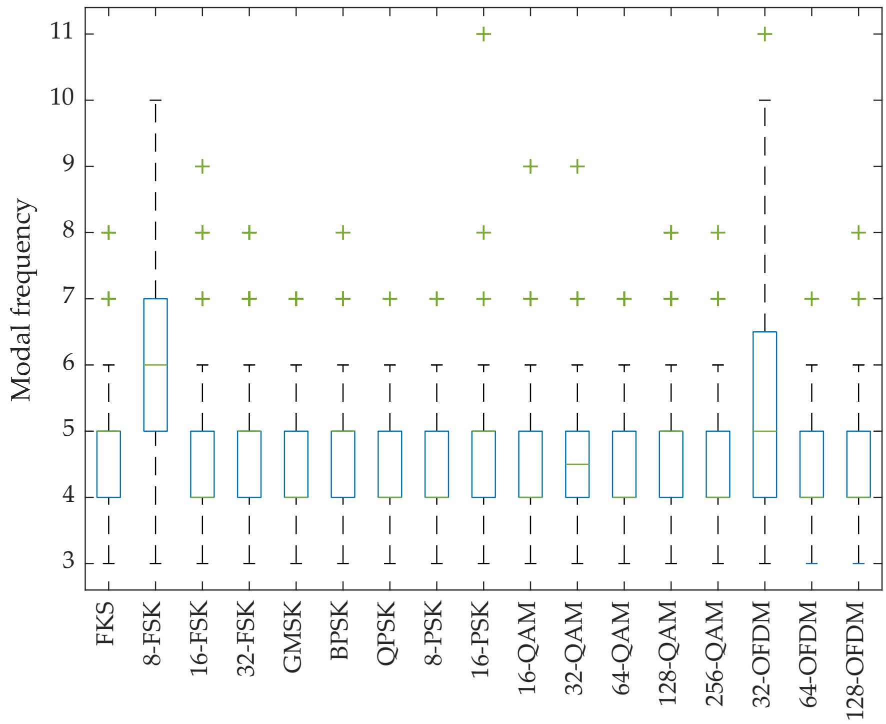

(b) 10 dB SNR AGWN channel.

Figure 3.16: Box plots for the results of 100 pMUSIC tests on various different modulation types.

3.7 Conclusion

In this chapter, several methods for blindly determining the parameters of an OFDM signal were explored and evaluated. It was determined that the Giannakis–Tsatsanis test cannot be used to distinguish OFDM signals from several other modulation techniques. A MUSIC algorithm based test to determine the number of sub-carriers present in an OFDM signal was also evaluated. A shortcoming of this test, namely that it is computationally intensive, was addressed by improving the test to use the MATLAB® `pmusic` function. This greatly reduced the computational complexity of the test. Finally, it was determined that this pMUSIC algorithm could also be used to determine the presence of OFDM, thereby addressing a shortcoming of existing methods by developing a suitable method.

Table 3.5: Results of the pMUSIC test to determine the presence of OFDM.

	average modal frequency	
Modulation	AWGN 10 dB	AWGN 30 dB
FSK	4.8	5.7
8-FSK	5.9	5.6
16-FSK	4.6	5.5
32-FSK	4.9	5.4
GMSK	4.6	4.9
BPSK	4.9	5.4
QPSK	4.5	4.6
8-PSK	4.5	4.6
16-PSK	4.7	4.8
16-QAM	4.4	4.6
32-QAM	4.7	4.6
64-QAM	4.6	4.6
128-QAM	4.8	4.6
256-QAM	4.5	4.6
32-OFDM	5.5	16.9
64-OFDM	4.2	27.7
128-OFDM	4.3	13.5

Table 3.6: Accuracy of the pMUSIC test to determine the presence of OFDM.

	% results	
Modulation	OFDM	not OFDM
FSK	12	88
8-FSK	5	95
16-FSK	8	92
32-FSK	11	89
GMSK	4	96
BPSK	3	97
QPSK	1	99
8-PSK	–	100
16-PSK	1	99
16-QAM	1	99
32-QAM	2	98
64-QAM	1	99
128-QAM	–	100
256-QAM	1	99
32-OFDM	100	–
64-OFDM	100	–
128-OFDM	97	3

Chapter 4

Experiments in Various Channels

In this chapter, the pMUSIC test of the previous chapter will be further explored by examining the effects of different test conditions and different channels on the accuracy of the test. The reason for focusing on the pMUSIC test and not the other tests is that the pMUSIC test has been developed in this study, while the others are existing tests. The first thing that will be examined is the effect that both the inner modulation of the OFDM signal and the effect of the number of OFDM samples being tested have on the accuracy of the test. Next, the effects of different channels will be considered. The test will be repeated in AWGN channels with different SNRs, as well as in different TDL channel models.

4.1 Experiments in an Ideal Channel

The purpose of this section is to determine the effect of different inner modulations, as well as the number of OFDM symbols being tested (N_s), on the accuracy of the pMUSIC test.

4.1.1 Experimental Setup

The test performed in Section 3.4 were repeated under different conditions to examine the performance of this test in these conditions. The tests were performed in an ideal channel because it is not the effect of the channel that is being considered here, but rather other test parameters. The test looked at the effects of different inner modulations and the number of OFDM samples being tested. For the inner modulations, QPSK, 16-QAM and 64-QAM were considered. This is because these are common inner modulations for OFDM signals as discussed in Section 2.9. For this experiment, $N_s \in \{50, 100, 200\}$ and $N_c \in \{16, 32, 64, 128\}$. The tests were repeated 100 times for each combination of these conditions.

4.1.2 Results and Conclusion

Table 4.1 shows the results of each of the different combinations of inner modulation, number of symbols, and the number of sub-carriers. The left side of the table shows the inner modulation of the OFDM signal, the number of symbols used in the test and the number of sub-carriers in the OFDM signal. The right side of the table shows the percentage of times that the test result was in each of the categories, where these categories are:

1. Less than the actual number of sub-carriers minus one.
2. Equal to the actual number of sub-carriers minus one.
3. Equal to the actual number of sub-carriers.
4. Equal to the actual number of sub-carriers plus one.
5. Greater than the actual number of sub-carriers plus one.

The results are also summarised per parameter in Table 4.2. This summary is visualised in Figures 4.1 to 4.3. These figures show histograms of the result of the test, where in each case one of the test parameters were varied. In Figure 4.1, the inner modulation is varied, in Figure 4.2, N_s is varied, and in Figure 4.3, N_c is varied.

As mentioned in Section 3.4.4 and as can be seen in the results of the test, off-by-one errors are fairly common for this test, especially $N_c - 1$ errors. This is due to the pseudo nature of the algorithm. This problem can be solved by limiting the solution space, for example, in this case, $N_c \in \{16, 32, 64, 128\}$. The last column in Table 4.2 shows the results if off-by-one errors are calculated as correct. These results can lead to insights that are not as easily seen from the other results.

From these results, we can see that the inner modulation of the OFDM signal does not have a significant impact on the accuracy of the tests. The inner modulation will, therefore not be evaluated again in future tests.

It can also be seen that the accuracy of the test increases as the number of samples being tested increases. This is especially clear in the case of $N_c \pm 1$ in Table 4.2. It should also be noted that this only holds up to a certain point. The number of samples cannot be increased indefinitely to increase accuracy. Looking at $N_c = 16$ and $N_c = 32$ it can be seen that an increase has no significant effect, but the effect becomes significant as the number of sub-carriers increase.

Finally, it can be seen that the accuracy decreases as the number of sub-carriers increase. This is probably linked to the previous observation in that a certain number of sub-carriers require a certain number of samples in order to be accurate, but increasing the number of samples beyond this point does not provide any benefit. It should also be noted that the off-by-one errors increase as the number of sub-carriers increase.

Table 4.1: Results of pMUSIC tests in an ideal channel.

Actual Inner Modulation	N_s	N_c	Results of the test (% of iterations) $< N_c - 1$	$N_c - 1$	N_c	$N_c + 1$	$> N_c + 1$
QPSK	50	16	2	17	75	3	3
16-QAM	50	16	1	8	89	1	1
64-QAM	50	16	2	5	80	8	5
QPSK	100	16		13	87		
16-QAM	100	16		13	87		
64-QAM	100	16		16	84		
QPSK	200	16		15	85		
16-QAM	200	16		16	84		
64-QAM	200	16		13	87		
QPSK	50	32	2	25	70	3	
16-QAM	50	32	2	24	62	8	4
64-QAM	50	32	3	28	61	6	2
QPSK	100	32		28	70	2	
16-QAM	100	32		26	72	2	
64-QAM	100	32		28	72		
QPSK	200	32		25	75		
16-QAM	200	32		35	65		
64-QAM	200	32		27	73		
QPSK	50	64	6	31	51	9	3
16-QAM	50	64	4	32	49	13	2
64-QAM	50	64	5	36	47	6	6
QPSK	100	64		43	56	1	
16-QAM	100	64		40	60		
64-QAM	100	64		49	50	1	
QPSK	200	64		56	44		
16-QAM	200	64		59	41		
64-QAM	200	64		56	44		
QPSK	50	128	10	34	40	12	4
16-QAM	50	128	24	24	32	14	6
64-QAM	50	128	16	41	25	11	7
QPSK	100	128	1	73	24	2	
16-QAM	100	128		64	36		
64-QAM	100	128	1	70	27	2	
QPSK	200	128		82	18		
16-QAM	200	128		81	19		
64-QAM	200	128		80	20		

Table 4.2: Summary of results of pMUSIC tests in an ideal channel.

Actual		Results of the test (% of iterations)					
		$< N_c - 1$	$N_c - 1$	N_c	$N_c + 1$	$> N_c + 1$	$N_c \pm 1$
Inner Modulation	QPSK	1.8	36.8	57.9	2.7	0.8	97.4
	16-QAM	2.6	35.2	58.0	3.2	1.1	96.4
	64-QAM	2.3	37.4	55.8	2.8	1.7	96
N_s	50	6.4	25.4	56.8	7.8	3.6	90
	100	0.2	38.6	60.4	0.8		99.8
	200		45.4	54.6			100
N_c	16	0.6	12.9	84.2	1.3	1.0	98.4
	32	0.8	27.3	68.9	2.3	0.7	98.2
	64	1.7	44.7	49.1	3.3	1.2	97.1
	128	5.8	61.0	26.8	4.6	1.9	92.4

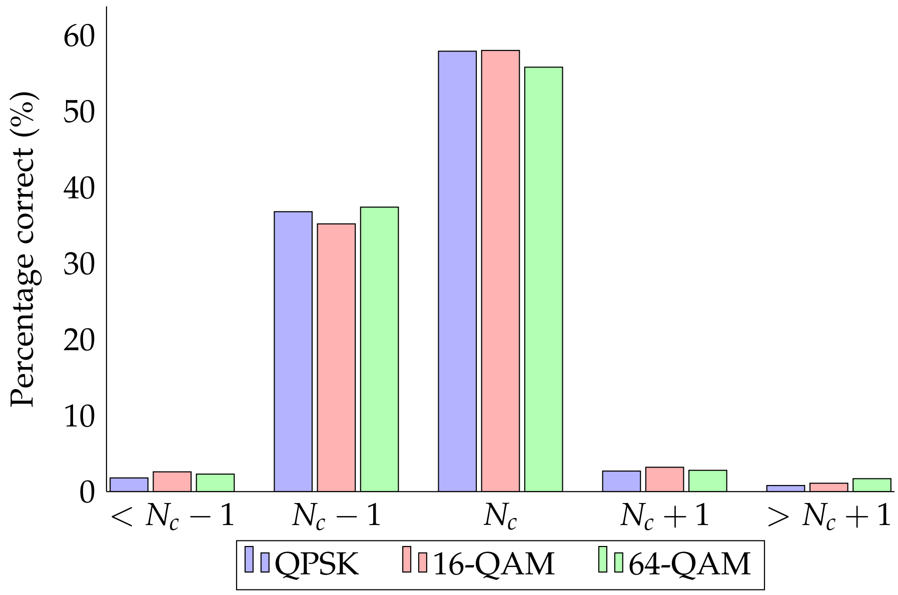

Figure 4.1: Results of pMUSIC tests in an ideal channel per inner modulation.

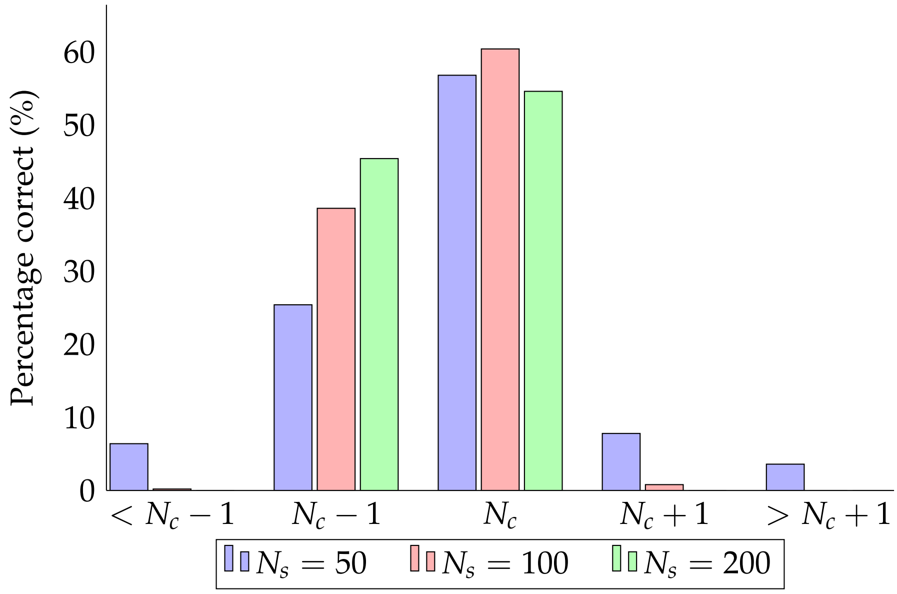

Figure 4.2: Results of pMUSIC tests in an ideal channel per number of symbols.

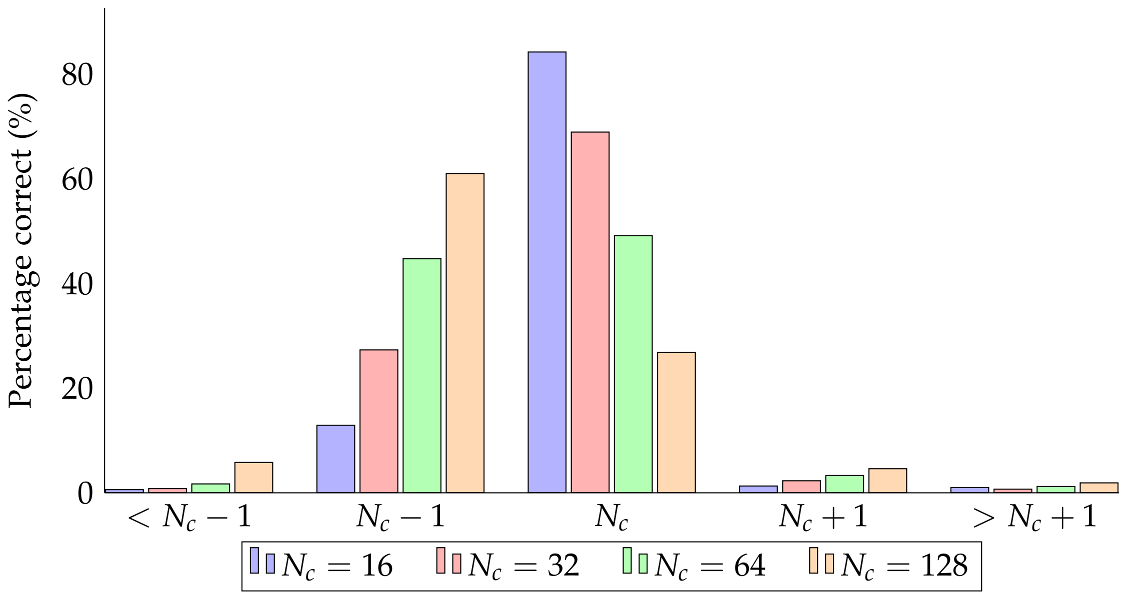

Figure 4.3: Results of pMUSIC tests in an ideal channel per number of sub-carriers.

4.2 Experiments in AWGN Channels

The purpose of this section is to determine the effect of different SNR values in an AWGN channel on the accuracy of the pMUSIC test. The effect of N_s is also revisited.

4.2.1 Experimental Setup

For this section, the tests of Section 4.1 were repeated in AWGN channels. The AWGN channel of the MATLAB® Communications System Toolbox was used for these tests. This test looked at the effect of 30 dB, 20 dB and 10 dB SNR AWGN channels of the accuracy of the test. For this experiment, $N_s \in \{100, 200\}$ and $N_c \in \{16, 32, 64, 128\}$. An inner modulation of 16-QAM was used. The tests were repeated 100 times for each combination of these conditions.

4.2.2 Results and conclusion

Table 4.3 shows the results of each of the different combinations of SNR, the number of symbols, and the number of sub-carriers. The left side of the table shows the inner modulation of the OFDM signal, the number of symbols used in the test and the number of sub-carriers in the OFDM signal. The right side of the table shows the percentage of times that the test result was in each of the categories, where these categories are:

1. Less than the actual number of sub-carriers minus one.
2. Equal to the actual number of sub-carriers minus one.
3. Equal to the actual number of sub-carriers.
4. Equal to the actual number of sub-carriers plus one.
5. Greater than the actual number of sub-carriers plus one.

The results are also summarised per parameter in Table 4.4. This summary is visualised in Figures 4.4 to 4.6. These figures show histograms of the result of the test, where in each case one of the test parameters were varied. In Figure 4.4, the SNR of the AWGN channel is varied, in Figure 4.5, N_s is varied, and in Figure 4.6, N_c is varied.

From these results, it can be seen that the test performed well in the 30 dB AWGN channel, and resonantly well in the 20 dB AWGN channel, but it performed very badly in the 10 dB AWGN channel. This means that an understanding of the channel conditions is required in order to understand the accuracy of the test. As in the previous case, the accuracy increased as N_s increased, and the accuracy decreased as N_c increased. The off-by-one errors also increased as N_c increased.

Table 4.3: Results of pMUSIC tests in AWGN channels.

Actual			Results of the test (% of iterations)				
SNR	N_s	N_c	$< N_c - 1$	$N_c - 1$	N_c	$N_c + 1$	$> N_c + 1$
30 dB	100	16		13	85	2	
20 dB	100	16		10	86	3	1
10 dB	100	16	14	9	17	9	51
30 dB	200	16		12	88		
20 dB	200	16		17	83		
10 dB	200	16	6	9	48	12	25
30 dB	100	32		22	78		
20 dB	100	32	2	17	74	6	1
10 dB	100	32	49	3	3	5	40
30 dB	200	32		37	63		
20 dB	200	32		28	71	1	
10 dB	200	32	43	10	11	8	28
30 dB	100	64		48	52		
20 dB	100	64	17	22	32	10	19
10 dB	100	64	49		2	2	47
30 dB	200	64		58	42		
20 dB	200	64	1	32	61	6	
10 dB	200	64	57		4	3	36
30 dB	100	128	2	50	41	5	2
20 dB	100	128	45	3	2	7	43
10 dB	100	128	64				36
30 dB	200	128		73	27		
20 dB	200	128	25	22	17	17	19
10 dB	200	128	68				32

Table 4.4: Summary of results of pMUSIC tests in AWGN channels.

Actual		Results of the test (% of iterations)					
		$< N_c - 1$	$N_c - 1$	N_c	$N_c + 1$	$> N_c + 1$	$N_c \pm 1$
Channel	30 dB	0.3	39.1	59.5	0.9	0.3	99.5
	20 dB	11.3	18.9	53.3	6.3	10.4	78.4
	10 dB	43.8	3.9	10.6	4.9	36.9	19.4
N_s	100	20.2	16.4	39.3	4.1	20.0	59.8
	200	16.7	24.8	42.9	3.9	11.7	71.7
N_c	16	3.3	11.7	67.8	4.3	12.8	83.8
	32	15.7	19.5	50.0	3.3	11.5	72.8
	64	20.7	26.7	32.2	3.5	17.0	62.3
	128	34.0	24.7	14.5	4.8	22.0	44.0

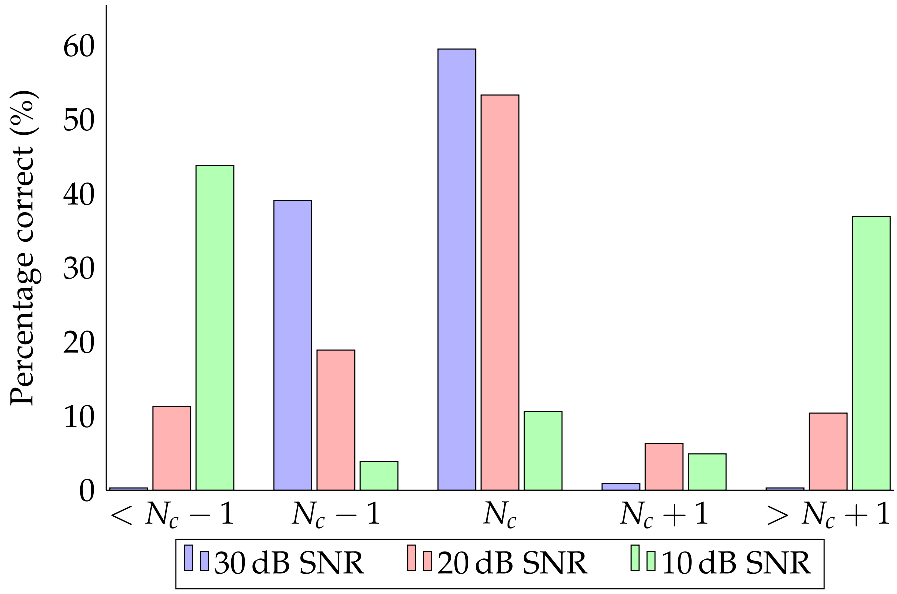

Figure 4.4: Results of pMUSIC tests in AGWN channels per SNR.

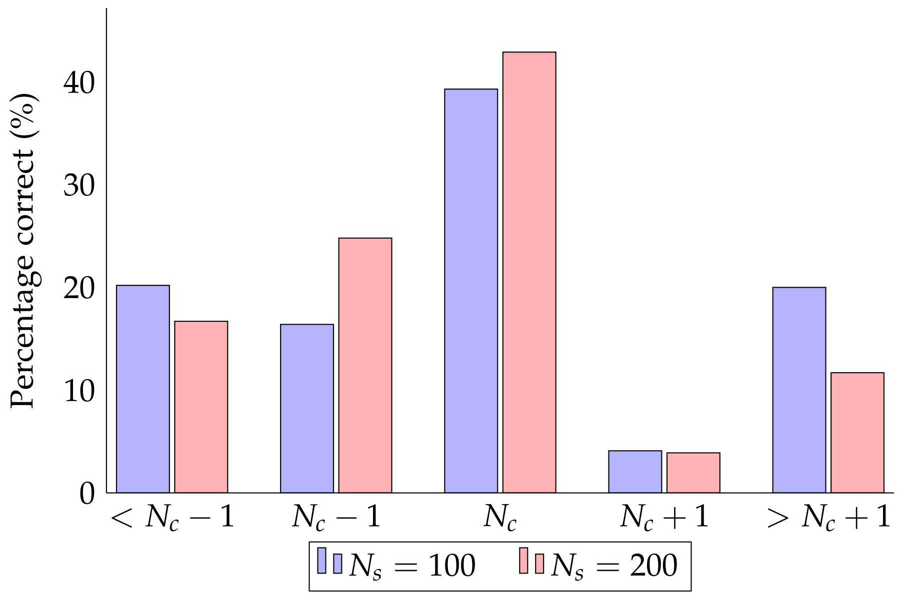

Figure 4.5: Results of pMUSIC tests in AGWN channels per number of symbols.

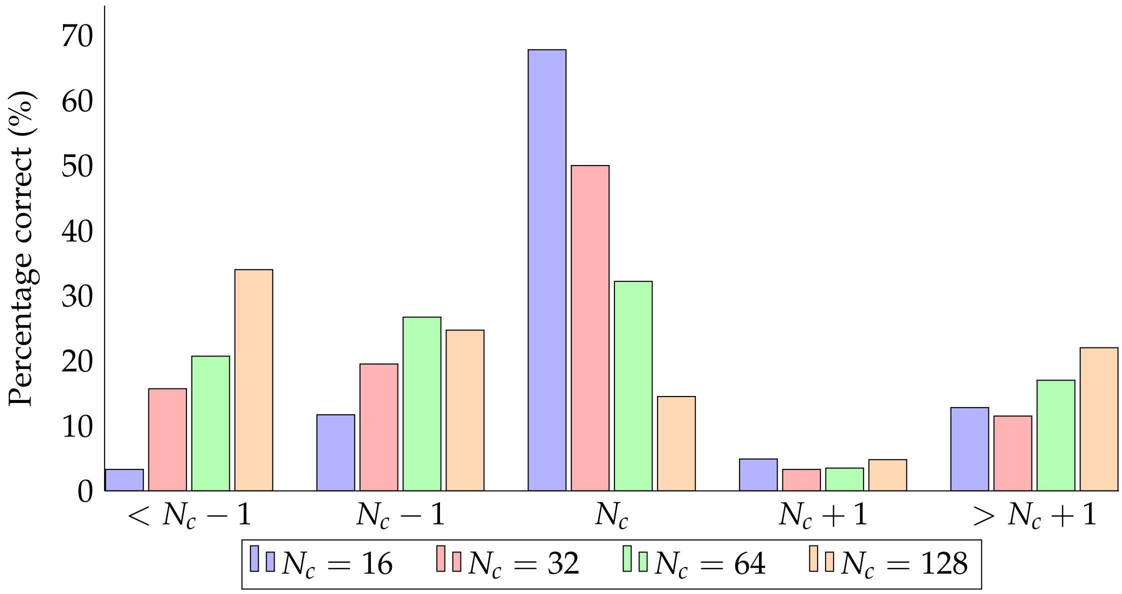

Figure 4.6: Results of pMUSIC tests in AWGN channels per number of sub-carriers.

4.3 Experiments in TDL Channels - LTE

The purpose of this section is to determine the accuracy of the pMUSIC test under more realistic channel conditions. This will be done by selecting one of the common OFDM signals from Section 2.9 and performing the test using the parameters and test conditions prescribed by the relevant standard.

4.3.1 Experimental Setup

For this section, the tests of the previous sections were repeated in the LTE channel models. LTE was chosen as a test case because from the signals mentioned in Section 2.9, and it is the only signal that has a variable number of sub-carriers and a comparably low number of sub-carriers. The values for the sub-carrier spacing and inner modulation used in this experiment are values typically found in an LTE signal.

The channel models used are the following SISO Rayleigh TDL models as described in the LTE standard [47]:

- Extended Pedestrian A (EPA) model with 5 Hz maximum Doppler shift (f_D)
- Extended Vehicular A (EVA) model with $f_D = 70\,\text{Hz}$
- Extended Typical Urban (ETU) model with $f_D = 70\,\text{Hz}$

The channel parameters used in the tests are the same as those proposed for the LTE standard by 3GPP, release 15 [47].

From the channel models in the LTE standard, the SISO Rayleigh TDL models were chosen above the AWGN and MIMO models, because AWGN channels were already tested and MIMO channels are outside the scope of this study.

The channels were implemented using the `comm.RayleighChannel` system object from the MATLAB® Communications System Toolbox. The object was setup using the path gains, path delays and maximum Doppler shift from the LTE channel specification [47]. The sub-carrier spacing from the specification was also used.

The number of OFDM samples (N_s) tested were 200. For this test, $N_c \in \{16, 32, 64, 128\}$. An inner modulation of 16-QAM was used as this is one of the inner modulations used in LTE [40]. As shown in Section 4.1, the choice of inner modulation does not have a significant impact on the results. The tests were repeated 100 times for each combination of these conditions.

4.3.2 Results and Conclusion

The results of these are shown in Table 4.5 and summarised in Table 4.6. It is also visualised in Figures 4.7 and 4.8.

From these results, it can be seen that the test performed reasonably well in the EPA channel, while not performing very good in the EVA channel, and performing badly in the ETU channel. The increase in N_c produced similar results than in the previous test.

It should also be noted that the test tends to overestimate the number of sub-carriers in these channels, with a significantly larger number of results in the $> N_c + 1$ bin than in the previous test. This effect increases as the number of sub-carriers increase.

Table 4.5: Results of pMUSIC tests in LTE channels.

Actual		Results of the test (% of iterations)				
Channel	N_c	$< N_c - 1$	$N_c - 1$	N_c	$N_c + 1$	$> N_c + 1$
EPA	16		14	86		
EVA	16	1	11	75	5	8
ETU	16	7	4	44	13	32
EPA	32	1	28	65	2	4
EVA	32	3	13	40	22	22
ETU	32	1	7	26	19	47
EPA	64		35	49	6	10
EVA	64	5	14	18	19	44
ETU	64	7	4	8	13	68
EPA	128	8	30	32	17	13
EVA	128	17	21	14	16	32
ETU	128	5	3	5	5	82

Table 4.6: Summary of results of pMUSIC tests in LTE channels.

Actual		Results of the test (% of iterations)					
		$< N_c - 1$	$N_c - 1$	N_c	$N_c + 1$	$> N_c + 1$	$N_c \pm 1$
Chan-nel	EPA	2.3	26.8	58.0	6.3	6.8	91.0
	EVA	6.5	14.8	36.8	15.5	26.5	67.0
	ETU	5.0	4.5	20.8	12.5	57.3	37.8
N_c	16	2.7	9.7	68.3	6.0	13.3	84
	32	1.7	16.0	43.7	14.3	24.3	74
	64	4.0	17.7	25.0	12.7	40.7	55.3
	128	10.0	18.0	17.0	12.7	42.3	47.7

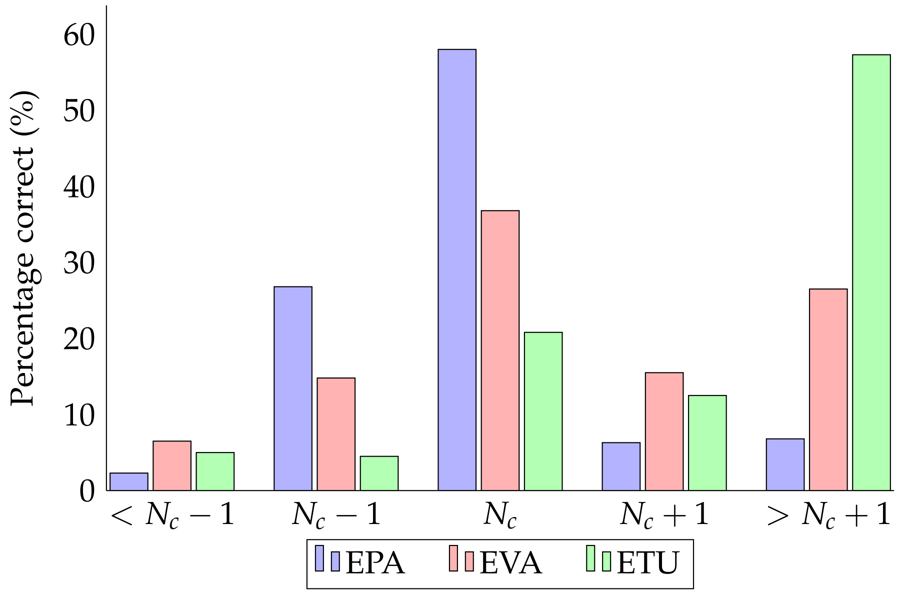

Figure 4.7: Results of pMUSIC tests in LTE channels per channel scenario.

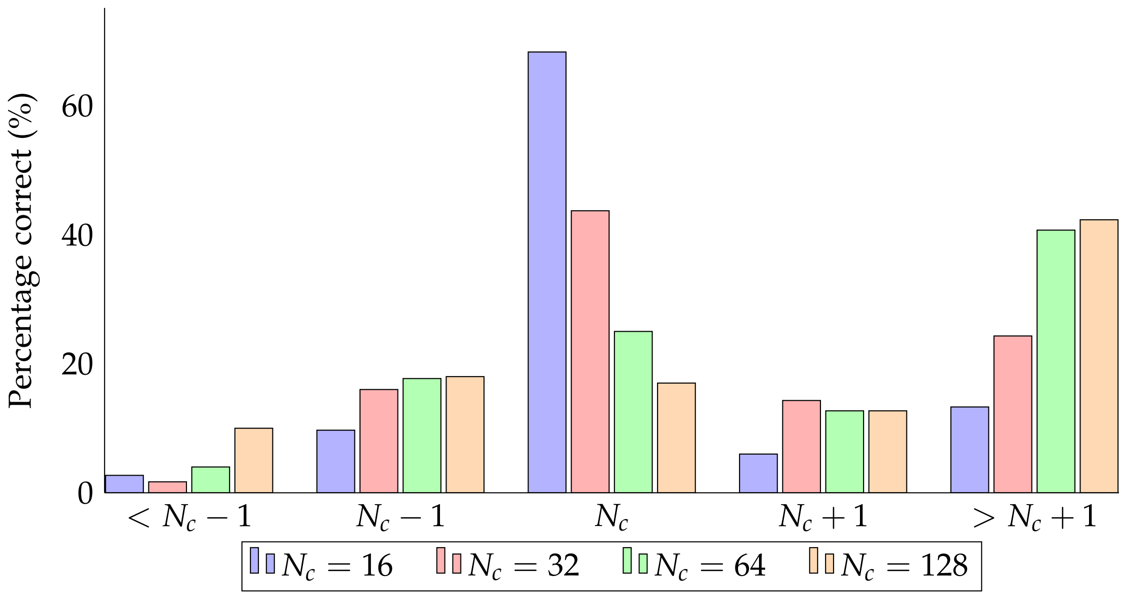

Figure 4.8: Results of pMUSIC tests in LTE channels per number of sub-carriers.

4.4 Comparison of Channels

The results for the different channels were compared for the case of a 16-QAM inner modulation, and 200 OFDM symbols. This comparison is provided in Table 4.7.

Table 4.7: Comparison of results of pMUSIC tests in AWGN and multi-path channels.

Channel	Results of the test (% of iterations)					
	$< N_c - 1$	$N_c - 1$	N_c	$N_c + 1$	$> N_c + 1$	$N_c \pm 1$
ideal		47.8	52.3			100
30 dB SNR		45	55			100
20 dB SNR	6.5	24.8	58	6	4.8	88.8
10 dB SNR	43.5	4.8	15.8	5.8	30.3	26.3
EPA	2.3	26.8	58.0	6.3	6.8	91.0
EVA	6.5	14.8	36.8	15.5	26.5	67.0
ETU	5.0	4.5	20.8	12.5	57.3	37.8

It can be seen that under these conditions, the results are similar for the ideal channel and the 30 dB AWGN channel. The 20 dB AWGN channel also performed similarly to the EPA LTE channel. The 10 dB AWGN channel performed the worst of all the channels tested.

This means that this test is not suitable in cases where the AWGN SNR is equal to or worse than 10 dB or where the conditions are comparable to the LTE ETU channel.

4.5 Conclusion

In this chapter, an in-depth examination was performed regarding the performance of the pMUSIC test as developed in this study. It was noted to perform well in 30 dB and 20 dB AWGN channels, as well as in EPA and EVA LTE channels.

Chapter 5

Verification and Validation

In this Chapter, the verification and validation of the work presented in Chapters 3 and 4 are done. The various components of the experimental setup will be verified and validated.

5.1 Introduction

Verification and validation is the process of determining if a model and its output are correct for its intended purpose [64, 65]. More specifically, verification is determining if the model and its implementation are correct, and validation is determining if the model is sufficiently accurate and consistent for its intended application [64, 65].

The three specific verification and validation techniques used here as proposed by [64, 65] are *Comparison to Other Models*, *Comparison Using Graphical Displays*, and *Explore Model Behaviour*.

The *Comparison to Other Models* technique consists of comparing the output of the model being validated to the results obtained from a known model [64, 65]. The *Comparison Using Graphical Displays* technique is similar to *Comparison to Other Models*, but the comparison is made graphically, rather than numerically or analytically [64, 65].

In the *Explore Model Behaviour*, the output of the model is examined using various qualitatively or quantitatively techniques [64, 65].

Referring back to Section 3.1, recall that the experimental setup is as shown in Figure 5.1. Each component of this setup needs to be verified, and the output of the tests validated. This will be done in the following sections.

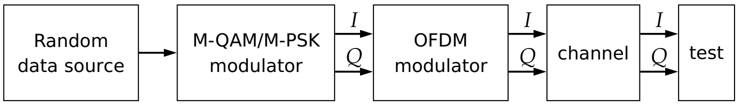

Figure 5.1: The experimental setup.

5.2 Verification of Random Data Source

The random data source is implemented using the `randi` MATLAB® function as explained in Section 3.1. The MATLAB® random number generator has been extensively tested by [66], and although it does not exhibit perfect pseudorandom properties, it is good enough for the purpose in which it is used here.

5.3 Verification of Inner Modulation

According to [67], the modulation of signals can be verified by plotting the constellation diagrams of the modulated signals and comparing it to the expected result. A constellation diagram is a diagram showing the in-phase and quadrature components of a signal's signal elements on a complex plane [32, 68]. The amplitude and phase of the signal elements can also be seen on the constellation diagram [32, 68]. This concept is shown in Figure 5.2.

Figure 5.3 shows the results of constellation plots of the modulation schemes used in the absence of noise. By comparing this to the expected result as seen in [32, 68], it can be seen that it is correct. This verifies the modulators using the *Comparison Using Graphical Displays* technique.

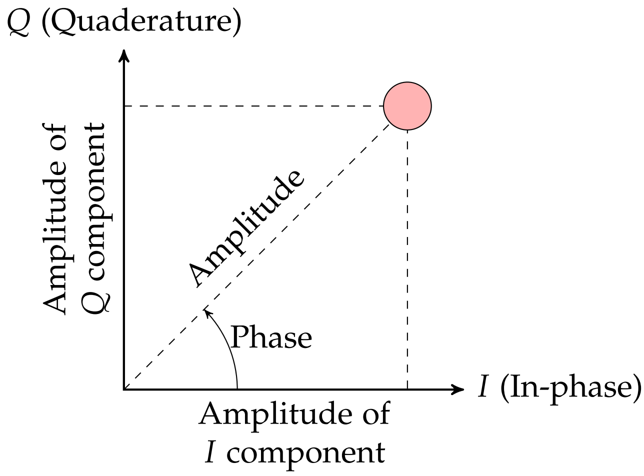

Figure 5.2: The layout of a constellation diagram [68].

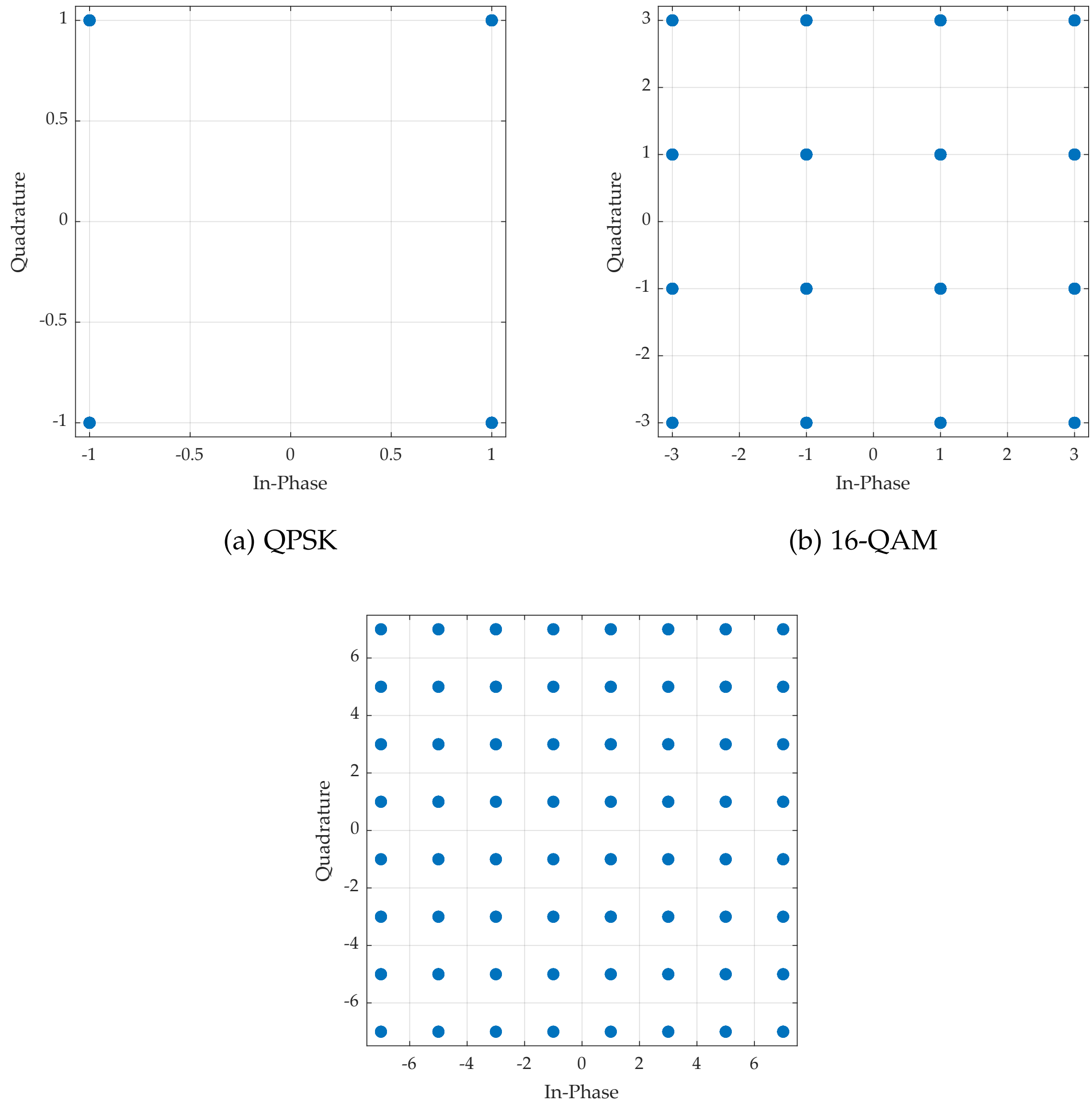

(a) QPSK (b) 16-QAM

(c) 64-QAM

Figure 5.3: The constellation diagrams of the inner modulations used in this study.

5.4 Verification of OFDM Modulator

In order to verify that the generated OFDM signals are correct, the signal generated by the MATLAB® Communications Toolbox was compared to the signal generated by OFDM code from [10]. This setup is shown in Figure 5.4. For the test case, an OFDM signal with $N_c = 64$ and $N_s = 100$ was generated using both methods and compared. In this case, the signal has a maximum magnitude of 0.4 and mean squared error (MSE) of 5.51×10^{-34}, which means that the signals are functionally identical. The small difference can be attributed to floating-point rounding errors. This verifies these OFDM modulators using the *Comparison to Other Models* technique.

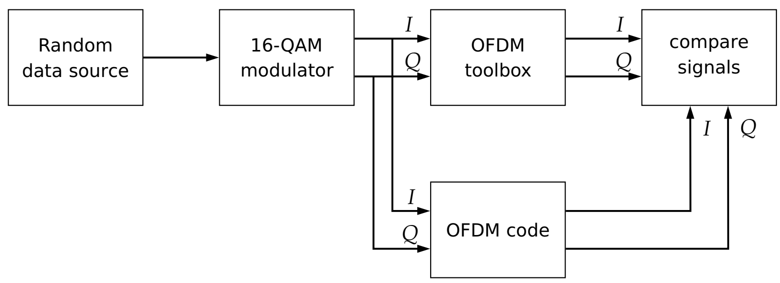

Figure 5.4: OFDM verification process.

5.5 Verification of the AGWN Channel Model

An AWGN channel can be verified by plotting a distribution of the amplitudes of an 8-PSK that has been sent through the channel and seeing if the resulting data has a Gaussian distribution [67]. This was tested for AWGN channels with an SNR of 30 dB and 10 dB, and the result can be seen in Figure 5.5. A modulation scheme of 8-PSK was chosen as this is what is suggested by [67]. From this, it can be seen that the channel does indeed exhibit the correct behaviour. This verifies the AWGN channel used using the *Comparison Using Graphical Displays* technique.

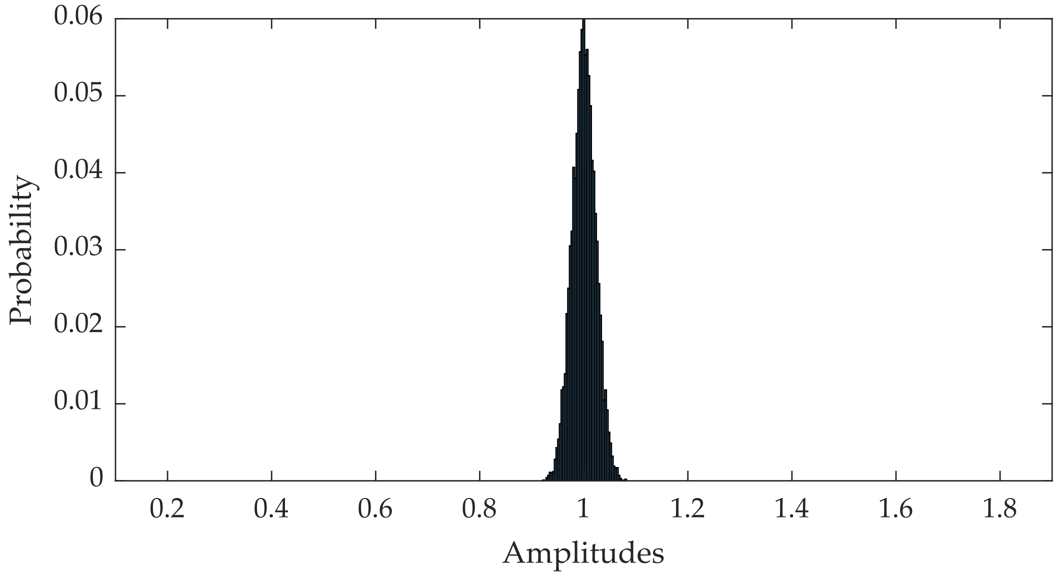

(a) 30 dB AWGN

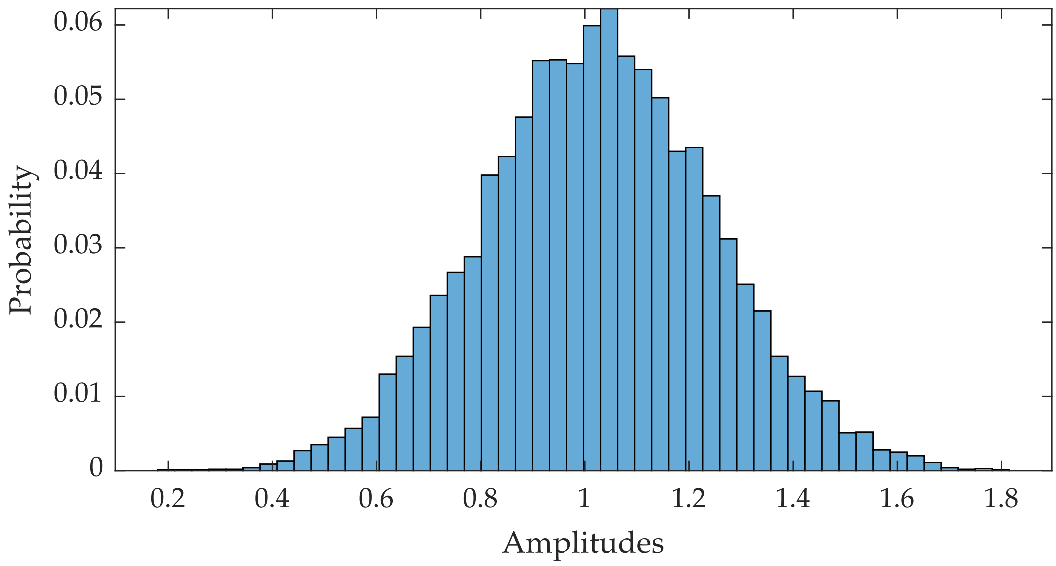

(b) 10 dB AWGN

Figure 5.5: A distribution of the amplitudes of received 8-PSK symbols.

5.6 Verification of the LTE Channel Models

The verification of the LTE channel models is done visually by looking at the impulse and frequency responses of the channels and seeing if they vary over time and match the expected result. The impulse and frequency responses at a point in time are shown in Figures 5.6 to 5.8. When observing these responses over time, they can be seen to change. They exhibit comparable responses than seen in similar graphs in [69] and can, therefore, be verified by *Comparison Using Graphical Displays* and *Comparison to Other Models*.

5.7 Verification and Validation of the Giannakis–Tsatsanis Test

The Giannakis–Tsatsanis test, as implemented in Section 3.2, can be both verified and validated by the fact that similar results were obtained under similar conditions than in the original paper [58]. This fact also contributes to the verification and validation of the general experimental setup used throughout the study. The implementation of this test was therefore verified and validated by reproducing published results and using the *Comparison to Other Models* technique.

5.8 Validation of pMUSIC Algorithm

The validation of the pMUSIC algorithm is provided by the extended tests done in Chapter 4. The fact that the test can produce accurate results across several iterations under certain conditions shows that the test is accurate and consistent under these conditions using the *Explore Model Behaviour* technique. Conversely, it also demonstrates the conditions under which this test cannot perform accurately and will, therefore, not be suitable as discussed in Section 4.4.

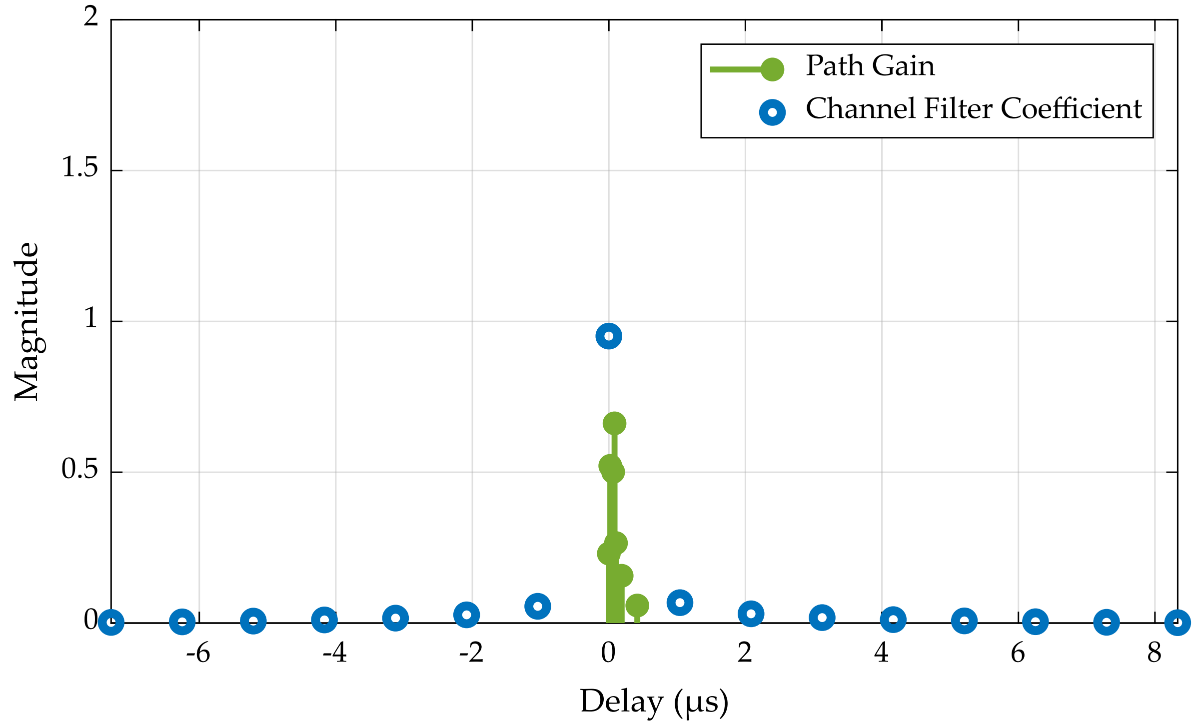

(a) Impulse Response

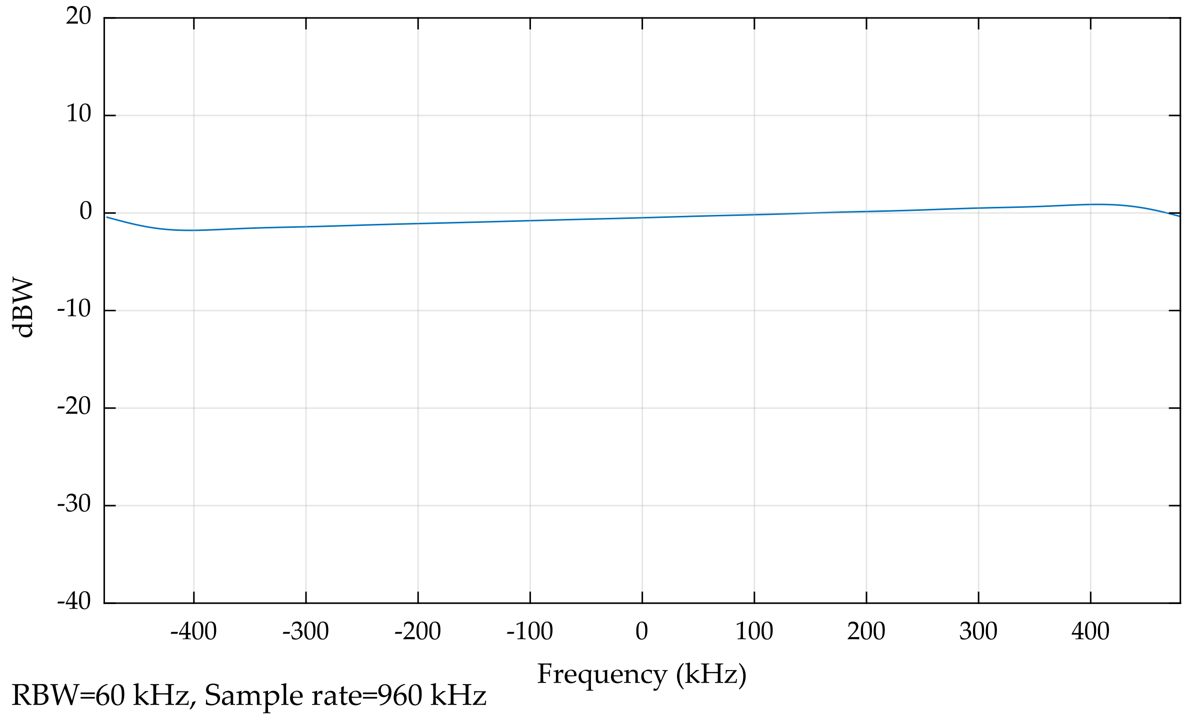

(b) Frequency Response

Figure 5.6: The response of the LTE EPA channel at a point in time.

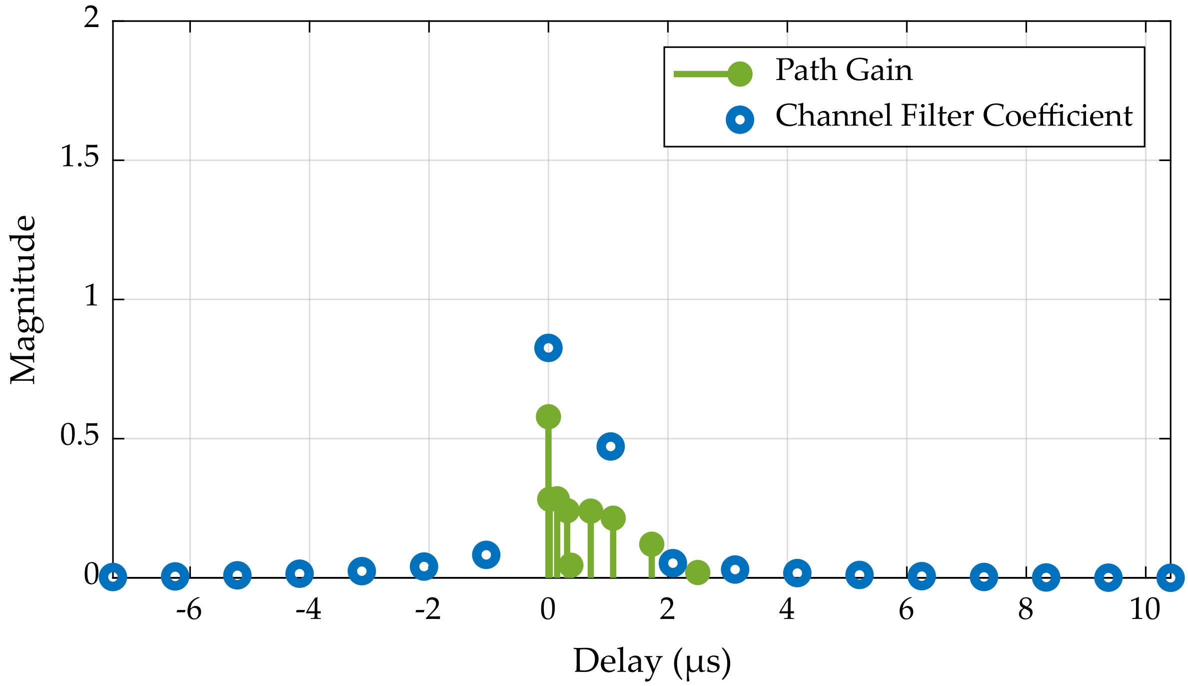

(a) Impulse Response

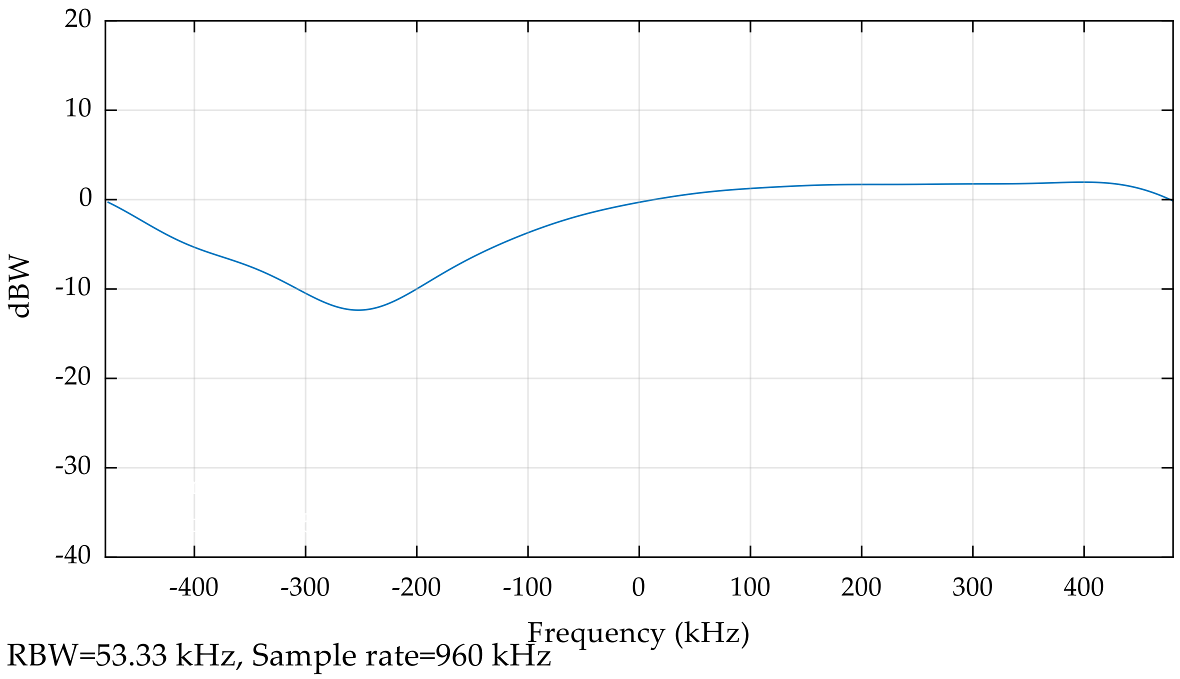

(b) Frequency Response

Figure 5.7: The response of the LTE EVA channel at a point in time.

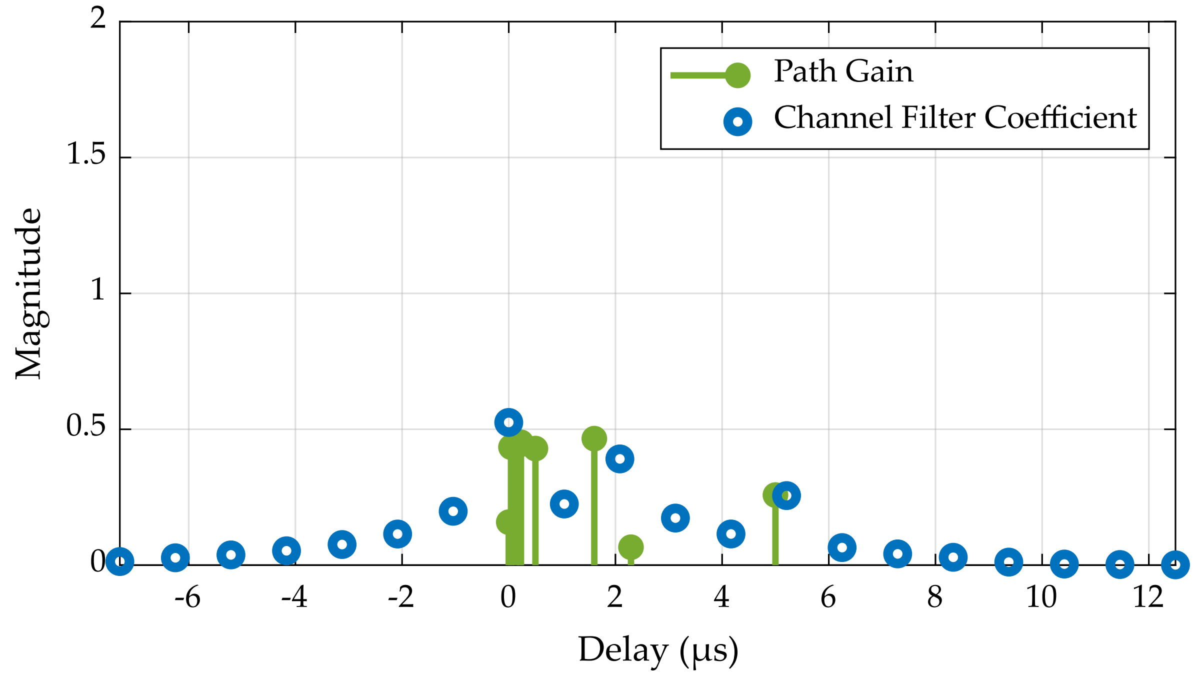

(a) Impulse Response

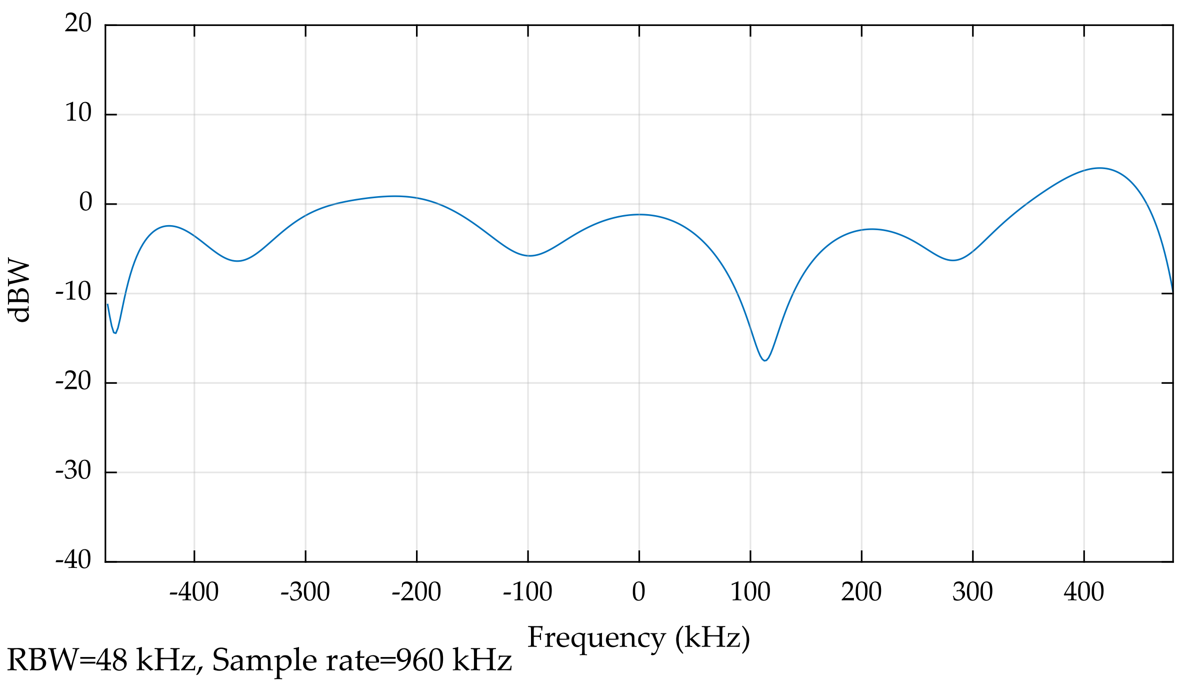

(b) Frequency Response

Figure 5.8: The response of the LTE ETU channel at a point in time.

5.9 Conclusion

In this chapter, the components of the experimental setup were verified and validated. This was done to provide credibility to the experiments done in Chapters 3 and 4.

Chapter 6

Conclusion

This chapter will conclude the study by revisiting the aim of the study as presented in Chapter 1, summarising the results obtained in Chapters 3 and 4 and exploring future work to be done in succession of this study.

6.1 Research Aim

As indicated in Chapter 1, the aims of this research were to:

1. Identify the applicable OFDM modulations
2. Identify the modulation parameters
3. Identify the appropriate tests for parameter extraction
4. Evaluate existing tests for parameter extraction
5. Develop or improve tests for parameter extraction
6. Perform experiments in increasingly realistic channels

Items 1 to 3 were addressed by means of an extensive literature study in Chapter 2. A survey of commonly found OFDM signals was compiled and from this, the typical values for OFDM parameters were determined. The theoretical background of the Giannakis–Tsatsanis test and MUSIC algorithm were also discussed.

Items 4 and 5 were addressed in Chapter 3 by evaluating the applicability of the Giannakis–Tsatsanis test and MUSIC algorithm. An improvement to the MUSIC algorithm was also made.

Item 6 was addressed in Chapter 4 by repeating the experiments of Chapter 3 in various different channel models and observing the results.

6.2 Research Results

An extensive literature study was done in Chapter 2. An overview of related work showed that there are few existing AMC techniques for OFDM signals. It also found that AMC systems are most often tested in AWGN channels and seldom in multipath fading channels. The theoretical background behind OFDM signals was discussed and the related modulation parameters and their typical values given. Tests for determining the presence of OFDM signals and the parameters of these signals were shown.

These tests were implemented in Chapter 3. It was found that the Giannakis–Tsatsanis test cannot successfully distinguish OFDM from all single-carrier modulation schemes. The MUSIC test was successfully implemented to determine the number of sub-carriers in an OFDM signal, but it was found that it is too computationally complex to be practically used. The novel use of the MUSIC algorithm to determine the presence and number of guard carriers was also done. To address the complexity problem of the MUSIC test, an improvement to this test was made and proposed as the pMUSIC test. This test was able to successfully determine the number of sub-carriers in an OFDM signal. It was also found that this developed pMUSIC test can be used to determine the presence of OFDM from amongst more modulation schemes than the Giannakis–Tsatsanis test can. This increased versatility comes at a significant cost, namely computational complexity. This means that the pMUSIC test can be used as an

AMC system that is capable of distinguishing OFDM from other modulation schemes and determining the number of OFDM sub-carriers in a signal.

The pMUSIC test developed in this study was evaluated extensively in Chapter 4. It was noted to perform well in 30 dB and 20 dB AWGN channels, as well as in EPA and EVA LTE channels.

Finally, in Chapter 5, the components of the experimental setup were verified and the outputs of the tests validated.

6.3 Contributions of this Study

This study has the following novel contributions as developed by the author:

1. Using the Giannakis–Tsatsanis test on a wider range of modulation techniques.
2. MATLAB® implementation of MUSIC algorithm and visual interpretation of results.
3. Extension of the MUSIC algorithm to give results in the presence of guard carriers.
4. Development of the pMUSIC algorithm for testing the number of sub-carriers in an OFDM signal.
5. Using the pMUSIC algorithm to determine the presence of OFDM.
6. Extensive tests of this algorithm in various channels, including multipath fading channels.

6.4 Future Work and Recommendations

The work presented here provides an AMC system capable of determining the presence of an OFDM signal and the number of sub-carriers in the signal under certain conditions, as shown in Chapters 3 and 4. Future work building on this study will be to expand the system to be able to determine more of the OFDM parameters as mentioned in Section 2.8. Doing this will work towards the goal of being able to blindly demodulate an OFDM signal.

The run-time of the pMUSIC test can be reduced by iterating over a smaller range of values in which the result is expected instead of iterating over the entire range of values. Effective techniques for accomplishing this can be examined.

Other future work would be incorporating the work of [67] into this system to enable the determination of the inner modulation of an OFDM signal.

Finally, the system should be tested in increasingly realistic conditions. This can be done by performing hardware-in-the-loop tests in a laboratory setup and finally testing it against real-world physical signals and channels.

6.5 Closure

AMC is an important and evolving field with several applications in both military and civilian domains. This study addressed a gap in the existing AMC body of knowledge by providing efficient techniques for determining the presence of OFDM and determining the number of OFDM sub-carriers present in a signal.

References

[1] T. Rappaport, *Wireless Communications: Principles and Practice*, 2nd ed. Upper Saddle River: Prentice Hall PTR, 2002.

[2] A. Goldsmith, *Wireless communications*. New York: Cambridge University Press, 2005.

[3] J. Proakis and M. Salehi, *Digital Communications*, 5th ed. Boston: McGraw-Hill Education, Nov. 2007.

[4] Z. Zhu and A. K. Nandi, *Automatic Modulation Classification: Principles, Algorithms and Applications*. Chichester: John Wiley & Sons, Dec. 2014.

[5] F. Benedetto, A. Tedeschi, and G. Giunta, "Automatic Blind Modulation Recognition of Analog and Digital Signals in Cognitive Radios," in *2016 IEEE 84th Vehicular Technology Conference (VTC-Fall)*, Sep. 2016.

[6] O. A. Dobre, A. Abdi, Y. Bar-Ness, and W. Su, "Survey of automatic modulation classification techniques: classical approaches and new trends," *IET Communications*, vol. 1, no. 2, pp. 137–156, Apr. 2007.

[7] M. W. Aslam, Z. Zhu, and A. K. Nandi, "Automatic Modulation Classification Using Combination of Genetic Programming and KNN," *IEEE Transactions on Wireless Communications*, vol. 11, no. 8, pp. 2742–2750, Aug. 2012.

[8] Z. Yu, "Automatic modulation classification of communication signals," Ph.D., New Jersey Institute of Technology, New Jersey, USA, 2006. [Online]. Available: http://search.proquest.com/pqdtglobal/docview/855816225/abstract/7BEEBD0847B64EE9PQ/8

[9] H. Guldemir and A. Sengur, "Online modulation recognition of analog communication signals using neural network," *Expert Systems with Applications*, vol. 33, no. 1, pp. 206–214, Jul. 2007.

[10] Y. S. Cho, J. Kim, W. Y. Yang, and C. G. Kang, *MIMO-OFDM Wireless Communications with MATLAB*. Singapore: John Wiley & Sons, Aug. 2010.

[11] V. G. Chavali and C. R. C. M. da Silva, "Classification of Digital Amplitude-Phase Modulated Signals in Time-Correlated Non-Gaussian Channels," *IEEE Transactions on Communications*, vol. 61, no. 6, pp. 2408–2419, Jun. 2013.

[12] F. Wang and X. Wang, "Fast and Robust Modulation Classification via Kolmogorov-Smirnov Test," *IEEE Transactions on Communications*, vol. 58, no. 8, pp. 2324–2332, Aug. 2010.

[13] D. L. Adamy, *EW101: A First Course in Electronic Warfare*. Norwood: Artech House, 2001.

[14] H. Xiao, "Blind recognition of analog modulation schemes for software defined radio," Ph.D., New Jersey Institute of Technology, New Jersey, USA, 2012. [Online]. Available: http://search.proquest.com/pqdtglobal/docview/1667738502/abstract/7BEEBD0847B64EE9PQ/10

[15] H. C. Wu, M. Saquib, and Z. Yun, "Novel Automatic Modulation Classification Using Cumulant Features for Communications via Multipath Channels," *IEEE Transactions on Wireless Communications*, vol. 7, no. 8, pp. 3098–3105, Aug. 2008.

[16] G. Kalivas, *Digital Radio System Design*. Chichester: John Wiley & Sons, Oct. 2009.

[17] A. F. Molisch, *Wireless Communications*, 2nd ed. Chichester: Wiley-IEEE Press, 2011.

[18] A. F. Molisch and F. Tufvesson, "Multipath Propagation Models for Broadband Wireless Systems," in *Signal processing for mobile communications handbook*, M. Ibnkahla, Ed. Boca Raton, Florida: CRC Press, 2005, pp. 53–96.

[19] M. Failli, *COST 207: Digital land mobile radio communications*. Luxembourg: Commission of the European Communities, 1989. [Online]. Available: https://publications.europa.eu/en/publication-detail/-/publication/61fc77e7-bca2-4229-8eb4-77741f0d2ab2

[20] ITU-R M.1225, "Guidelines for evaluation of radio transmission technologies for IMT-2000," 1997. [Online]. Available: https://www.itu.int/rec/R-REC-M.1225-0-199702-I/en

[21] W. Banzhaf, P. Nordin, R. E. Keller, and F. D. Francone, *Genetic Programming: An Introduction: on the Automatic Evolution of Computer Programs and Its Applications*. San Francisco: Morgan Kaufmann Publishers Inc., 1998.

[22] Z. Zhu, A. K. Nandi, and M. W. Aslam, "Robustness enhancement of distribution based binary discriminative features for modulation classification," in *2013 IEEE International Workshop on Machine Learning for Signal Processing (MLSP)*, Sep. 2013.

[23] A. K. Nandi and E. E. Azzouz, "Algorithms for automatic modulation recognition of communication signals," *IEEE Transactions on Communications*, vol. 46, no. 4, pp. 431–436, Apr. 1998.

[24] M. L. D. Wong and A. K. Nandi, "Automatic digital modulation recognition using artificial neural network and genetic algorithm," *Signal Processing*, vol. 84, no. 2, pp. 351–365, Feb. 2004.

[25] V. Choqueuse, S. Azou, K. Yao, L. Collin, and G. Burel, "Blind modulation recognition for MIMO systems," *Military Technical Academy Review*, vol. 19, no. 2, pp. 183–196, 2009.

[26] W. C. Headley and C. R. C. M. da Silva, "Asynchronous Classification of Digital Amplitude-Phase Modulated Signals in Flat-Fading Channels," *IEEE Transactions on Communications*, vol. 59, no. 1, pp. 7–12, Jan. 2011.

[27] J. J. Popoola, "Sensing and detection of a primary radio signal in a cognitive radio environment using modulation identification technique," Ph.D., University of the Witwatersrand, Johannesburg, South Africa, Jul. 2012. [Online]. Available: http://wiredspace.wits.ac.za/handle/10539/11600

[28] J. J. Popoola and R. van Olst, "The performance evaluation of a spectrum sensing implementation using an automatic modulation classification detection method with a Universal Software Radio Peripheral," *Expert Systems with Applications*, vol. 40, no. 6, pp. 2165–2173, May 2013.

[29] M. S. Mühlhaus, M. Öner, O. A. Dobre, and F. K. Jondral, "A Low Complexity Modulation Classification Algorithm for MIMO Systems," *IEEE Communications Letters*, vol. 17, no. 10, pp. 1881–1884, Oct. 2013.

[30] R. Prasad, *OFDM for Wireless Communications Systems*. Boston: Artech House, 2004.

[31] J. J. van de Beek, P. O. Börjesson, P. Ödling, and S. K. Wilson, "Orthogonal Frequency Division Multiplexing (OFDM)," in *Review of Radio Science 1996-1999*, W. R. Stone, Ed. Oxford: Oxford University Press, 1999, pp. 177–206.

[32] L. Frenzel, *Principles of Electronic Communication Systems*, 3rd ed. New York: McGraw-Hill Education, 2008.

[33] D. Grimaldi, S. Rapuano, and L. De Vito, "An Automatic Digital Modulation Classifier for Measurement on Telecommunication Networks," *IEEE Transactions on Instrumentation and Measurement*, vol. 56, no. 5, pp. 1711–1720, Oct. 2007.

[34] E. Dahlman, S. Parkvall, J. Sköld, and P. Beming, *3G Evolution, Second Edition: HSPA and LTE for Mobile Broadband*, 2nd ed. Amsterdam: Academic Press, Oct. 2008.

[35] ETSI EN 300 401 V2.1.1, "Radio Broadcasting Systems; Digital Audio Broadcasting (DAB) to mobile, portable and fixed receivers," Jan. 2017. [Online]. Available: https://www.etsi.org/deliver/etsi_en/300400_300499/300401/02.01.01_60/en_300401v020101p.pdf

[36] ETSI EN 302 755 V1.4.1, “Digital Video Broadcasting (DVB); Frame structure channel coding and modulation for a second generation digital transmission system for cable systems (DVB-T2),” Jul. 2015. [Online]. Available: http://www.etsi.org/deliver/etsi_en/302700_302799/302755/01.04.01_60/en_302755v010401p.pdf

[37] 3GPP TS 36.201 V15.1.0, “Evolved Universal Terrestrial Radio Access (E-UTRA); LTE physical layer; General description,” Jun. 2018. [Online]. Available: http://www.3gpp.org/DynaReport/36201.htm

[38] IEEE Std 802.11-2016, “Telecommunications and information exchange between systems Local and metropolitan area networks–Specific requirements - Part 11: Wireless LAN Medium Access Control (MAC) and Physical Layer (PHY) Specifications,” Dec. 2016.

[39] 3GPP TS 36.101 V15.4.0, “Evolved Universal Terrestrial Radio Access (E-UTRA); User Equipment (UE) radio transmission and reception,” Sep. 2018. [Online]. Available: http://www.3gpp.org/DynaReport/36101.htm

[40] 3GPP TS 36.211 V15.2.0, “Evolved Universal Terrestrial Radio Access (E-UTRA); Physical channels and modulation,” Jun. 2018. [Online]. Available: http://www.3gpp.org/DynaReport/36211.htm

[41] ITU-R BT.2254-3, “Frequency and network planning aspects of DVB-T2,” Mar. 2017. [Online]. Available: https://www.itu.int/pub/R-REP-BT.2254-3-2017

[42] ETSI TS 103 461 V1.1.1, “Digital Audio Broadcasting (DAB); Domestic and in-vehicle digital radio receivers; Minimum requirements and Test specifications for technologies and products,” Aug. 2017. [Online]. Available: https://www.etsi.org/deliver/etsi_ts/103400_103499/103461/01.01.01_60/ts_103461v010101p.pdf

[43] ETSI TS 102 831 V1.2.1, “Digital Video Broadcasting (DVB); Implementation guidelines for a second generation digital terrestrial television broadcasting system (DVB-T2),” Aug. 2012. [Online]. Available: https://www.etsi.org/deliver/etsi_ts/102800_102899/102831/01.02.01_60/ts_102831v010201p.pdf

[44] ETSI TR 101 190 V1.3.2, “Digital Video Broadcasting (DVB); Implementation guidelines for DVB terrestrial services; Transmission aspects,” May 2011. [Online]. Available: https://www.etsi.org/deliver/etsi_tr/101100_101199/101190/01.03.02_60/tr_101190v010302p.pdf

[45] IEEE 802.11-03/940r4, “TGn Channel Models,” May 2004.

[46] IEEE 802.11-09/0308r12, “TGac Channel Model,” Mar. 2010.

[47] 3GPP TS 36.104 V15.4.0, “Evolved Universal Terrestrial Radio Access (E-UTRA); Base Station (BS) radio transmission and reception,” Sep. 2018. [Online]. Available: http://www.3gpp.org/DynaReport/36104.htm

[48] ITU, “Final Acts of the Regional Administrative Conference for the Planning of VHF/UHF Television Broadcasting in the African Broadcasting Area and Neighbouring Countries,” 1989. [Online]. Available: https://www.itu.int/pub/R-ACT-RRC.11-1989/en

[49] ITU, “Final Acts of the Regional Administrative Conference for the Planning of VHF Sound Broadcasting (Region 1 and Part of Region 3),” 1984. [Online]. Available: https://www.itu.int/pub/R-ACT-RRC.5-1984/en

[50] ITU, “Final Acts of the Regional Radiocommunication Conference for the revision of the Geneva 1989 Agreement (RRC-06-Rev.GE89),” Jun. 2006. [Online]. Available: https://www.itu.int/pub/R-ACT-RRC.16-2006/en

[51] ITU, “Final Acts of the Regional Radiocommunication Conference for planning of the digital terrestrial broadcasting service in parts of Regions 1 and 3, in the frequency bands 174-230 MHz and 470-862 MHz (RRC-06),” Jun. 2006. [Online]. Available: https://www.itu.int/pub/R-ACT-RRC.14-2006

[52] J. Medbo and P. Schramm, “Channel Models for HIPERLAN/2 in Different Indoor Scenarios,” Mar. 1998. [Online]. Available: https://web.archive.org/web/20181015091711/http://read.pudn.com/downloads121/ebook/516255/Hiperlan/HIPERLAN%20-%203ERI085b.pdf

[53] J. G. Liu, X. Wang, and J. Y. Chouinard, "Iterative Blind OFDM Parameter Estimation and Synchronization for Cognitive Radio Systems," in *2012 IEEE 75th Vehicular Technology Conference (VTC Spring)*, May 2012.

[54] A. Punchihewa, V. K. Bhargava, and C. Despins, "Blind Estimation of OFDM Parameters in Cognitive Radio Networks," *IEEE Transactions on Wireless Communications*, vol. 10, no. 3, pp. 733–738, Mar. 2011.

[55] O. Azarmanesh and S. G. Bilén, "I-Q diagram utilization in a novel modulation classification technique for cognitive radio applications," *EURASIP Journal on Wireless Communications and Networking*, vol. 2013, p. 289, Dec. 2013.

[56] E. Kanterakis and W. Su, "Blind OFDM parameter estimation techniques in frequency-selective rayleigh channels," in *2011 IEEE Radio and Wireless Symposium*, Jan. 2011, pp. 150–153.

[57] G. B. Giannakis and M. K. Tsatsanis, "Time-domain tests for Gaussianity and time-reversibility," *IEEE Transactions on Signal Processing*, vol. 42, no. 12, pp. 3460–3472, Dec. 1994.

[58] W. Akmouche, "Detection of multicarrier modulations using 4th-order cumulants," in *MILCOM 1999. IEEE Military Communications. Conference Proceedings (Cat. No.99CH36341)*, vol. 1, 1999, pp. 432–436 vol.1.

[59] O. Azarmanesh, "A Novel Approach to Modulation Classification in Cognitive Radios," Ph.D., Pennsylvania State University, University Park, PA, USA, 2011.

[60] M. H. Hayes, *Statistical digital signal processing and modeling*. New York: John Wiley & Sons, 1996.

[61] W. Akmouche, E. Kerherve, and A. Quinquis, "OFDM spectral characterization: estimation of the bandwidth and the number of sub-carriers," in *Proceedings of the Tenth IEEE Workshop on Statistical Signal and Array Processing (Cat. No.00TH8496)*, Aug. 2000, pp. 48–52.

[62] J. L. Devore and N. R. Farnum, *Applied statistics for engineers and scientists*, 2nd ed. Belmont, CA: Brooks/Cole, 2005.

[63] C. D. Brown and H. T. Davis, "Receiver operating characteristics curves and related decision measures: A tutorial," *Chemometrics and Intelligent Laboratory Systems*, vol. 80, no. 1, pp. 24–38, Jan. 2006. [Online]. Available: http://www.sciencedirect.com/science/article/pii/S0169743905000766

[64] R. G. Sargent, "Verification and validation of simulation models," in *Proceedings of the 2011 Winter Simulation Conference (WSC)*, Dec. 2011, pp. 183–198.

[65] R. G. Sargent, "An introductory tutorial on verification and validation of simulation models," in *Proceedings of the 2015 Winter Simulation Conference (WSC)*, Dec. 2015, pp. 1729–1740.

[66] P. L'Ecuyer and R. Simard, "TestU01: A C Library for Empirical Testing of Random Number Generators," *ACM Transactions on Mathematical Software*, vol. 33, no. 4, pp. 22:1–22:40, Aug. 2007.

[67] H. K. Blackie, "Comparison of feature-based classifiers in Automatic Modulation Classification systems," Masters Dissertation, North-West University, Potchefstroom, South Africa, May 2018. [Online]. Available: https://repository.nwu.ac.za/handle/10394/31727

[68] B. A. Forouzan, *Data Communications and Networking*, 5th ed. New York: McGraw-Hill Education, 2013.

[69] P. Muñoz, I. de la Bandera, R. Barco, F. Ruiz, M. Toril, and S. Luna-Ramírez, "Estimation of link-layer quality parameters in a system-level LTE simulator," in *2010 Fifth International Conference on Broadband and Biomedical Communications*, Dec. 2010.

Appendix A

Publications

A subsection of the work presented in this dissertation was presented at and appeared in the proceedings of the *Southern Africa Telecommunication Networks and Applications Conference (SATNAC)* in 2018 as follows:

M. Rossouw and M. Ferreira, "Parameter Estimation of OFDM Signals in Gaussian Channels," in *Proc. Southern African Telecommun. and Netw. Access Conf. SATNAC 2018*, Arabella, Hermanus, Western Cape, South Africa, 2018.